Role of the MoFe Protein β-95-Cysteinyl Residue in Nitrogenase Catalysis in *Azotobacter vinelandii*

by

Haibing Xie

Thesis submitted to the faculty of the Virginia Polytechnic Institute and State University in partial fulfillment of the requirements for the degree of

Master of Science in Biochemistry

Approved by:

_____
Dr. William E. Newton, Chairman

_____ _____
Dr. Jiann-Shin Chen Dr. Timothy J. Larson

August 20,1998

Blacksburg, Virginia

Keywords: Nitrogenase, MoFe protein, P cluster, ***A. vinelandii***, β-95^{Cys}, β-95^{Asp}

Acknowledgment

I would like to take this opportunity to thank my advisor, Dr. William E. Newton, for his unconditional support, outstanding scientific guidance and fatherly care for me. Without him, I could not have accomplished this work and could not have overcome all the difficulties that I encountered during these past several years. I also would like to thank Dr. Jiann-shin Chen and Dr. Timothy J. Larson for their valuable advice, kind encouragement and understanding as my committee members. This excellent combination of professional expertise on my committee provided me with such a valuable experience. I will carry the wonderful memory for the rest of my life.

I especially thank my wife, Hong Zhu, for her silent support behind me. Without her, I could not have finished this work.

Thanks also to all the faculty members in this department, particularly Dr. Bevan, Dr. Kennelly, Dr. Sitz, Dr. Hess, Dr. Gregory and Dr. Storrie, to name a few. I appreciate their kind help and encouragement.

Special acknowledgment to Peggy, Mary Jo, Karen and Sheila for their efforts in helping me.

I would like to emphasize the friendship, encouragement and help coming from both graduate students and coworkers in our Lab.

This work was supported by a grant to Dr. Newton from National Institutes of Health (DK-37255).

Role of MoFe Protein β-95-Cysteinyl Residue in Nitrogenase Catalysis in *Azotobacter vinelandii*.

by

Haibing Xie

Committee Chairman: **William E. Newton**

Department of Biochemistry

(**Abstract**)

Previous studies revealed that β-95-Cys provides an essential ligand to one of the Fe atoms on the P cluster within the MoFe protein of nitrogenase, and a limited number of substitutions at this position resulted in inactive nitrogenase. It was also found that the counterpart of β-95-Cys, α-88-Cys, which also acts as a cysteinyl ligand to the P cluster, is replaceable without a complete loss of activity. In order to study the structure-function relationship of the protein environment in this region with respect to the P-cluster, subtle changes were introduced at β-95-Cys in ***Azotobacter vinelandii*** nitrogenase through site-directed mutagenesis and gene replacement method. Some crude extracts from the mutants with substitutions at β-95-Cys contain typical FeMo cofactor EPR signal. The β-95^{Asp} MoFe protein also has significant nitrogenase activity, but lower, suggesting that β-95-Cys is not absolutely required for both FeMo cofactor insertion and nitrogenase activity.

In order to characterize its catalytic features, the β-95^{Asp} MoFe protein was purified from mutant strain DJ1096. It has significantly reduced H^+ reduction, C_2H_2-reduction and N_2-reduction activity. It was found that a higher percentage of electron flux goes to

H^+ compared to the wild type MoFe protein. It was also found that reductant independent ATP hydrolysis occurs during H^+ reduction, suggesting that the altered MoFe protein has an increased affinity for Fe protein-ADP complex. Surprisingly, CO has a significant enhancement effect on H^+ reduction at low electron flux, but not at high electron flux, and highly couples the electron transfer to ATP hydrolysis. These results indicate that the binding of CO to the MoFe protein may either decrease the affinity of Fe-ADP complex for the β-95^{Asp} MoFe protein or facilitate electron acceptance by the P cluster, thus improving the electron transfer to substrate.

Table of Contents

List of the Figures

List of the Tables

Chapter 1. Literature Review

1.1. Biological Nitrogen Fixation

Nitrogen is an essential element for life. It cannot be substituted for in the proteins and nucleic acids of living organisms. Global inventories show that more than 99.9% of nitrogen on the earth is present as the dinitrogen molecule (N_2), of which somewhat more than 97% is trapped in primary rocks ($2x10^{17}$ metric tons) and sedimentary rocks ($4x10^{14}$ tons), and about 2% ($4x10^{15}$ tons) is free in the atmosphere (Burns and Hardy, 1975; Delwiche, 1977). In comparison, there are only about $1x10^{11}$ tons of fixed nitrogen distributed in the land and sea. Atmospheric dinitrogen (N_2) is chemically unreactive due to the high energy required to break its strong triple bond. Thus, it cannot be directly utilized by either plant or animal, both of which lack the ability to convert N_2 to a fixed, useable form. Fixed forms of nitrogen are produced naturally by either the non-biological oxidation of N_2 or the biological reduction of N_2. Unlike plants and animals, certain prokaryotic organisms, which are called diazotrophs, have the ability to reduce N_2 to ammonia. Diazotrophy is a characteristic shared by many different genera of prokaryotes with representatives among Gram-positive and Gram-negative bacteria. About 60% of the newly fixed nitrogen is contributed by diazotrophs (Eady, 1992). At least 35 genera have been found to be able to fix dinitrogen. They fall into three categories based on their ability to grow in the presence of dioxygen; they are anaerobes, aerobes or microaerobes (Silvester and Musgrave, 1991) .

The dramatic growth of large cities and populations after the 19th century led to increased demands for fixed nitrogen. This demand led to the beginning of the nitrogenous fertilizer industry. Several commercial nitrogen-fixation processes were developed like the Birkeland-Eyde process, the Frank-Caro Cyanamide process and the Serpak process (Ernst, 1928; Vancini, 1971; Appl, 1976). Currently, the industrial

production of ammonia-based fertilizer employs only the Haber-Bosch process (Leigh, 1981), which requires both high temperature (ca. 350^{o}C) and pressure (ca. 400 atm). In the presence of a catalyst composed of finely divided iron plus Mo, K and Al oxides, N_2 and H_2 combine to produce ammonia. However, the current use of commercial fertilizer poses a potential hazard to natural ecosystems due to run-off of the fertilizer into ground waters. Another shortcoming is its high cost and sophisticated industrial installation.

Thus, biological nitrogen fixation has become a major topic of research in attempts to find complementary processes for producing fixed nitrogen. Biological nitrogen fixation is confined to prokaryotic microorganisms, i.e., those without an organized nucleus, namely Eubacteria (including cyanobacteria and actinomycetes) and Archaea. Such bacteria can be either free livers, like ***Azotobacter*** and ***Clostridium***, or can form symbiotic associations with higher plants, such as the ***Rhizobium***-legume system. Because many of these legume systems, like beans and peas, are basic foods, biological nitrogen fixation has obvious significance in agriculture. A better understanding of the molecular mechanism of biological nitrogen fixation should also prove valuable in attempts to simulate the N_2-fixation activity of bacteria in purely chemical systems.

1.2. Nitrogenase

Biological nitrogen fixation in bacteria is carried out by the enzyme called nitrogenase. It is well established that the enzyme responsible for nitrogen fixation can exist in three different forms: a Mo- and Fe-containing form called Mo-nitrogenase; a V- and Fe-containing form called V-nitrogenase (Robson et al., 1986; Hales et al., 1986); and a third form, called nitrogenase-3 (Chisnell, 1988), which may only contain Fe. All three nitrogenases consist of two separable proteins called Component 1 (or the MoFe, VFe or FeFe protein) and Component 2 (or the Fe protein). Component 2 acts

as a specific electron donor to Component 1, where substrates are reduced. Little is currently known about nitrogenase-3, however, the Component 1 proteins of both the Mo- and V- nitrogenases appear to be very similar. Both proteins contain two types of metal-containing prosthetic groups; these are the cofactor clusters (FeMo-cofactor and FeV-cofactor, respectively; Shah and Brill, 1977; Smith et al., 1988), which constitute the substrate-binding and -reduction site (Hawkes et al., 1984; Scott et al., 1990; 1992), and the P clusters (Zimmermann et al., 1978), which appear to be involved in the initial acceptance of electrons from Component 2 (Dean et al., 1990). The amino-acid sequence of the two polypeptide subunits of the Component 1 proteins, for example, from ***Azotobacter vinelandii*** (Joerger et al., 1989)**,** are highly homologous. Magnetic circular dichroism (Morningstar et al., 1987) and X-ray absorption spectroscopic studies (Arber et al., 1987; George et al., 1988; Arber et al., 1989; Chen et al., 1993) of the two cofactors have revealed only minor differences. The V-nitrogenase and nitrogenase-3 will not be discussed further in this thesis because they are not part of author's research interest.

Both component proteins of Mo-nitrogenase, the molybdenum-iron protein (MoFe protein) and the iron protein (Fe protein) contain non-heme iron and acid-labile sulfur. Physiologically, Mo-nitrogenase catalyzes the six-electron reduction of one molecule of N_2 to give two molecules of ammonia with the concurrent transfer of two electrons to protons to produce H_2. This overall eight-electron reaction is coupled to the hydrolysis of 16 molecules of MgATP. The nitrogenase-catalyzed nitrogen-fixation reaction can be described as shown below:

$$N_2 + 8H^+ + 8e^- + 16\ MgATP = 2\ NH_3 + H_2 + 16\ MgADP + 16\ Pi$$

Mo-nitrogenase can also catalyze the reduction of other substrates like C_2H_2, N_3^-, CN^- and so on.

1.2.1. Iron Protein (Fe protein)

Encoded by ***nifH*** gene, the iron protein (Fe protein) is a γ_2 homodimer with its two identical subunits bridged by a single 4Fe-4S cluster. The molecular mass of all Fe proteins is around 60,000 Daltons (Dean and Jacobson, 1992). The Fe protein from ***Azotobacter vinelandii*** was crystallized with diffraction quality material being obtained (Rees and Howard, 1983). The crystal structure of this iron protein has been determined at 2.9 A^o resolution (Georgiadis et al., 1992). The quarternary structural arrangement of the Fe protein shows both identical subunits folded as a single α/β-type domain and bridged at one surface by the 4Fe-4S cluster. A ribbons diagram is shown as Figure 1-1. The overall shape of Fe protein has been described as an “iron butterfly” with the 4Fe-4S cluster being the head. An eight β-sheet (with seven of the eight β strands oriented in parallel fashion), flanked by nine α helices, is found at the core of each subunit. This general type of fold is a common structure for nucleotide-binding proteins. The 4Fe-4S cluster is symmetrically coordinated by four cysteinyls. These are Cys-97 and Cys-132 from each subunit, which confirmed the prediction of chemical modification, genetics and spectroscopic studies (Hausinger et al., 1983; Meyer et al., 1988; Howard et al., 1989).

Two other residues of the Fe protein, which have been identified as interacting with the MoFe protein, namely Arg-100 and Glu-112, are located on the same “top” surface of Fe protein as the 4Fe-4S cluster. ADP-ribosylation of one Arg-100 residue results in blocking productive complex formation between the Fe protein and the MoFe protein (Pope et al.,1985; Murrell et al., 1988). The interaction between the Fe protein and the MoFe protein is sensitive to substitution of Arg-100, which has been interpreted as indicating that this residue is involved in a salt bridge to the MoFe protein (Wolle et al., 1992). Chemical cross-linking studies indicate that Glu-112 is involved in the

Figure 1-1. Ribbon Structure of Fe Protein γ_2 dimer from *A. vinelandi*i Nitrogenase.

This picture was provided by Dr. Jeff Bolin at Purdue University.

interaction between the Fe protein and MoFe protein as well (Willing et al., 1989; Willing et al., 1990).

A nucleotide-binding sequence, GXXXXGKS/T (where G is Gly, K is Lys, S is Ser, T is Thr and X represents any amino acid), which is known as Walker's motif A (Walker et al., 1982), is found in Fe protein. This sequence adopts a β strand-loop-α helix structure and the possible involvement of this region in nucleotide binding was first recognized by sequence analysis (Robson, 1984). This suggestion was later confirmed by the crystal structure that this region adopted a β strand-loop-α helix structure with partially occupancy by a bound MgADP molecule (Georgiadis, et al., 1992).

During biological nitrogen fixation, the reduction of dinitrogen by nitrogenase involves a series of three electron-transfer steps. The first step is the reduction of the Fe protein by an electron carrier, such as ferredoxin or flavodoxin; the second step is transfer of a single electron to the MoFe protein; and the third step is the transfer of an electron and a proton to the substrate. This last step is believed to occur at the FeMo-cofactor of the MoFe protein. The first two steps must be repeated because all nitrogenase substrates need at least two electrons to be reduced. Thus, it is necessary for the Fe protein and MoFe protein to undergo a cycle of obligatory association and dissociation of the protein complex. The dissociation step has been identified as rate-determining for the overall reaction (Hageman and Burris, 1978; Thorneley and Lowe, 1983; Thorneley and Lowe, 1984). It is proposed that the Fe protein docks to the MoFe protein with its 4Fe-4S cluster located near to the MoFe-protein's P cluster.

The ability of the Fe protein to bind the nucleotides, MgATP and MgADP, plays a significant role in the association and dissociation of nitrogenase complex. Differences in cluster-chelation behavior provide an insight into the Fe protein-

nucleotide interaction. It was found that α,α'-dipyridyl chelates iron slowly from the Fe-protein in the absence of nucleotides. In the presence of MgATP, however, the iron is readily chelated by α,α'-dipyridyl, whereas in the presence of MgADP, iron chelation is inhibited. The chelation behavior is also sensitive to the oxidation state of the Fe protein(Anderson and Howard, 1984; Deits and Howard, 1989). Thus,, MgATP binding to the Fe protein somehow influences the environment of the 4Fe-4S cluster (Burgess et al., 1993; Yates et al., 1991), even though the binding site for the terminal phosphate is located about 20 A^o away from 4Fe-4S cluster. MgATP binding also lowers the reduction potential, $E^{o'}$, of the 4Fe-4S cluster by about 100 mV (Morgan et al., 1986; Zumft et al., 1974) and changes the rhombic shape of the S = 1/2 EPR signal exhibited by the 4Fe-4S cluster to a more axial shape (Zumft et al., 1972; Smith et al., 1973). The O_2 sensitivity of the Fe protein increases and the CD spectrum of the oxidized Fe protein changes significantly on MgATP binding (Stephens et al., 1982). Thus, MgATP binding appears to induce a long-distance conformational change in the Fe protein. In contrast, although MgADP binding causes the change in both the CD spectrum and reduction potential E^o (Burgess et al., 1983; Morgan et al., 1986; Zumft et al., 1974; Stephens et al., 1982), it is an inhibitor of the chelation reaction (Walker et al., 1973; Walker et al., 1974). Therefore, although MgATP and MgADP appear to bind to the same site on the Fe protein, they have different effects on protein structure. SAXS (small angle x-ray scattering) studies confirm MgATP-induced conformational changes in the Fe protein from ***A. vinelandii*** (Chen et al., 1994). Site-directed mutagenesis studies indicate that Ala-157 is crucial for the Fe protein to establish the electron-transfer-favored conformation induced by MgATP binding (Chen et al., 1994).

The conformational change induced by MgATP binding appears to serve at least three important functions in the mechanism of the nitrogen-fixation reaction. It: (1) allows the Fe protein to dock to the MoFe protein; (2) drives a single electron transfer first to the P cluster (which is a proposed intermediate electron acceptor) and then to the FeMo-cofactor; and (3) leads to the dissociation of the Fe protein from the MoFe

protein (Ryle et al., 1996; Lanzilotta et al., 1996). A signal-transduction pathway from the nucleotide-binding site to the 4Fe-4S cluster was determined as the peptide chain from Asp-125 to Cys-132 and is referred to as Switch II (Ryle et al., 1996).

In summary, the 4Fe-4S cluster, the redox center of the Fe protein, is responsible for accepting and delivering single electrons to the MoFe protein. Binding of MgATP to the Fe protein and its subsequent hydrolysis is essential for electron transfer. The mechanistic details concerning MgATP hydrolysis, electron transfer and nitrogenase complex association and dissociation are still under intense investigation.

1.2.2. The Molybdenum-Iron (MoFe) protein

The MoFe-protein, also referred to as nitrogenase Component 1, is a $\alpha_2\beta_2$ tetramer with total molecular mass of 230 KDa. The α subunit is encoded by the ***nifD*** gene and the β subunit is encoded by ***nifK*** gene. In ***A. vinelandii***, the subunits have molecular masses of ca. 55,000 Da and 59,000 Da, respectively. The MoFe protein contains two Mo atoms, 30 Fe atoms and 32 acid-labile sulfides, which are organized into two types of metallocluster, the P Cluster and the FeMo-cofactor. Based on the crystal structure of the MoFe protein from ***A. vinelandii***, the α- and β- subunits in the $\alpha_2\beta_2$ tetramer have similar polypeptide folds. A ribbon diagram of the ***A. vinelandii*** oxidized state MoFe protein $\alpha_2\beta_2$-subunit tetramer is shown in Figure 1-2. The individual α and β subunits of the ***A. vinelandii*** MoFe protein consists of 491 and 522 amino acids, respectively (Brigle et al., 1985). Sequence comparisons revealed the similarities between the sequences of the amino-terminal regions of the α and β subunits (Lammers et al., 1983). They also exhibit similar polypeptide folds consisting of three domains (designated as I, II, III, in the α and β subunits, respectively) of the α/β-type (Figure 1-3). The sequence alignment of regions containing conserved Cys (and His)

Figure 1-2. Ribbon diagram of *A. Vinelandii* MoFe Protein $\alpha_2\beta_2$ tetramer. The picture was provided by Dr. Jeff Bolin at Purdue University.

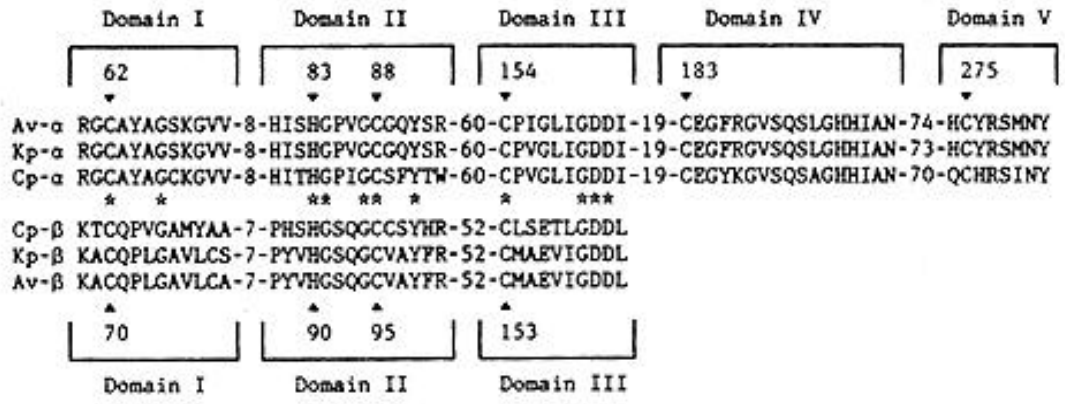

Figure 1-3. Alignment of interspecifically conserved Cys residues from the MoFe Protein α- and β-subunits from *A. vinelandii* (Av), *K. pneumoniae* (Kp), and *C. pasteuriaum* (Cp).

Cys Residues which are conserved in both subunits are indicated by black dot. Numbers refer to the A. vinelandii sequence. The ***A. vinelandii*** MoFe protein α- and β-subunits have 492 and 523 residues, respectively. Domain I, II, III are targeted as potential P-cluster environments and domain IV, V are targeted as FeMoco environments.

residues from the MoFe protein α and β-subunits of several species is shown in Figure1-3. Each subunit contains a wide shallow cleft between the three domains. The FeMo-cofactor occupies the bottom of the cleft in the α subunit. The site in the β-subunit corresponding to the location of the FeMo cofactor in the α-subunit contains the side chains of residues β-His-193, β-Gln-294, β-His-297 and β-Asp-372. There are extensive contacts between the pairs of α- and β-subunits, especially in the region surrounding the P cluster that bridges domain I of the α- subunit and domain I' of the β- subunit. The α- and β subunit are roughly related by a 2-fold rotation axis that passes through the P cluster (Kim and Rees, 1992).

1.2.3. Environments of MoFe Protein Metal Clusters

In 1979, Kurtz et al. (1979) found that about 16 Fe atoms can be extracted from each MoFe protein molecule as approximately four 4Fe-4S clusters by treatment of the native protein with thiols in a denaturing organic solvent. These protein-bound Fe-S clusters are called P cluster because of their covalently protein-bound nature (Zimmerman et al., 1978). Whereas the redox and spectroscopic properties were thought to be compatible with their formation as four 4Fe:4S clusters, the spectroscopic properties of the P cluster are very unusual. It was later proposed that P clusters exist as two 8Fe-8S clusters (Hagen et al., 1985) and supported by X-ray anomalous diffraction data, which indicated that the Fe atoms of the P cluster were associated with just two regions of high electron density in the tetramer (Bolin et al., 1990). X-ray crystallographic studies established a model in which each P cluster contains two 4Fe-4S sub-clusters that share a common sulfide. These sub-clusters are also bridged by the thiolate S of two cysteinyl residues (from α-Cys-88 and β-Cys-95), each of which, therefore, coordinately binds to two iron atoms. The remaining 4 Fe atoms, two in each sub-cluster, are ligated by singly coordinating cysteinyl

thiolates (from α-Cys-62, α-Cys-154, β-Cys-70 and β-Cys-153). The β-Ser-188 residue is also involved in P cluster binding. Thus, it was found that P-cluster of the MoFe protein ***from A. vinelandii*** contains only 7 S atoms instead of 8 (Peters, et. al, 1997) (Figure 1-4).

The protein environment around the P cluster is mainly provided by hydrophobic residues, including α-Tyr-64, α-Pro-85, α-Tyr-91, α-Pro-155, α-Phe-186, β-Pro-72, β-Phe-99, β-Tyr-98, β-Met-154 and β-Phe-189. Hydrophilic residues around the P cluster, namely α-Glu-153, α-Glu-184 and α-Ser-92, are not conserved. The strictly conserved Gly residues (α-Gly-87, β-Gly-94 and α-Gly-185) are structurally important for the P cluster's function. For example, substitution of α-Gly-185 with Asp results in a mutant with a Nif^- (non-nitrogen-fixing) phenotype (Kim and Rees, 1992).

The FeMo-cofactor, first identified by Shah and Brill (1977), is believed to be the substrate-binding and substrate-reduction site on the MoFe protein (Hawkes et al., 1984; Scott et al., 1990; 1992). Two FeMo-cofactors exist in each MoFe protein molecule. Each FeMo-cofactor contains two sub-clusters, which have the compositions of 4Fe:3S and Mo:3Fe:3S, respectively, and are bridged by three non-protein sulfide ligands (Figure 1-5). As an essential component of FeMo-cofactor (Hoover et al., 1987; 1989), homocitrate is coordinated to the Mo through one hydroxyl oxygen and one carboxyl oxygen (Kim and Rees, 1992; Chan et al., 1993). The FeMo-cofactor is buried at least 10 A^o below the protein surface (Kim and Rees, 1992).

Around the FeMo-cofactor environment, the residues α-Cys-275, α-His-442 and α-Ser-278 are strictly conserved. The residues, α-Gly-356 and α-Gly-357, which are required to avoid steric interference with the FeMo-cofactor, are also conserved. Residues, α-Arg-96 and α-Arg-359, which can potentially form hydrogen bonds to

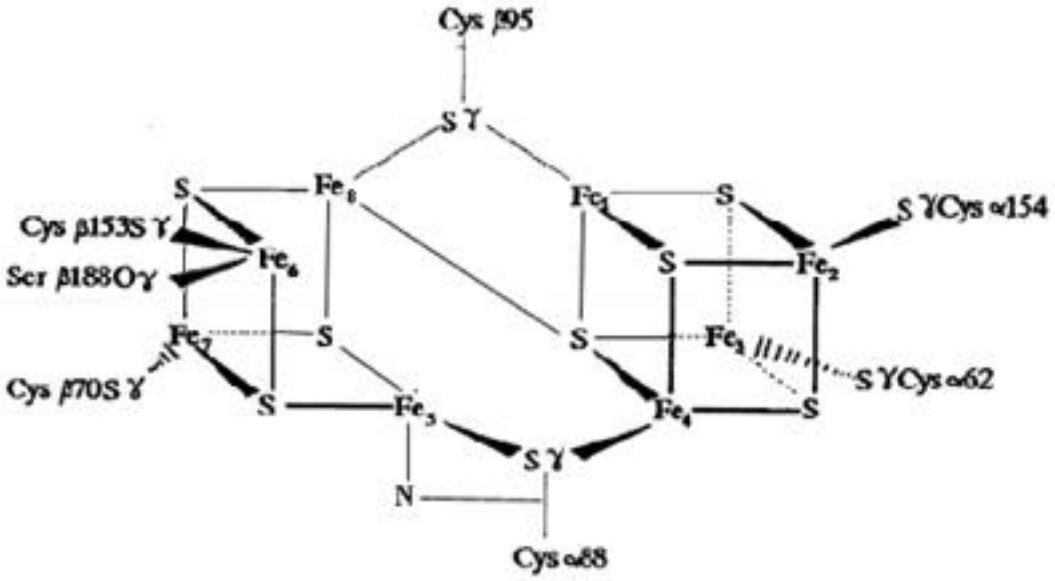

Figure 1-4. Schematic representation of the oxidized state P-cluster model.

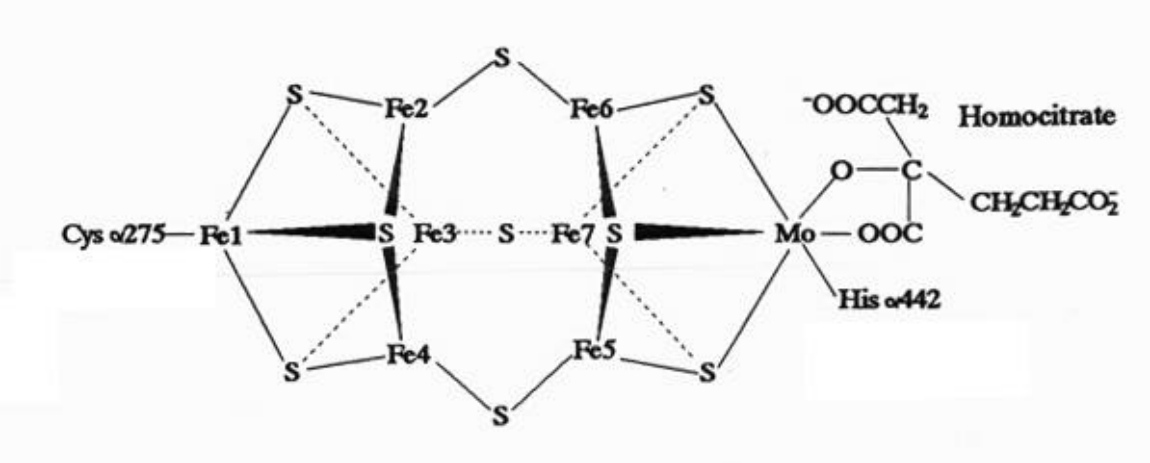

Figure 1-5. Schematic representation of the FeMoco model (Adapted from Kim and Rees, 1992a).

cluster sulfides of FeMo-cofactor, may serve to stabilize the FeMo-cofactor and the partially reduced intermediates formed during substrate reduction. α-His-195 may function in the proton-transfer reaction. α-Gln-191, α-Gln-440 and α-Glu-427 are near the homocitrate and interact with this group either directly or indirectly through water molecules. FeMo-cofactor is buried in a hydrophobic protein environment formed by α-Tyr-229, α-Ile-231, α-Val-70, α-Phe-381, α-Leu-358 and α-Ile-355. Only two residues directly ligate to the FeMo cofactor; α-Cys-275 coordinates Fe1, whereas α-His-442 coordinates the Mo atom (Kim and Rees, 1992). The side chains of α-Arg-96 and α-His-195 and the NH groups of α-Gly-356 and α-Lys-358 form hydrogen bond to sulfides of the FeMo-cofactor and may provide a channel for protons to be transferred to substrate bound to the FeMo-cofactor (Howard and Rees, 1994).

1.2.4. Functions of the Metalloclusters

The function of the two metallocenters is believed to be as redox centers, which mediate electron delivery from the Fe protein to substrate. Mutagenesis studies (Peters et al., 1995b; May et al., 1991) and kinetic measurements (Lowe et al., 1993) provide indirect evidence that P clusters serve as an intermediate in electron transfer from the 4Fe-4S cluster of the Fe protein to the FeMo-cofactor at the substrate-reduction site. Studies of the redox properties of the P cluster, employing Mossbauer spectroscopy, indicated that, in the dithionite-reduced MoFe protein (in its native state; P^N), all of its iron atoms were in the ferrous state (Surerus et al., 1992). No more-reduced forms of the P cluster are detectable, but some oxidized forms have been identified, including a two electron-oxidized form designated as P^{OX} (Zimmerman et al., 1978), which can be reversibly generated from P^N state. The P cluster in each of the redox states is found to contain 8 Fe and 7 S atoms. The interconversion of between two redox states causes movement of two of the Fe atoms and an exchange of protein-based coordination by ligation supplied by the central S atom. In the P^{ox}

state, the P cluster is coordinated by the protein through the thiolates of six cysteinyl ligands, the O_γ of β-Ser-188 and the backbone amide of α-Cys-88; whereas in the native P^N state, β-Ser-188 and the amide N of α-Cys-88 no longer coordinate the cluster due to the movement of their coordinated Fe atoms toward the central sulfur. This redox-mediated structural change of the P cluster implies a role for the P-cluster in coupling electron transfer and proton transfer in nitrogenase (Peters et al., 1997).

The FeMo-cofactor exhibits a biologically unique S=3/2 electron paramagnetic resonance (EPR) signal in its as-isolated semi-reduced form (native form; M^N) within the MoFe protein. However, the isolated FeMo-cofactor has a considerably broader line shape (Rawlings et al., 1978; Figure 1-6). This result indicates that the polypeptide environment of FeMo-cofactor affects its spectroscopic features.

Mutant strains in which the ***nifE***, ***nifN*** or ***nifB*** genes have been disrupted fail to synthesize FeMo-cofactor and lack both catalytic activity and S=3/2 EPR signal (Shah and Brill, 1977; Shah et al., 1973; Paustian et al., 1990). The catalytic activity and EPR signal can be recovered by the addition of FeMo-cofactor extracted from wild type. The electron paramagnetic resonance (EPR) spectra of both the MoFe protein of wild type nitrogenase from ***A. vinelandii*** and isolated FeMo-cofactor in NMF (***N***-methylformamide) are shown in Figure 1-6. The correlation of the presence of FeMo-cofactor with both catalytic and spectroscopic features of the MoFe protein provided the first evidence that the FeMo-cofactor is located at or is part of the substrate-reduction site (Newton and Dean, 1993).

Certain mutant strains, which have a defective ***nifV*** gene, produce an altered form of FeMo-cofactor with homocitrate replaced by citrate (Hawkes et al., 1984) because these $NifV^-$ mutant strains are not able to synthesize homocitrate. The MoFe protein purified from these mutant strains has the properties of decreased N_2-fixation capacity and CO-sensitive proton reduction (see later; McLean and Dixon, 1981; Hawkes et al.,

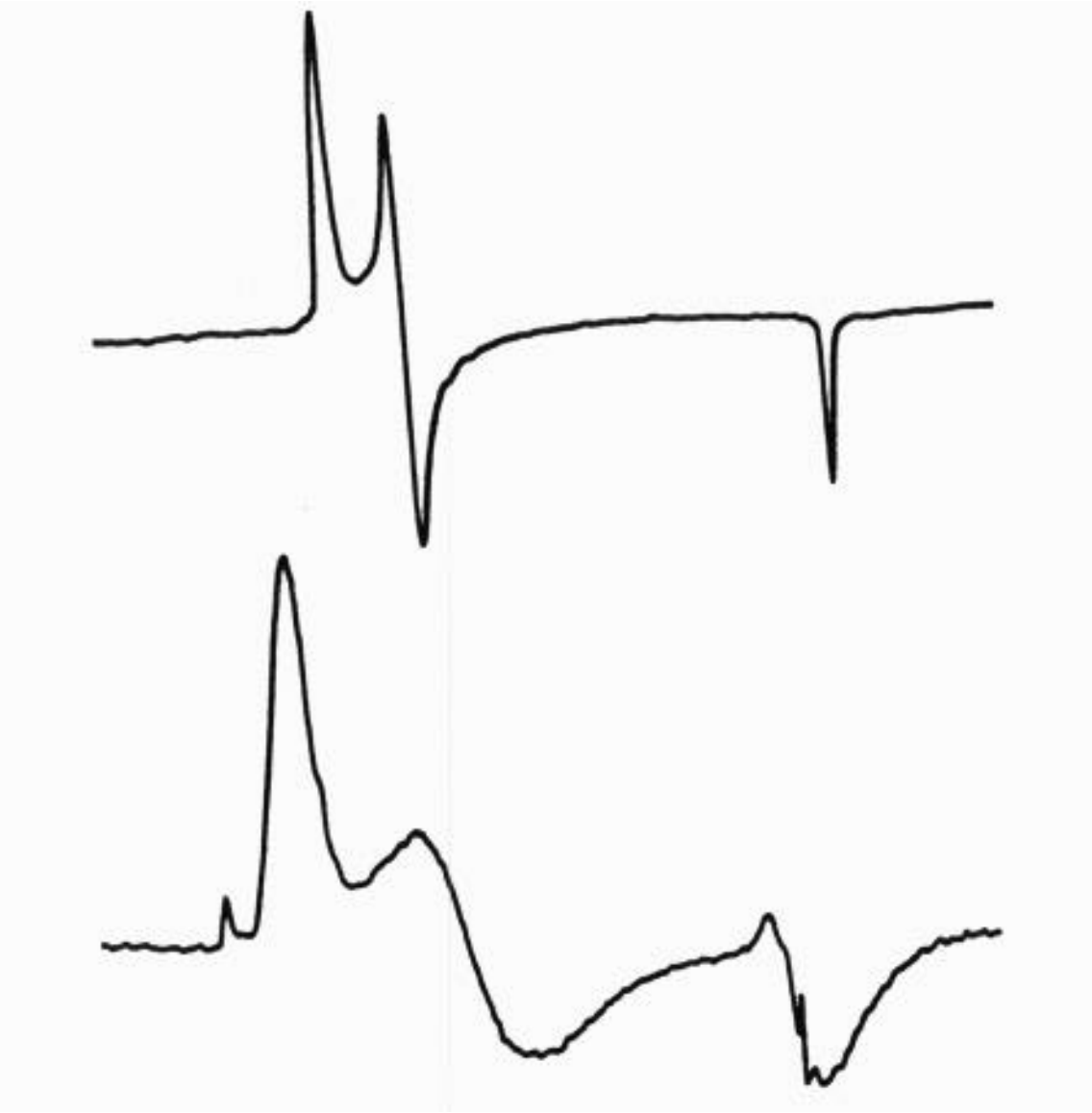

Figure 1-6.Comparision of S=3/2 EPR signals of protein-bound FeMoco (g=3.65, 4.34) (top); and of isolated FeMoco (g=3.3, 4.7) (bottom) at 13K (Adapted from Newton and Dean, 1992).

1984). The MoFe protein produced by a $NifV^+$, but FeMo-cofactor deficient, mutant strain can be reconstituted by FeMo-cofactor prepared from the $NifV^-$ mutant strain. The resulting MoFe protein has altered catalytic properties exactly like MoFe protein from the $NifV^-$ mutant. This result suggested that the properties of the $NifV^-$ mutant are the consequence of a defective FeMo-cofactor (Hoover et al., 1987; 1989). Taken together, all evidence points to a reasonable suggestion that FeMo-cofactor is at the substrate-reduction site. However, efforts to reduce substrates using extracted FeMoco have either failed or been equivocal (Newton, et al,1992; Burgess, 1990; Shah et al., 1978; McKenna et al., 1979), indicating again that the polypeptide environment of FeMo-cofactor must have one or more critical functions in effecting substrate binding and reduction (Newton and Dean, 1993).

1.3. The Genetic Organization of the *nif* Genes.

The genes, which encode nitrogenase and related proteins, are called ***nif*** genes. The early work concerning the identification of N_2-fixation genes centered mainly on ***Klebsiella pneumoniae***, because ***K. pneumoniae*** was the only diazotrophic organism amenable to the application of the classical bacterial genetic manipulations developed for ***Escherichia coli***. Twenty ***nif***-specific genes have been identified in ***K. pneumoniae*** by genetic complementation experiments, biochemical reconstitution studies and in ***vivo*** DNA-directed expression studies (Arnold et al., 1988; Beynon et al., 1988; Denefle et al., 1987; Elmerich et al., 1978; Houmard et al., 1980; MacNeil et al., 1978; Merrick, 1980; Paul et al., 1987; Puhler et al., 1980; Riedel et al., 1979; Roberts et al., 1980; Roberts et al., 1978). Nucleotide sequences are now available for all these genes: ***nifJ*** (Arnold et al., 1988; Cannon et al., 1988) , ***nifH*** (Arnold et al., 1988; Scott et al., 1981; Sundaresan and Ausubel, 1981); ***nifD*** (Arnold et al., 1988; Scott et al., 1981; Ioannidis et al., 1987); ***nifK*** (Arnold et al., 1988; Holland et al., 1987; Steinbauer et al., 1988); ***nifT*** (Arnold et al., 1988; Beynon et al., 1988); ***nifY*** (Arnold et al., 1988; Beynon et al., 1988), ***nifE, nifN, nifX*** (Arnold et al., 1988; Setterquist et al.,

1988); ***nifU, nifS, nifV*** (Arnold et al., 1988; Beynon et al., 1987); ***nifW*** (Arnold et al., 1988; Beynon et al., 1988; Paul et al., 1987); ***nifZ, nifM*** (Arnold et al., 1988; Paul et al., 1987); ***nifF*** (Arnold et al., 1988; Drummond, 1985); ***nifL*** (Arnold et al., 1988; Drummond and Wootton, 1987); ***nifA*** (Arnold et al., 1988; Drummond, 1986; Buikema, 1985); and ***nifB, nif Q*** (Arnold et al., 1988; Buikema, 1987) .

These genes are organized into 8 transcription units as shown in Figure 1-7. Two of these, which are contained within the ***nifUSVWZM*** gene cluster, appear to overlap. The ***nifJ*** gene has not been found in ***Azotobacter vinelandii*** and a dozen more open reading frames (designated as ORF1 and so on; refer to Figure 1-7 for details) are scattered within the ***Azotobacter nif*** cluster. The function of many of their products remains unclear. Because the ***nifJ*** gene is a pyruvate:flavodoxin oxidoreductase and is essential for nitrogen fixation in ***K. pneumoniae***, it is proposed that there must be another, as yet unidentified, ***nif*** gene product that serves a similar role in electron transfer to ***Azotobacter*** nitrogenase (Martin et al., 1989).

Various aspects of structure and function of the ***nif***-specific gene products for both ***A. vinelandii*** and ***K. pneumoniae*** are summarized in Table 1-1.

1.4. Site-directed Mutagenesis Studies

1.4.1. Effect of Amino-Acid Substitution in the Immediate P-Cluster Environment

The primary sequences of the MoFe protein α- and β-subunits from different species reveal the presence of five conserved cysteinyl residues, α-Cys-62, α-Cys-88, α-Cys-154, α-Cys-183 and α-Cys-275, in the α subunit and three, β-Cys-70, β-Cys-95 and β-Cys-153, in the β subunit (Mazur and Chui, 1982; Lammers and Haselkorn, 1983; Kaluza and Hennecke, 1984; Weinman et al., 1984; Brigle et al., 1985; Thony et al.,

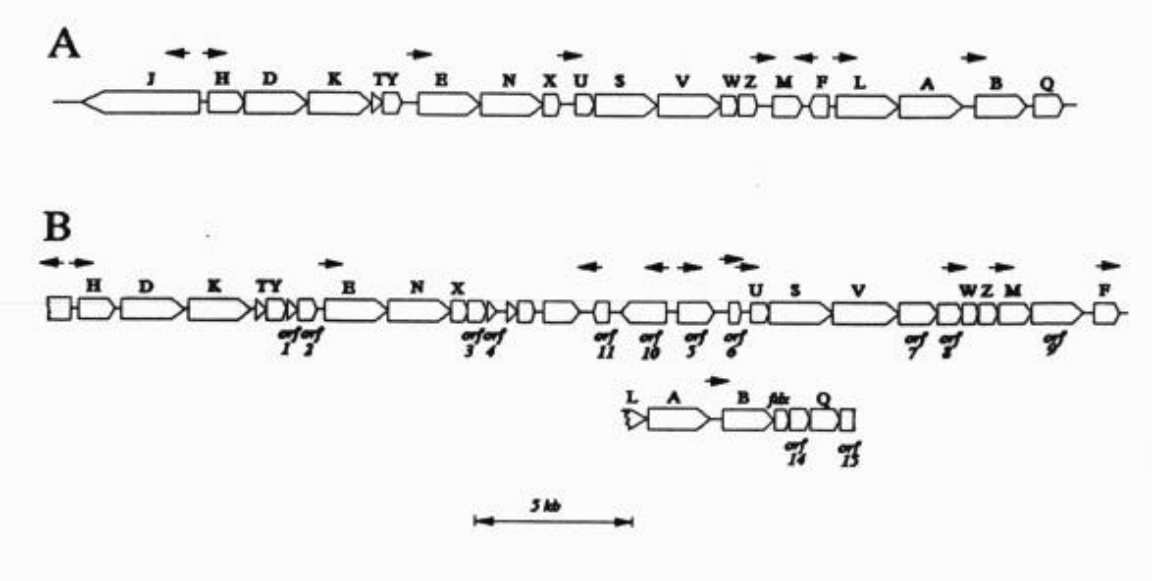

Figure 1-7. Comparision of the physical organization of nif genes from (A) *K. pneumoniae* and (B) *A.vinelandii* (Adapted from Dean and Jacobson, 1992).

Table 1-1 *nif* gene products and their known or proposed functions in *A. vinelandii*

Gene	Product and Known or Proposed Function
nifH	Fe protein subunit, forms homodimer (M_r=63,000), has a single [4Fe-4S] cluster bridged between the two subunits, required for FeMoco biosynthesis
nifD	MoFe protein α-subunit, forms the MoFe protein holoprotein with β-subunit as $\alpha_2\beta_2$ tetramer (M_r=230,000), 2 P clusters and 2 FeMocos
nifK	MoFe protein β-subunit, forms the MoFe protein apoprotein with α-subunit as $\alpha_2\beta_2$ tetramer (M_r=230,000), 2 P clusters and 2 FeMocos
nifF	Flavodoxin, physiological reductant of the Fe protein
nifE	Required for the FeMoco biosynthesis, forms $\alpha_2\beta_2$ tetramer (M_r=210,000) with the *nifN* gene product, exhibits a fair level of sequence identity when compared to the MoFe protein α-subunit
nifN	Required for the FeMoco biosynthesis, forms $\alpha_2\beta_2$ tetramer (M_r=210,000) with the *nifE* gene product, exhibits a fair level of sequence identity when compared to the MoFe protein β-subunit
nifB	Required for the FeMoco biosynthesis
nifQ	Involved in the FeMoco biosynthesis, possibly in forming the $MoFe_3S_3$ in the FeMoco, the *nifQ* (defective in FeMoco synthesis) can be suppressed by elevated levels of Mo, cysteine or cystine[a]
nifU	Stabilization of the Fe protein, possibly involved in providing Fe for nitrogenase metallocluster synthesis[b]
nifS	L-cysteine desulfurase, involves in donating inorganic sulfide for nitrogenase metallocluster synthesis[b]
nifV	Homocitrate synthase, synthesis of the organic component of FeMoco
nifW	Function not known, might be involved in processing homocitrate[c]
nifZ	Function not known, required for full activity of the MoFe protein, might have a function related to FeMoco formation or insertion[c]
nifM	Required for Fe protein activation[d]
nifA	Positive regulatory element
nifL	Negative regulatory element
nifX	A possible negative regulatory element[e]
nifT	Function not known, not required for diazotrophic growth[e]
nifY	Function not known, not required for diazotrophic growth, possibly involved in stabilizing the conformation of apo-MoFe protein for FeMoco insertion[e]

(This table is adapted from Shen, 1994)

[a] Ugalde et al,. 1985; Joerger& Bishop, 1988. [b] Jacobson et al., 1989; Miller & Orme-Johnson, 1992; Zheng et al., 1993. [c] Jacobson et al., 1989; Paul& Merrick, 1989. [d] Howard et al., 1986; Jacobson et al., 1989; Paul & Merrick 1989. [e] Gosinl et al., 1990; White et al., 1992; Homer et al., 1993.

1985; Holland et al., 1987; Ioannidis and Buck,1987; Arnold et al., 1987; Steinbauer et al., 1988; Wang et al., 1988; Rawlings et al., 1989). The alignment of inter-specifically conserved Cys residues from the MoFe protein α- and β-subunits from ***A. vinelandii***, ***K. pneumoniae*** and ***Clostridium pasteurianum*** is shown in Figure 1-3. The x-ray crystal structure (Kim and Rees, 1992) confirms the prediction (Brigle et al., 1985; Dean et al., 1990) that the residues, α-Cys-62, α-Cys-88, α-Cys-154, β-Cys-70, β-Cys-95 and β-Cys-153 serve as ligands to the P cluster.

Individual substitution of Ser for α-Cys-62, α-Cys-154, β-Cys-70 or β-Cys-95 of the ***A. vinelandii*** MoFe protein shows that these residues are essential for nitrogen-fixation activity (Dean et al., 1990). However, the substitution by Asp for β-Cys-95 results in a diazotrophically viable mutant strain, although both its fixation and diazotrophic-growth rates are slower than wild type. Studies of this last mutant stain constitute the body of the author's research, which is described in subsequent chapters. Also, substitution by Asp, Thr or Gly for α-Cys-88 decreased its nitrogenase activity, but still allowed the mutant strain to grow diazotrophically (J.S. Cantwell, Ph. D. Thesis, Virginia Tech, 1998). Substitution of β-Cys-153 with Ser does not significantly decrease the diazotrophic growth rate for either ***A. vinelandii*** or ***K. pneumoniae*** mutants (Dean et al., 1988; Kent et al., 1989; May et al., 1991).

1.4.2. Effect of Amino-Acid Substitutions of α-Gln-191 and α-His-195.

The FeMo-cofactor biosynthetic gene products, NifEN, form a tetrameric scaffold (resembling the ***nifDK*** gene products) on which FeMo-cofactor is biosynthesized (Brigle et al., 1987; Paustian et al., 1990). The immature FeMo-cofactor must escape from this NifEN scaffold to the NifDK tetramer to form the mature MoFe protein. Thus, the domains that harbor the FeMo-cofactor within each of these tetramers are likely to

be structurally related to each other. Within the α-subunit, this domain encompasses α-Gln-191 and α-His-195 residues, which are highly conserved. This theoretical rationale formed the original basis in a site-directed mutagenesis strategy that targeted the α-Gln-191 and α-His-195 residues (Scott et al., 1990).

Two mutant strains with either α-Gln-191 substituted by Lys or α-His-195 substituted by Asn were constructed based on the presence of these substituting residues at corresponding positions in the ***nifE*** gene product (Figure 1-8). Both mutants lost their capability for diazotrophic growth (Scott et al., 1990; Scott et al., 1992; Kim et al., 1995). However, both strains exhibit S=3/2 EPR signals that, although different both to wild-type and to each other, suggests that the global structure of both altered MoFe proteins is not dramatically affected. The altered MoFe proteins from both strains are still able to catalyze the reduction of acetylene and protons but at a slow rate. Amazingly, these altered nitrogenases also show a change of catalytic specificity by directing 15-40% of their electron flux to reduce acetylene by four electrons to ethane (Scott et al., 1990; Scott et al., 1992). This catalytic property had been suggested as a characteristic of vanadium-dependent nitrogenase (Dilworth et al., 1987; Dilworth et al., 1988), however, the V-nitrogenase and these altered Mo-nitrogenases do not share the same catalytic mechanism (Scott et al., 1992).

Further studies on the purified α-Lys-191 MoFe protein showed that its H_2-evolution behavior is also changed. First, 91% of the electron flux under 10% acetylene produces H_2 compared with only 10-15% for wild-type. Second, unlike wild type, addition of 1-10% CO to an argon, N_2 or 10% acetylene atmosphere inhibits H_2 evolution by about 65%, whereas addition of CO has no inhibitory effect on H_2 evolution by wild type (Scott et al., 1992).

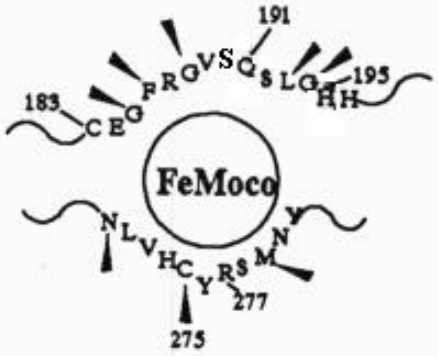

MoFe Protein α-subunit

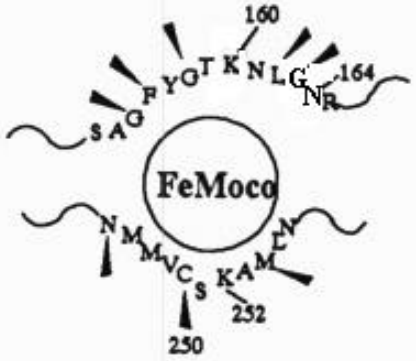

nifE Product

Figure 1-8 Schematic representation of FeMoco binding within the proposed α-subunit (α-183-Cys and α-275-Cys region) and the corresponding region in the *nifE* gene product which is proposed for FeMoco biosynthesis (Adapted from Dean and Jacobson, 1992). Arrow heads indicate the conserved residues within the corresponding area of both *nifE* gene product and the MoFe protein α-subunit.

A similar phenomenon was encountered previously with the NifV$^-$ MoFe protein in which an integral component of the FeMo-cofactor, homocitrate, is not incorporated. Homocitrate is an organic entity that plays an important role in directing the MoFe protein's substrate-reduction and inhibitor-susceptibility properties(McLean et al., 1981; Hoover et al., 1987; Hoover et al., 1988; Imperial et al., 1989). Homocitrate has been shown to be coordinated to the Mo atom of the FeMo-cofactor (Kim and Rees, 1992) with one of its uncoordinated terminal carboxylates involved in hydrogen bonding to α-Gln-191. Thus, the effect of substitution of α-Gln-191 on the properties of the FeMo-cofactor may be mediated by homocitrate (Figure 1-5).

N-ligation of protein-bound FeMo-cofactor, as demonstrated by a pulsed EPR technique called Electron Spin Echo Envelope Modulation spectroscopy or ESEEM, was shown to be affected by substitution at the α-subunit residue, His-195, as was the ability to fix N_2 (Thomann et al., 1991; Kim et al., 1995; DeRose et al., 1995). However, α-His-195 is not directly coordinated to any constituent atom of the FeMo-cofactor but is close enough to be hydrogen bonded to one of FeMo-cofactor's central bridging sulfides (Kim and Rees, 1992). All substitutions at α-His-195 were reported to result in a Nif$^-$ phenotype (Kim et al., 1995**)**, although recent work has shown that the α-Gln-195 MoFe protein reduces N_2 to ammonia but at only 1-2% of the wild-type rate (Dilworth et al., unpublished results). It was found that, when Thr substitutes for α-His-195, catalyzed H_2 evolution under argon is about 50% inhibited by addition of 10% CO and 25% inhibited under an 100% N_2. In contrast, with the α-Gln-195 MoFe protein, H_2 evolution is insensitive to the presence of CO but is significantly (about 65%) inhibited by N_2 and this inhibition is reversible (Kim et al., 1995). Thus, the α-His-195 residue is not absolutely required for N_2 binding but it may play a significant role in N_2 reduction. Furthermore, MgATP hydrolysis is uncoupled from electron transfer in the α-Gln-195 nitrogenase under 100% N_2 where a ratio of about 20 MgATP

hydrolyzed per electron pair transferred is measured versus about 5 for wild type. The addition of CO can relieve the N_2-induced inhibition of H_2 evolution. Acetylene reduction to ethylene in this strain is also inhibited by N_2 in a competitive manner (K_i=0.22atm). Taken together, these data suggest that all these effects are occurring on a single site , which cannot reach the oxidation-reduction level required to reduce N_2 effectively (Newton and Dean, 1993; Kim et al., 1995).

1.4.3. Effect of Amino-Acid Substitutions around the α-Cys-275 Residue of the MoFe protein.

Isolated FeMo-cofactor (Shah and Brill, 1977) is reported to be reactive to a variety of chemical reagents, including thiols, EDTA, ***o***-phenanthroline, α,α'-bipyridyl and CN^- (Rawlings et al., 1978; Burgess et al., 1980; Smith, 1985). Phenylthiol reacts with isolated FeMo-cofactor in a 1:1 stoichiometry, which is interpreted to indicate that the FeMo-cofactor is bound to its polypeptide matrix by only one cysteinyl residue (Brigle et al., 1985; Burgess et al., 1985). NMR and x-ray absorption spectroscopy studies (Masharak et al., 1982; Newton et al., 1985) on isolated FeMo-cofactor clearly show that the thiol-binding site is an Fe atom and not the Mo atom. Before the crystal structure of the MoFe protein became available, the responsible cysteinyl-coordinating residue was proposed to be α-Cys-275 based on both amino-acid sequence comparisons and site-directed mutagenesis studies (Brigle et al., 1985; Newton and Dean, 1993). This suggestion was supported by the fact that the α-subunit cysteinyl residues, 62, 88 and 154, and the β-subunit cysteinyl residues, 70, 95 and 153, appeared more likely to be P cluster ligands and because the substitution by either Ser or Ala for α-Cys-275 result in a FeMo-cofactor-deficient "apo-MoFe protein" (Brigle et al., 1985; Brigle et al., 1987).

Substitution at α-275 also increases the pool of accessible FeMo-cofactor in crude extracts of the mutant strains (Kent et al., 1989), which is shown by mixing extracts of α-Ala-275 mutant strain with an extract of a nifB$^-$ mutant (a NifB$^-$ mutant accumulates an inactive “apo-MoFe protein” lacking FeMo-cofactor) to reconstitute an active nitrogenase. The extracts of these mutant strains also exhibit an EPR signal, which is significantly shifted (g values of 4.5 and 3.5 versus the wild-type g values of 4.3 and 3.7) and broadened. These phenomena are simply explained by having the FeMo-cofactor only loosely associated with its altered protein matrix due to the absence of α-Cys-275, whose presence would to help anchor the FeMo-cofactor. This hypothesis is also supported by the observation that altered MoFe proteins with substitutions at α-Cys-275 exhibit an electrophoretic mobility similar to “apo-MoFe protein” (Kent et al., 1990). The α-Cys-275 residues were finally proved by the X-ray crystal structure to be the thiol ligand to Fe1 of FeMo-cofactor (Kim and Rees, 1992).

1.5. Mechanism of Nitrogenase Action.

1.5.1. The Lowe-Thorneley Kinetic Model

A kinetic model of the nitrogenase reaction mechanism has been derived from pre-steady-state kinetic studies (Lowe and Thorneley, 1984a,b; Thorneley and Lowe, 1984a,b). It consists of two major parts: the Fe-protein cycle(Figure 1-9) and the MoFe-protein cycle(Figure 1-10).

The Fe-protein cycle is a redox cycle during which an electron is transferred from the Fe protein to the MoFe protein. The Fe protein is denoted as Av2 in the Lowe-Thorneley Scheme and goes from its reduced Av2(red) state to its oxidized Av2(ox) state. The MoFe protein is denoted as Av1. The Fe-protein cycle consists of five steps:

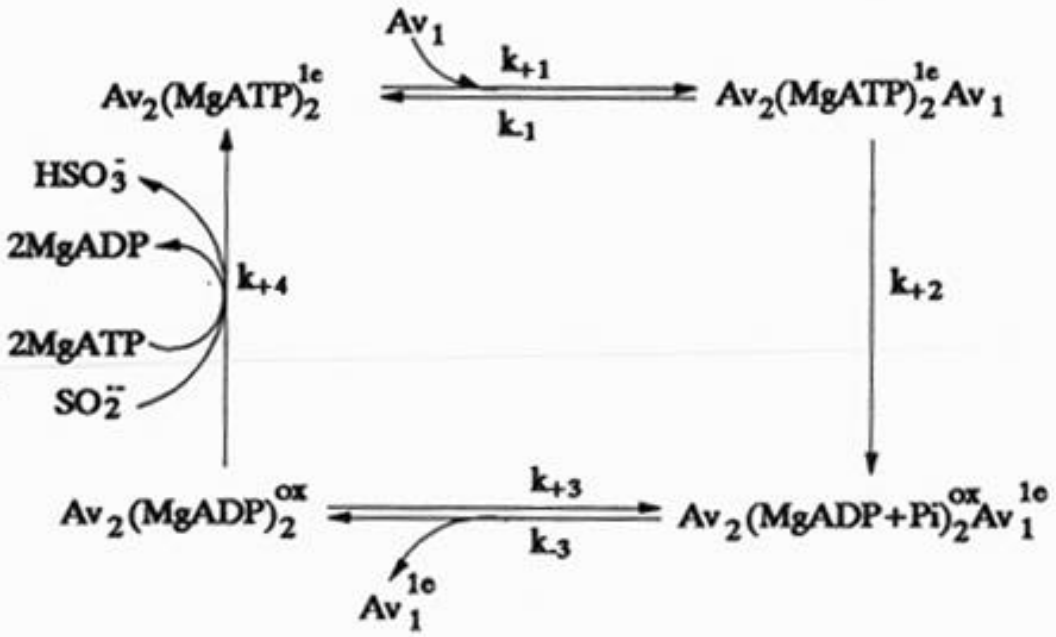

Figure 1-9 Oxidation-reduction cycle for the Fe protein from *A. vinelandii* (Adapted from Thorneley & Lowe, 1985). In the diagram, Av_1 represents the MoFe protein from *A. vinelandii* and Av_2 represents the Fe protein.

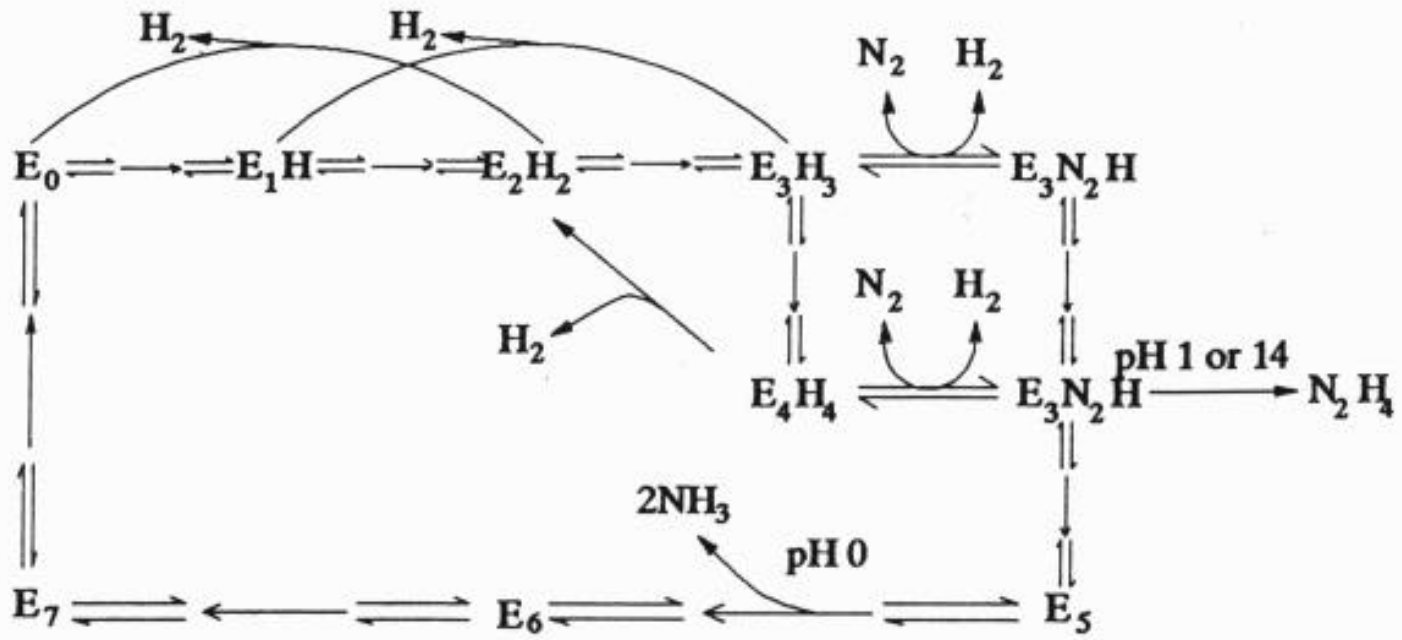

Figure1-10. MoFe-protein cycle. E_n represents Av_1 ($\alpha\beta$ dimer of the MoFe protein), and n refers to the number of times Av_1 completes the Fe protein cycle, which is indicated by the three arrow reactions linking the E_n and E_{n+1}.

1. Av2(ox)$(MgADP)_2$ is reduced by an exogenous electron donor to Av2(red)$(MgADP)_2$;

2. MgADP is then replaced by MgATP;

3. Av2(red)$(MgATP)_2$ complexes with Av1;

4. MgATP hydrolysis is accompanied by electron transfer to Av1; and

5. The complex dissociates into Av1(red) and Av2(ox)$(MgADP)_2$

The MoFe-protein cycle is concerned with the fact that reduction of one N_2 molecule to give two molecules of NH_3 plus one molecule of H_2 is an overall eight-electron process. Therefore, the Fe-protein cycle has to operate eight times to progressively reduce the MoFe protein, which binds and reduces substrate and then finally returns to its highest oxidation state, denoted as E_o. To simplify the situation, this scheme divides the MoFe protein into two equal and independent αβ dimers, each of which is serviced by an Fe protein. The scheme was devised to explain the lag and burst phase of product appearance during substrate reduction and the slowness of the overall process. For example, H_2 production under argon shows a lag phase, the length of which depends on the ratio of Av2 to Av1 (Thorneley and Lowe, 1985). H_2 production under N_2 shows the same lag phase, followed by a burst of H_2 production, before attaining a steady rate. The lag was explained by assuming two slow reduction steps before H_2 was released and the burst was due to rapid replacement of H_2 by N_2 binding. Determination of the rate constants for each of the individual reactions led to the following conclusions.

1. The rate-limiting step (with k = 6.4 sec^{-1}) was the protein-protein dissociation of the complex [Av2(ox)$(MgADP)_2$-Av1(red)] rather than ATP hydrolysis, electron transfer or substrate reduction.

2. The dissociation rate of the [Av2(ox)$(MgADP)_2$-Av1(red)] complex is independent of the oxidation state of the reduced Av1 species.

3. Substrate binding and product release could only occur with uncomplexed Av1.

4. N_2 is bound to a more reduced form of Av1 (probably E_3) than that which could release H_2.

5. The hydrazido(2-) group (=N-NH_2) is a likely bound intermediate, which releases hydrazine on quenching with either acid or alkali, and is probably bound to the MoFe protein in its oxidation state E_4.

6. One molecule of NH_3 may be released at oxidation state E_5, leaving a readily reducible, bound nitride group, which on further reduction, under physiological or assay conditions, yields the second NH_3 molecule and restores the original MoFe protein state of E_0.

7. If the reducing power is low, e.g., at a low Fe protein-to-MoFe protein ratio, then the MoFe-protein state, E_2H_2, which is formed after the two electron and two proton have been transferred to the reduction site, will lose H_2 and revert to state E_0 without reducing N_2. This situation is prevented by having sufficient reductant, MgATP and a large molar excess of the Fe protein over the MoFe protein. Given these conditions, then the reduction of Av2(ox)$(MgADP)_2$ (about 200 sec^{-1}), the rate of MgATP-MgADP exchange on the reduced Fe protein, and the rate of [Av2(red)$(MgATP)_2$-Av1] complex formation will all be considerably faster than the rate-limiting complex dissociation

step. This situation would minimize the steady-state concentration of free Av1 and the state E_2H_2 and so decrease the wasteful production of H_2. However, because the first-order rate constants for MgATP/MgADP exchange and of H_2 loss from E_2H_2 are very similar, it is very important to have a pool of excess Av2(red)$(MgATP)_2$ to complex Av1 at the E_2H_2 state.

8. In contrast, if the reductant concentration is low and the reduction of Av2(ox) $(MgADP)_2$ becomes the rate-limiting step, then the reformation of complex [Av2(ox)$(MgADP)_2$-Av1(red)] could also prevent H_2 evolution. This would have the benefit of "freezing" the E_2H_2 state and thus saving energy.

9. A final requisite of the mechanism is a high concentration of the nitrogenase proteins. Because complex formation [Av2(red)$(MgATP)_2$-Av1], which prevents H_2 release from oxidation state E_2H_2, is a second-order reaction, for the rate to be very much faster than the rate of H_2 release from E_2H_2, the concentration of nitrogenase should be 100 μM. At very low concentration, complex formation rather than dissociation becomes the rate-limiting step.

1.5.2. Factors Affecting Complex Formation by the Nitrogenase Component Proteins and Inter-Protein Electron Transfer.

Substrate reduction by nitrogenase first requires electron transfer in a complex of the Fe-protein and MoFe protein coordinated with the hydrolysis of 2 MgATP/e^- (Hageman and Burris, 1978). The inhibitory effect of salt on nitrogenase activity has been known for sometime (Deits and Howard, 1990; Burns et al., 1985; Wolle et al., 1992). This observation supports the hypothesis that the formation of the nitrogenase complex depends on ionic interactions. Furthermore, ADP-ribosylation of the Arg-100 residue of the Fe protein is reported to block complex formation between Fe protein and MoFe protein (Pope et al., 1985; Murrell et al., 1988). Site-directed mutagenesis studies

(Lowery et al., 1989) also imply that Arg-100 plays an important role in complex formation. Furthermore chemical cross-linking studies show that cross-linking occurs between Glu-112 of Fe protein and the β-Lys-300 on the MoFe protein (Willing and Howard, 1990). The three- dimensional structure of the Fe protein (Georgiadis et al., 1992) shows that Glu-112 and Arg-100 are located on the same protein surface as the 4Fe-4S cluster, thus ensuring the closest possible approach of 4Fe-4S cluster to the MoFe protein. These data all support the hypothesis that ionic interactions contribute to the formation of the active complex.

MgATP binding causes an, as yet, uncharacterized conformational change in the Fe protein that affects the properties of its 4Fe-4S cluster (see earlier) and, further, MgATP hydrolysis occurs only after the Fe protein and MoFe protein form a complex. However, energy transduction, which results from MgATP hydrolysis and phosphate release, does not drive complex dissociation because the dissociation rate of 6.4 sec^{-1} can be measured in the absence of phosphate (Thorneley and Lowe, 1983). It may be that the MgATP-induced conformational change is all that is required for electron transfer from the Fe protein to the MoFe protein. A variety of kinetic studies have indicated that MgATP hydrolysis may precede, follow or occur simultaneously with electron transfer within the Fe-protein-MoFe protein complex (Eady et al., 1978; Hageman et al., 1980; Mensink et al., 1992; Thorneley et al., 1989). However, none of the probes used are unambiguous in interpreting the effect being measured. For example, rapid quenching cannot distinguish among ATP cleavage on the enzyme complex and subsequent phosphate release, whereas heat changes and pH changes are difficult to assign to a particular partial reaction.
Recent studies, using a direct, real-time assay for rapidly measuring phosphate release, suggest that phosphate release occurs after electron transfer but before complex dissociation (Lowe et al., 1995). Thus, MgATP hydrolysis and phosphate release apparently drive a subsequent energy-transduction event. What this event is remains unclear. The most often suggested possibilities include: (a) modulation of

the redox potential of one or both of the metalloclusters within the MoFe protein; and (b) the coupling of proton transfer with electron transfer. In the case of either of these possibilities and assuming that the MgATP-binding sites identified through the x-ray crystal structure are those effective in catalysis, the docking surface of the Fe protein and the MoFe protein must play an important role in energy transduction. The energy made available from MgATP hydrolysis and phosphate release on the Fe protein must be transduced through this interface to the metalloclusters of the MoFe protein. Further, the rates of electron transfer, MgATP hydrolysis and complex dissociation all decrease proportionally if this interface is disturbed (Lowe et al., 1993), suggesting that a concerted conformational change of both proteins occurs within the complex when MgATP is hydrolyzed and phosphate is released. The overall reaction leads to reduction of FeMo-cofactor mediated through the P cluster and the oxidation of the Fe-protein's 4Fe-4S cluster by one electron each, while the P cluster remains in the same oxidation state at the beginning and the end of the redox cycle (Howard and Rees, 1994).

1.6. Substrate Reactions of Nitrogenase

1.6.1. General Requirements for Nitrogenase Action.

Mo-nitrogenase catalytic activity requires the presence of MgATP, an electron source, substrates, and an anaerobic condition. In addition to N_2, a variety of compounds, such as N_2O, azide ion and hydrazoic acid, acetylene, hydrogen cyanide, and various organic isocyanides, can act as substrates (Mozen and Burris, 1954; Schollhorn and Burris, 1966; Schollhorn and Burris, 1967a,b; Dilworth, 1966; Hardy and Knight, Jr., 1967; Kelly et al, 1967). H_2 is usually a concomitant product except that, when no other substrate is present, H^+ serves as an unique substrate (Bulen et al., 1965).

$Na_2S_2O_4$ is a convenient low-potential electron donor, which is usually chosen for the ***in vitro*** nitrogenase reaction assay. Because nitrogenase turnover requires the hydrolysis of MgATP to MgADP and inorganic phosphate (Mortenson, 1964) and because its product, MgADP, is inhibitory to nitrogenase catalysis (Moustafa and Mortenson, 1967), an ATP-regenerating system was developed. It consists of creatine phosphate, creatine phosphate kinase, $MgCl_2$ and ATP (Bulen and LeComte, 1966) to prevent the effect of MgADP. It is well known that pH, temperature, salt concentration and both $Na_2S_2O_4$ and MgATP concentrations all affect nitrogenase reactivity (Burns et al., 1985; Hwang and Burris, 1972). ***In v****ivo*, the electron is supplied by a ferredoxin or flavodoxin (Shah et al., 1983).

1.6.2. Dihydrogen Evolution.

Studies of the ratios of H_2:HD:D_2 produced by the action of nitrogenase in mixed H_2O-D_2O solutions demonstrate that hydronium ions are the ultimate source of H_2 evolution (Jackson et al., 1968).

$$2H_3O^+ + 2e^- \rightarrow H_2 + 2H_2O$$

The proton, like all other substrates, is believed to be reduced at the FeMo-cofactor, however, both the chemical mechanism and specific binding site remain unknown. In the Lowe-Thorneley model for the MoFe-protein cycle, H_2 is first evolved at the E_2 state, so a low electron-flux condition favors H_2 evolution. Further, this scheme suggests that N_2 binding occurs via H_2 displacement, thus, N_2 reduction is always accompanied by H_2 evolution.

1.6.3. Dinitrogen Reduction

Together with the proton, dinitrogen is reduced by nitrogenase to ammonia and dihydrogen coupled with the hydrolysis of a minimum of 16 molecules of MgATP in a reaction that can be described as shown below.

$$N_2 + 8H^+ + 8e^- + 16MgATP \rightarrow 2NH_3 + H_2 + 16\ MgADP + 16\ P_i$$

Reported K_m values for this reaction as measured ***in vitro*** range from 0.1-0.2 atm N_2 (Hardy, 1979). N_2 is the only substrate whose reduction is competitively inhibited by H_2. Even at 50 atm N_2 pressure, a minimum of 25% of the electron flux goes to H_2 evolution (Simpson and Burris, 1984). It was reported that hydrazine was released after either acid or base treatment of a turning-over nitrogenase under N_2, suggesting the existence of enzyme-bound intermediates during the 6-electron reduction of N_2 to ammonia (Thorneley et al., 1978).

1.6.4. Hydrazine Reduction

Bulen (1976) first demonstrated the nitrogenase-catalyzed reduction of hydrazine to ammonia, the reaction can be described as:

$$N_2H_4 + 2e^- + 2H^+ \rightarrow 2NH_3$$

However, N_2H_4 is a poor substrate because the K_m of the reaction is about 20~30 mM (Davis, 1980).

1.6.5. Azide and Hydrazoic Acid Reduction.

Azide reduction by nitrogenase was first reported by Schollhorn and Burris (1967). Using a crude preparation of nitrogenase from either ***C. pasteurianum*** or ***A. vinelandii***, they showed that azide was apparently reduced by two electrons to give stoichiometric

amounts of N_2 and NH_3. Like N_2, the reaction requires MgATP and reductant and was inhibited by carbon monoxide (CO). These results were confirmed and extended by Hardy and Knight, Jr. (1967). Although the latter group supported the one N_2 to one NH_3 stoichiometry proposed earlier, they did observe a one N_2 to two NH_3 stoichiometry at low azide concentrations and they suggested that the excess NH_3 arose from the further reduction of the N_2 formed. This result was clearly confirmed by Dilworth and Thorneley (1981) when examining azide reduction using purified nitrogenase from ***K. pneumoniae.*** Electron balance was achieved in this study demonstrating that all major products were accounted for with the molar ratio of the products shown to be $1N_2H_4$ to $2N_2$ to $5\text{-}6NH_3$ in the series of reactions described below:

$$N_3^- + 3H^+ + 2e^- \rightarrow N_2 + NH_3$$

$$N_3^- + 7H^+ + 6e^- \rightarrow N_2H_4 + NH_3$$

$$N_3^- + 9H^+ + 8e^- \rightarrow 3NH_3$$

This information was re-examined by Rubinson et al. (1983), using ***A. vinelandii*** nitrogenase, who modified the Dilworth-Thorneley proposal. They found that both azide ion (N_3^-) and hydrazoic acid (HN_3) were substrates, which were reduced according to the following equations:

$$HN_3 + 6H^+ + 6e^- \rightarrow N_2H_4 + NH_3$$

$$N_3^- + 3H^+ + 2e^- \rightarrow N_2 + NH_3$$

1.6.6. Acetylene Reduction.

The nitrogenase-catalyzed reduction of C_2H_2 to C_2H_4 was first demonstrated by Dilworth (1966), using crude extracts of ***C. pasterianum***. The reaction can be described as:

$$C_2H_2 + 2e^- + 2H^+ \rightarrow C_2H_4$$

With wild-type Mo-nitrogenase, the only product is C_2H_4, although some H_2 is evolved depending on the concentration of C_2H_2 used (Dilworth, 1966; Hardy, 1979). However, certain altered Mo-nitrogenases (Scott et al., 1990; 1992; Kim et al., 1995) and the alternative V-nitrogenase also produce C_2H_6 (Dilworth et al., 1978; 1988). Acetylene is considered a good substrate compared to other alternative substrates because of its high solubility in water and its K_m value, which ranges from 0.002-0.003 atm (Hardy, 1979). These properties, plus its easy detection by gas chromatography, make C_2H_2 the most commonly used substrate in assays for nitrogenase activity both ***in vivo*** and ***in vitro*** (Hardy et al., 1973).

The reduction of C_2H_2 in D_2O gives ***cis***-$C_2H_2D_2$ as the major product. This geometric specificity has been used to support a concerted $2H^+/2e^-$ transfer mechanism involving side-on bonding of acetylene to a metal atom in nitrogenase (Stiefel, 1973). C_2H_2 is also an inhibitor of N_2 reduction in a non-competitive mechanism depending on the ratio of two nitrogenase components as well as on the concentration of C_2H_2 used (Rivera-Ortiz and Burris, 1975; Shah et al., 1975).

1.6.7. Cyanide Reduction

Cyanide reduction by nitrogenase was first reported by Hardy and Knight, Jr. (1967). Using a crude nitrogenase preparation, they showed that cyanide was reduced by six electrons to methane plus ammonia with a small amount (10% of the NH_3 produced)

of another base, which was suggested to be the four-electron-reduced product, methylamine. The reaction can be completely inhibited by carbon monoxide (0.9 atm). Hardy and Knight (1967) suggested that cyanide reduction proceeded via the two-electron intermediates, methyleneimine and methylamine, and was good model for N_2 reduction. They were unable, however, to demonstrate the reduction of methylamine to methane and ammonia. Very small amounts of ethylene and ethane (about 0.08% of the CH_4 produced) were observed during cyanide reduction catalyzed by nitrogenase (Kelly et al., 1967). These authors suggested that these C2 products were formed by interaction of adjacent C1 radicals on adjacent cyanide-binding sites. Several investigators (Hardy and Knight, Jr., 1967; Hwang and Burris, 1972; Rivera-Ortiz and Burris, 1975) reported that cyanide reduction appeared to have a self-inhibition effect, which caused difficulties in determining the apparent K_m for cyanide reduction. However, K_m values ranging from 0.19 mM to 4 mM have been reported (Kelly, 1968; Hardy and Knight, Jr., 1967; Rivera-Ortiz and Burris, 1975). The cyanide-reduction reactions can be summarized as:

$$HCN + 2e^- + 2H^+ \rightarrow CH_2NH$$

$$HCN + 4e^- + 4H^+ \rightarrow CH_3NH_2$$

$$HCN + 6e^- + 6\ H^+ \rightarrow CH_4 + NH_3$$

Upon hydrolysis, the CH_2NH (metlyleneimine) from the first reaction would give NH_3 and HCHO (Li et al., 1982). These last authors also reported that CN^- was a potent reversible inhibitor of total electron flux (K_i = 27μM), whereas HCN was the nitrogenase substrate (Km = 4.5mM at an Av2/Av1 ratio of 8). CN^- inhibition is completely reversed by low levels of CO, implying a common binding site. Azide can

partially relieve this inhibitory effect, but other substrates and inhibitors (N_2, C_2H_2, N_2O , H_2) have no effect (Li et al., 1982) .

1.6.8. Methyl isocyanide reduction

Methyl isocyanide reduction was first demonstrated by Kelly et al. (1967), using a crude extract from ***A. chroococcum,*** and was later shown to be a general property of N_2-fixing organisms (Biggins and Postgate, 1969; Hardy and Jackson, 1967; Kelly, 1968; Munson and Burris, 1969). Formation of the major products observed can be described by the reactions below (Rubinson et al., 1983):

$$CH_3NC + 4e^- + 4H^+ \rightarrow CH_3NHCH_3$$

$$CH_3NC + 6e^- + 6H^+ \rightarrow CH_3NH_2 + CH_4$$

In addition, small yields of C-2 hydrocarbon products (ethylene and ethane) are observed:

$$2CH_3NC + 8e^- + 8H^+ \rightarrow C_2H_4 + 2CH_3NH_2$$

$$2CH_3NC + 10e^- + 10H^+ \rightarrow C_2H_6 + 2CH_3NH_2$$

Using labeled CH_3NC, these products were shown to arise from the terminal isocyanide C atom and were suggested to form by dimerization of two enzyme-bound C-1 radicals (Kelly, 1968). However, later studies support a mechanism that involves reduction to produce an enzyme-bound methylene or methyl group followed by insertion of a second substrate into the enzyme-C bond (Hardy, 1979; Rubinson et al., 1983).

CH_3NC is also a potent reversible inhibitor (K_i = 158μM) of total electron flow and it appears to uncouple MgATP hydrolysis from electron transfer to substrate (Rubinson et al., 1983).

1.6.9. Inhibition of Substrate Reduction

The best-studied inhibitor of nitrogenase catalysis is carbon monoxide (CO). With wild-type Mo-nitrogenase, it inhibits the catalyzed reduction of all substrates except that of the proton. CO is not an inhibitor of total electron flux through nitrogenase, its inhibitory action diverts electron flux away from substrate reduction to proton reduction until, at a sufficient CO concentration, all electrons are consumed as H_2 evolution. A second well-studied inhibitor is H_2. In contrast to CO, H_2 is specific as an inhibitor of only N_2 reduction by nitrogenase.

Early inhibition studies of nitrogenase-catalyzed reduction were performed under conditions where the concentration of electron acceptors and inhibitors did not affect nitrogenase-catalyzed ATP hydrolysis and where the concentration of the electron acceptor (substrate) was at least 1.8-times of its Michaelis constant to minimize the effect of concomitant H_2 evolution. Thus, the effects were centered on the reduction site. Based on Lineweaver-Burk plots, these experiments showed that CO was a noncompetitive inhibitor of N_2, acetylene and azide reduction. It did not inhibit H_2 evolution. H_2 was found to inhibit N_2 fixation competitively but it did not inhibit the reduction of azide, acetylene, cyanide, isocyanide and H^+(Hwang et al., 1973; Hardy, 1979; Burris,1979)

Other similar experiments, in which combinations of substrates were used, showed that: (a) acetylene and cyanide were noncompetitive with N_2; (b) acetylene and azide are noncompetitive with each other; and (c) cyanide and methylisocyanide were

competitive with azide. These observations were interpreted as showing that at least five sites exist on the nitrogenase complex for substrate reduction (Hwang et al., 1973). These were: (1) an N_2- and H_2-evolving site; (2) an acetylene-binding site; (3) a site shared by azide, cyanide and methylisocyanide; (4) a CO-binding site; and (5) an H^+ site.

If multiple sites as suggested above really exist, they are all likely to be located either on or very close to the FeMo-cofactor, which has been strongly implicated to be either part of or to contain the substrate-binding and -reduction site(s) (Hawkes et al., 1984; Scott et al., 1990). More recent studies, using MoFe proteins altered by directed mutagenesis within the FeMo-cofactor-binding pocket, (Kim et al., 1995; Shen et al., 1997) suggest some commonality among the N_2- and C_2H_2-binding sites and show that there are multiple CO-binding sites. Other altered nitrogenases, such as that resulting from the ***nifV***$^-$ mutation (McLean et al., 1983) or from the substitution of α-Glu-191 with Lys (Scott et al., 1992), have shown CO sensitivity of their H_2-evolution activity. Interestingly, this inhibition by CO is not complete and at least 25% of the electron flow remains. Together with the fact that 25% electron flow to H_2 evolution is observed even at very high dinitrogen concentrations with wild-type nitrogenase (Rivera-Ortiz and Burris, 1975; Simpson and Burris, 1984), these results may suggest that more than one H_2-evolution site exists. It has also been suggested (Kim et al., 1993) that a possible H_2-evolution site may be located on the P-cluster of the MoFe-protein. However, in light of the Lowe-Thorneley model, the noncompetitive nature of the inhibition kinetics may reflect binding to the different oxidation states of the enzyme during the MoFe protein cycle rather than to different sites on the enzyme. Thus, the location of the substrate-binding sites on nitrogenase and how the substrates are reduced still remains a mystery.

Chapter 2. Materials and Methods

2.1. General Materials.

General chemicals were purchased from Fisher Scientific Company (Pittsburgh, PA) unless otherwise specified. Chemicals used for buffer systems in this study, like Tris, Tes, Hepes, Hepps, Ches and Bis-tris, were purchased from Sigma Chemical Co. (St. Louis, MO).

Sodium dithionite ($Na_2S_2O_4$) was purchased from Mallinckrodt Chemical Company (Berkeley, CA).

Chromatographic media employed in the study were purchased from various companies. Q-Sepharose, Phenyl-Sepharose, Sephacryl S-200 and S-300 were purchased from Pharmacia Ltd (Uppsala, Sweden). Dowex AG1X2 resin and Bio-Gel P-6DG desalting gel were purchased from BioRad (Hercules, CA).

Gases, such as nitrogen, argon, hydrogen, helium and air, were purchased from AirCo (Radnor, PA) and carbon monoxide from Matheson Products Inc. (East Rutherford, NJ). Cylinder argon was first passed through a heated (120^{o}C) BASF copper catalyst column to remove dioxygen before being used as a flushing gas in the Schlenk lines. Acetylene was produced in the laboratory by the reaction of calcium carbide with water.

2.2. Anaerobic Techniques

Because all known nitrogenases are extremely sensitive to dioxygen, all procedures are performed in anaerobic buffer under an argon atmosphere. A Schlenk line

equipped with a vacuum pump and an argon gas line, that is controlled by two-way stopcocks, is designed to replace air with argon. The monitoring system consists of a mercury manometer, which measures the gas pressure in the Schlenk line, and a bubble flow monitor, which monitors the argon flow into the system. A dry-ice trap is also appropriately placed to avoid the mixing of moisture generated by evacuation with the pump oil. To replace the air in the buffer-containing flask with argon, the buffer-containing flask was first degassed under vacuum on the Schlenk line for more than 60 minutes, with 10% water of total volume added to offset the vaporizing. It was then flushed with argon gas, followed by the addition of sodium dithionite to a final concentration of 1mM in the solution. The “degassed” buffer-containing flask was then kept under argon until and while in use. If an anaerobic atmosphere needs to be generated in an empty container, a repeated cycle (at least three times) of evacuation and flushing with argon is performed and then it is kept under argon until used.

2.3. Cell Growth, Media and Nitrogenase Depression.

Growth of ***A. vinelandii*** cells was carried out on a modified Burk medium (Strandberg and Wilson, 1968). It consists of 0.8g K_2HPO_4, 0.2g KH_2PO_4, 0.2g $MgSO_4.7H_2O$, 20.0g sucrose, 0.05g $CaSO_4.2H_2O$, 0.027g $FeCl_3.6H_2O$ and 0.0024g $Na_2MoO_4.2H_2O$ per liter. If a fixed nitrogen source is needed for growth, the equivalent of 0.12g urea (NH_2CONH_2) per liter is added as an aliquot of a 20mM filter-sterilized solution. If the medium is to be used to make plates, 20g of agar is also added before the sterilization step.

Before each strain can be grown, cells must be transferred from a -70^oC stock culture to a Burk-plus-urea (BU) plate. The culture is grown at 30^oC for 2-3 days, then a single colony is transferred to another BU plate and grown at 30^oC for a further 2-3 days. This transfer is performed at least twice before the culture is used for growth on liquid media. Then, a small container, containing 50 ml of BU medium, is used to grow the

cells transferred from the plate. After about 16-hours of growth, when the Klett unit reading is 90-170, using a Klett-Summerson meter with a No. 54 filter (Klett Mfg. Co. Inc., New York), a 10-ml aliquot of the growing cells is transferred from this small flask to a Fernbach flask containing 500 ml BU medium. The resulting cell culture is grown under filtered air with a shaking speed of 250 rpm at 30^{o}C. The cell density is monitored until the density reaches 150-200 Klett units and then about 200-300ml of the culture is transferred to a 28-liter fermentor containing about 24 liters of BU medium. The cells are allowed to grow until the density reaches 200-220 Klett units. The culture is then concentrated with a Pellicon cassette filtration apparatus (with a 0.45µm membrane; Millipore Corporation, Bedford, MA) and a Watson-Marlow pump (Smith and Nephew Watson-Marlow, Falmouth, Cornwall, England) to a volume of 2 liters and the concentrated cells washed three times with 300 ml 50mM Tris (pH 8.0) buffer. These cells were then resuspended in 24 liters of Burk medium without a fixed-nitrogen source. The cells were allowed to grow and derepress, i.e., to synthesize nitrogenase, for up to 4 hours before the Pellicon harvester was employed again to concentrate the culture down to about 1.5 liters. Final harvest of the cells from the fermentor involved a wash with 6 liters of prechilled (4^{o}C) 50mM Tris-HCl (pH 8.0), followed by the concentration-filtration procedure to reduce the volume to 2 liters again. Removal of the remaining medium from cells was achieved by centrifuging the washed cultures at 10,400xg for 30 minutes at 4^{o}C, using a Sorval RC-5B centrifuge and Sorvall GS-3 rotor. The collected cells were stored at -70 ^{o}C in a freezer until used.

2.4. Crude Extract Preparation

To prepare a crude extract, prechilled (4^{o}C) degassed 50mM Tris-HCl, pH8.0, buffer, containing 2mM sodium dithionite, is used to dilute the thawed cells in a ratio of 1.0g cells to 2.0ml of buffer under anaerobic conditions. The cell suspension was then subjected to a 12-min. pulse of sonication using a Heat System Sonicator, Model

XL2015, in a rosette cooling cell (Heat Systems-Ultrasonic, Inc.), which was immersed in an ice-water bath to keep it cool. The broken-cell suspension was then transferred to a flask and incubated at 55^{o}C for about 5 minutes. The suspension was then transferred to centrifuge tubes anaerobically and centrifuged for 90 minutes at 98000xg at 4^{o}C, using a Beckman L5-50B ultracentrifuge and a Ti-45 rotor. The supernatant was removed from the centrifuge tubes under an argon flush, using a Hamilton syringe, pelleted into liquid nitrogen, and then stored in liquid nitrogen until used.

2.5. Protein Purification

The purification procedure designed here for both wild-type MoFe protein and altered MoFe protein consists of four chromatography steps: (1) an anion-exchange step over Q-Sepharose; (2) a gel-filtration step over Sephacryl S-300; (3) a hydrophobic-interaction step using phenyl-Sepharose; and (4) a second gel-filtration step using Sephacryl S-200. All columns were monitored at 405 nm using an Absorbance/Fluorescence Monitor (ISCO, Model UA-5). All fractions were pelleted in liquid nitrogen between steps.

2.5.1. Q-Sepharose step.

At room temperature (20^{0}C -25^{0}C), a Q-Sepharose column (5cmx25cm) was equilibrated and reduced with 25mM Tris-HCl (pH 7.4) containing 2mM $Na_2S_2O_4$. The thawed crude extract was loaded onto the column, followed by elution with a linearly increasing NaCl gradient from 0 M to 1.0 M in 25mM TrisHCl, pH 7.4 buffer, plus 1mM $Na_2S_2O_4$. The total elution volume is 1 liter. Several protein-containing fractions were detected at 405 nm and each was collected and further investigated by both SDS-PAGE and a proton-reduction assay. Fractions containing nitrogenase activity were used for the next purification step. The MoFe-protein fraction eluted at about 0.2M

NaCl and the Fe-protein fraction eluted at about 0.4M NaCl. The Fe protein was purified by passage over a second Q-Sepharose column.

2.5.2. Sephacryl S-300 Gel Filtration

At room temperature (20^0C -25^0C), a Sephacryl S-300 column (15cmx70cm) was equilibrated and reduced with a solution of 200mM NaCl in 25mM Tris-HCl, pH7.4, containing 1mM $Na_2S_2O_4$. The fractions from the Q-Sepharose step containing MoFe-protein activity were loaded onto a Sephacryl S-300 column and then eluted with 200mM NaCl in 25mM Tris-HCl, pH7.4, plus 1mM $Na_2S_2O_4$. The major elution peak was collected usually as at least four separate fractions (50-100ml/fractrion) and each fraction was investigated with SDS-PAGE and the H_2-evolution assay. For the altered MoFe protein, up to 20 fractions were collected. The fraction containing the wild-type MoFe protein was further purified by phenyl-Sepharose. The altered MoFe protein could not be purified further because it did not survive the hydrophobic-interaction step.

2.5.3. Phenyl-Sepharose Step

At room temperature (20^0C -25^0C), a column of phenyl-Sepharose (3cmx8cm) was first reduced and equilibrated with 25mM Tris-HCl, pH7.4, which was 0.4M in $(NH_4)_2SO_4$ and 1mM in $Na_2S_2O_4$. The appropriate wild-type fractions from the Sephacryl S-300 step were loaded anaerobically onto this column and eluted with a linearly decreasing 0.4-0.0M $(NH_4)_2SO_4$ gradient in 25mM Tris-HCl, pH 7.4, containing 1mM $Na_2S_2O_4$. The total elution volume is 1 liter. The eluting peak was separated into several fractions and assayed under argon for H_2-evolving activity. Usually, this step will give MoFe protein with a high purity.

2.5.4. Sephacryl S-200 Step.

Because Tris buffer is an inhibitor of the colorimetric ammonia assay used after the N_2-fixation reaction, it is necessary to change the buffer system for the above-obtained MoFe protein. Tris is also a general inhibitor of all nitrogenase activities. The pure MoFe protein sample was loaded onto a reduced Sephacryl S-200 column (3cmx50cm), which had been equilibrated with 200mM NaCl in 25mM Hepes-KOH pH7.4 buffer with 1mM $Na_2S_2O_4$, followed by elution with the same buffer. After buffer exchange, usually the total volume will expand about 10%. The eluted sample was concentrated by a Millipore concentrator to about 10 ml, pelleted into liquid nitrogen, and stored in liquid nitrogen until used.

2.6. Gel Electrophoresis.

SDS-PAGE (Sodium dodecyl sulfate-polyacrylmide gel electrophoresis) samples and gels were prepared according to Laemmli (1970) with a 12% polyacrylmide (1.35% cross linker) running gel and a 4% stacking gel. Electrophoresis was performed at 25mA/gel in a Hoefer Mighty Small apparatus (Hoefer, San Francisco, CA). After electrophoresis, the gels were stained with 0.1% Coomassie Blue (R-250), followed by destaining with 40% methanol/10%acetic acid/50% H_2O. A photographic record was kept of each gel after destaining. The SDS-PAGE technique was used extensively to monitor the progress of the nitrogenase purification process.

2.7. Protein Estimation

The Folin-Ciocalteu Protein Assay method, using bovine serum albumin (0-100µg/ml) as a standard (Smith et al., 1985), was employed to evaluate the protein concentration of crude extracts and solutions of purified proteins. Dithionite is known to give a

positive reaction on this assay, thus, samples must be vortexed vigorously in air to consume the dithionite.

2.8. Steady-State Assays for Nitrogenase Activity

2.8.1. Preparation of the Reaction Mixture

The following protocol was used to prepare the reaction mixture in 45-ml batches as needed:

Stock Solution	Volume Used (ml)
0.25M Hepes-KOH (pH7.4)	15.0
0.1M ATP	3.75
0.25M $MgSO_4$	3.0
0.3M Creatine phosphate	15.0
Creatine phosphate kinase	25,000 activity units
Deionized water	0.75

The reaction mixture is pre-prepared and stored in the -20^{o}C freezer in 10-ml aliquots to avoid unnecessary freezing and thawing to ensure the best performance.

2.8.2. Assay Preparation.

First, the required amount of both distilled water and the two component proteins of nitrogenase are calculated depending on the varying assays to be conducted. The total volume of these three components is 0.6ml. Then, water and 0.3ml of reaction mixture is added to a serum vial with an average volume of 9.3ml. The vial is then sealed with a rubber septum and then capped with a crimped aluminum seal (Alltech Associates, Inc., Deerfield, IL). These vials are then subjected to four cycles of evacuation and flushing using an automatic machine (Corbin, 1978) to replace the air

with either 100% argon or 100% N_2 depending on the assay to be performed. The internal pressure for each vial was then released by venting through a 16-gauge needle attached to a 3-ml disposable syringe filled with deionized water.

Second, 0.1ml of a freshly prepared 0.3M $Na_2S_2O_4$ solution is added to the reaction vials to serve as a reductant. All assays, except N_2-reduction assays, are performed under 100% argon. To prepare a C_2H_2/Ar gas mixture with a certain percentage of C_2H_2 present, the desired volume of 100% C_2H_2 was calculated as:

Desired Vol. = 8.4 x (desired conc. of C_2H_2)/(100% - desired conc.)

After the addition of the desired volume of 100% C_2H_2, the internal gas pressure was released again as described above. If, in a certain assay, CO or another gas is to be used, the same strategy was employed as described for C_2H_2.

2.8.3. Nitrogenase Activity Assay.

After the substrate was prepared and to assay the MoFe-protein activity, the calculated amount of wild-type Fe protein was added to the vial first, followed by the source of MoFe protein. For crude extracts, 100µl of crude extract was used to start each assay either with or without 10µl of wild-type Fe protein (at a concentration of ~18.5 mg/ml). With purified MoFe proteins, an appropriate amount (see below) of Fe protein was added to the reaction vial first, followed by purified MoFe protein to start the reaction. The amount of each protein used was determined by both the total protein concentration and the molar ratio required. Usually, a saturating ratio of 40:1 Fe protein-to-MoFe protein was used to ensure that the protein-protein interaction is not limiting the rate of the reaction. Total nitrogenase-protein concentrations in the assay were in the range of 0.25-1.00 mg/ml. The reactions were allowed to proceed at 30^{o}C

in a water bath with a shaking speed of about 100 rpm for certain time periods, e.g., 5 minutes, 8 minutes or 10 minutes, followed by the addition of 0.3 ml 0.5M EDTA to stop the reaction. Most products were then detected and quantified by gas chromatography (GC).

2.8.4. Product Analysis

2.8.4.1. Quantification of the Gases: C_2H_4, and H_2

C_2H_4, was quantified by gas chromatography on a Model GC-14A (Shimadzu, Tokyo, Japan) using a Poropak N column and a flame ionization detector (abbreviated as FID). H_2 was quantified by gas chromatography on a Model GC-8A (Shimadzu, Tokyo, Japan) on a molecular sieve 5-A column using a thermal conductivity detector (abbreviated as TCD).

The flame ionization detector (FID) is the most commonly used detector in GC. The detector consists of a small H_2-air diffusion flame burning at the end of a jet formed at the tip of a length of capillary tubing. When organic compounds are introduced into the flame from the column, electrically charged species are formed. These are collected by applying a voltage across the flame. The resulting current is amplified by an electrometer. When hydrocarbons are introduced into this flame, ionization takes place in strict proportion to the amount of compound present. This is due to the radical reaction:

$$CH + O \rightarrow CHO^{+} + e^{-}$$

This reaction is an almost quantitative measure of carbon atoms being burned. The GC-14A is connected to a CR-5A chromatography integrator (Shimadzu, Tokyo, Japan), where chromatographs are recorded and the area under each peak is

calculated. Calibrations are performed using standard gas mixtures of 1 ppm C_2H_4/100% helium, which was purchased from Scotty Specialty Gases (Plumsteadville , PA).

The TCD is a concentration-dependent detector that is sensitive to some overall property of the effluent. The measured property is a physical parameter rather than a chemical one. The larger the difference between the thermal conductivity of the carrier gas and the sample, the greater the detector response. In our case, H_2 is the sample, which has relative large thermal conductivity compared to Ar, thus making argon a good choice as a carrier gas (Schill, 1977). The TCD requires strictly isothermal conditions and, in our case, 40^oC is set for both column and injection/detection temperatures. A CR-5A integrator is connected to the GC-8A to record chromatographs as well as performing calculations as mentioned above. Calibration is done by using a standard gas mixture of 1% H_2/99% N_2 purchased from Scotty Specialty Gases (Plumsteadville, PA).

2.8.4.2. Ammonia Assay.

After termination of the N_2-fixation reaction, NH_3 was quantified by the phenol/hypochlorite colorimetric determination using ammonium sulfate as a standard as previously described by Dilworth et al. (1992). The liquid mixture (0.5ml) obtained from the terminated reaction from each vial was applied to a short Dowex AG1x2 ion-exchange column (Cl^- form, 200-400 mesh; BioRad), which was pre-prepared in a Pasteur pipet, to remove inhibitory components of the assay. The column was then flushed twice with 0.5-ml portions of distilled water. The total 1.5 ml was collected, from which 0.5 ml was taken and used in the ammonia assay. A 0.3-ml aliquot of a sodium phenolate solution (5 % w/v phenol plus 2.5 % w/v NaOH in distilled water), 0.45 ml sodium nitroprusside (0.02 % w/v in distilled water) and 0.45ml sodium hypochloride (10 % w/v in distilled water) was added in the above

order. This mixture was incubated at room temperature for 40 minutes before the visible absorbance of the mixture was measured at 630 nm against the $(NH_4)_2SO_4$ standard.

2.8.5. Measurement of ATP Hydrolysis by the Creatine Assay

The ATP hydrolyzed during the assay was estimated via measurement of creatine released from creatine phosphate. Because the ADP produced in the reaction is inhibitory to nitrogenase catalysis, it is recycled by a creatine phosphate-creatine phosphokinase system. As ADP is converted back to ATP by this system so creatine is released and is a direct measurement of ATP hydrolysis. The initial procedure was as described for the ammonia assay and the colorimetric measurement was as previously described by Ennor (1957). A 0.2-ml aliquot of the effluent from the Dowex AG1x2 column was mixed with 2 ml 1% α-naphthal (w/v in distilled water) and 1ml 0.05 % diacetyl (v/v in distilled water). The total volume was adjusted to 5 ml by addition of distilled H_2O. The mixture was incubated for 20 minutes at room temperature, followed by the measurement of absorbance at 530 nm. The concentration is calculated against the creatine standard of 0-2.0 µmol/ml creatine and then multiplied by the fold dilution.

2.9. Electron Paramagnetic Resonance (EPR) Spectroscopy

An electron possesses both charge and mass but also has angular momentum and spin. A spinning charge generates a magnetic field, so an electron may be thought of as a magnet orientated along the axis of spin (Knowles et al., 1976; Palmer, 1985). The strength of the magnetic field is expressed as the magnetic moment. The magnetic moment of an electron can assume one of the two possible orientations with respect to an externally applied magnetic field. An unpaired electron has a spin of

1/2 and these two orientations are expressed as either -1/2 (aligned with magnetic field) or +1/2 (aligned against the magnetic field). When electrons are paired, the spins oppose each other and are consequently diamagnetic. Molecules containing one or more unpaired electrons are paramagnetic and therefore can be studied by EPR (Zavoisky, 1945). EPR spectroscopy gives information about the existence of an unpaired electron and about its immediate surroundings (as the g value is affected by the environment surrounding the unpaired electron). For a free electron, g = 2.0023 and the resonances in the g=2 region are generally characteristic of non-metal, free radicals. EPR is particularly useful as a method of studying the Fe-S clusters in iron-sulfur proteins (Lowe, 1992). The single-electron oxidation and reduction of these centers are very easily detected. A characteristic EPR spectrum of the nitrogenase MoFe protein is illustrated in Figure 1-6; that of the Fe protein is not discussed in this thesis because it is peripheral to the author's research. The spectra of whole cells and purified proteins were recorded on a Varian Associates E-line instrument at 9.22 GHz and 20 mW at 13 K maintained by liquid helium boil-off.

2.10. Preparation of Crude Extract and Purified Protein Samples for EPR Analysis

The crude extracts were first concentrated to 40-80 mg/ml, and then injected into EPR tubes (3x200 mm) (Wilmad Glass Co. Inc., Buena, NJ), which had been previously flushed and filled with argon using an automatic machine (Corbin, 1978). Purified MoFe protein samples at 8-20 mg/ml were injected into similarly degassed EPR tubes. The sample-filled EPR tubes were then slowly immersed to liquid nitrogen until all the EPR tube was immersed and the sample completely frozen. The samples were stored in liquid nitrogen until examined.

Chapter 3. Role of MoFe Protein β-95-Cysteinyl Residue in Nitrogenase Catalysis in *A. vinelandii*

3.1. Introduction

Molybdenum-dependent nitrogenase (Mo-nitrogenase) is the catalytic component of biological nitrogen fixation. It is composed of the MoFe protein and the Fe protein. The Fe protein (a homodimer, encoded by ***nifH***), is a one-electron donor to the MoFe protein. The MoFe protein is a $\alpha_2\beta_2$ tetramer, which is encoded by ***nifDK*** genes. The MoFe protein contains two types of prosthetic groups, the FeMo-cofactor (FeMoco) and the P cluster. Significant evidence has been gathered to support FeMoco as the substrate-binding and -reducing site (Shah et al., 1972; Hawkes et al., 1984; Scott et al., 1990). One FeMoco is located in each of the α subunits of the MoFe protein. Each FeMoco consists of 1 Mo, 7 Fe, and 9 inorganic sulfides, plus one molecule of homocitrate. FeMoco is responsible for the characteristic electron paramagnetic resonance (EPR) signal of nitrogenase due to its S=3/2 spin system. The S=3/2 EPR signal of FeMoco within the MoFe protein shows apparent g values of 4.34, 3.65 and 2.01; however, those of "isolated" FeMoco, after their extraction from the MoFe protein using ***N***-methylformamide, are 4.7, 3.3 and 2.0 (reviewed by Newton, 1992).

The recent solution of the three-dimensional crystal structure of the MoFe protein, with models for both prosthetic groups bound within the protein, from both ***Azotobacter vinelandii*** and ***Clostridium pasteurianum*** has provided insights into: (i) the structure, orientation and relative location of these prosthetic groups; (ii) their potential functions; and (iii) the mechanism of biological nitrogen fixation by indicating potential protein-protein interaction sites, electron-transfer routes, etc. (Kim & Rees, 1992a, b; Kim et al., 1993; Chan et al., 1993; Bolin et al., 1993b; Howard & Rees, 1994). Within

the three metal clusters, which are believed to be involved in electron transfer and substrate reduction, the [4Fe:4S] cluster in the Fe protein is responsible for accepting an electron from an exogenous donor and then initiating intermolecular electron transfer to the MoFe protein with FeMoco as the substrate-reduction site. In contrast, the catalytic role of the P cluster, which is an [8Fe:7S] cluster, is not well understood, although it is believed to be involved in accumulating electrons delivered from the Fe protein and then transferring the electrons within the MoFe protein molecule to the substrate-reducing site. A nitrogenase docking model, which is based on the crystallographic structure of the components and which pairs the 2-fold symmetric surface of the Fe protein with the exposed surface of the MoFe protein's pseudosymmetric αβ interface, has been developed. It shows that, during the component-protein interaction, the P cluster is located directly between the Fe protein's [4Fe:4S] cluster and FeMoco. This alignment supports the concept that the P cluster is involved in mediating intramolecular electron transfer between the other two clusters(Howard and Rees, 1996).

The P cluster is located at the α/β-subunit interface and is coordinated equally by cysteinyl (Cys) residues from both subunits. These are α-62-Cys, α-88-Cys, α-154-Cys, β-70-Cys, β-95-Cys and β-153-Cys (numbers refer to the primary sequences of the ***A. vinelandii*** MoFe protein subunits). In addition, the residue, β-188-Ser, can coordinate the same Fe atom of the P cluster as β-153-Cys (see below). Residues α-62-Cys, α-154-Cys, β-70-Cys and β-153-Cys are terminal ligands to one Fe atom each, whereas residues α-88-Cys and β-95-Cys each bridge two Fe atoms, one from each sub-cluster. A third bridge between the sub-clusters is formed by a shared sulfide ion.

Recent EPR studies on the MoFe-protein crystals have helped to explain some apparent differences observed at the P cluster in the various reported structures. It was found that the two observed structures correspond to two spectroscopically assigned states of the MoFe protein. The first is the native, dithionite-reduced (P^N/M^N) state of the MoFe protein in which the P cluster is diamagnetic and EPR-silent and FeMoco is paramagnetic and EPR-active. The second is the oxidized (P^{ox}/M^{ox}) state, in which both the P cluste and FeMoco are oxidized relative to the native state but now the P cluster is paramagnetic and EPR-active and FeMoco is diamagnetic and EPR-silent. The P cluster undergoes a structural change as it converts between these two redox states and this change explains the observed structural differences at the P cluster in the reported structures. In both states, each sub-cluster retains both its cysteinyl γ-S terminal ligands as well as its two cysteinyl bridges. However, the nature of the third bridge varies, as does the ligation of some of the Fe atoms, between the two states. In the native P^N state, both sub-clusters may be effectively described as [4Fe:3S] with the seventh sulfide forming a central bridge to six Fe atoms, three from each sub-cluster. Thus, the P cluster may be thought of as two [4Fe:4S] cubes sharing a common, six-coordinate sulfide. In forming the P^{ox} state, two of these six Fe atoms, both from the same sub-cluster that is associated with the β-subunit, move away from the central sulfide. The result is that the seventh sulfide becomes four-coordinate and more closely associated with the sub-cluster in the α-subunit. The P cluster may now be thought of as being composed of a [4Fe:4S] sub-cluster bridged to a [4Fe:3S] sub-cluster. The loss of sulfide coordination suffered by these two Fe atoms is compensated by (i) the binding of the Oγ of β-188-Ser to one of the Fe atoms and (ii) by the binding of the backbone amide N of α-88-Cys to the other. Because both the β-188-serinyl and the backbone amide N are protonated in their unbound state and likely unprotonated in their bound state, these structural changes have led to the suggestion that the P cluster may be involved in coupling proton transfer with electron transfer during nitrogenase catalysis (Peters, ***et al***., 1997).

Previously, using site-directed mutagenesis of the ***A. vinelandii*** MoFe protein, single amino-acid substitutions of each of the six cysteinyl ligands of the P-cluster were introduced and showed that only α-88-Cys and β-153-Cys can tolerate replacement (Dean ***et al***., 1990; May ***et al***., 1991). This result is striking because these are the same residues that coordinate the two Fe atoms, which undergo substantial motion during the P^{ox}-P^{N} interconversion. However, the mechanistic significance of this observation is unclear and many questions concerning the role of the P cluster in catalysis remain. For example, how does the P cluster mediate the delivery of an electron from the Fe protein's [4Fe:4S] cluster to the FeMoco, how many electrons can be accumulated by the P cluster, and what is the pathway of the electron through the P cluster. In this thesis, we have: (i) compared the characteristics of eight altered MoFe proteins from ***A. vinelandii***, each having a single amino-acid substitution at the β-95-Cys position, with those of wild type at the crude-extract level; (ii) purified the altered β-95^{Asp} MoFe protein and compared its substrate-reduction characteristics with those of purified wild-type MoFe protein; (iii) used EPR spectroscopy to detect possible changes in the FeMoco environment due to the substitutions; and (iv) used inductively coupled plasma atomic emission spectroscopy (ICP-AES) to determine metal content and the P cluster-to-FeMoco ratio in the altered β-95^{Asp} protein in order to detect any instability in the binding of FeMoco to the MoFe protein due to changes in the polypeptide environment of the P cluster.

3.2. Experimental Procedures

3.2.1. Mutant strain construction

Site-directed mutagenesis, gene replacement and the isolation of mutant strains were performed as described previously (Brigle ***et al***., 1987a,b). The strategy for

making a number of mutants at one specific amino-acid residue is to chemically synthesize an oligonucleotide on which the codon for the desired amino-acid residue has been degenerately replaced. For substitution at β-95-Cys of the MoFe protein, the oligonucleotide having the following sequence was synthesized:

5'-CCCTACGTGCACGGTTCCCAGGGTXXXGTCGCCCTACTTC-3'

where XXX represents the degenerate codon at the designated residue. Each altered MoFe protein having a substitution within the MoFe protein β-subunit primary sequence is designated by the name of the subunit (in this case, β), the number of the amino-acid position substituted, followed by the three letter code for the substituting amino acid in superscript form. Eight mutants were obtained with the following substituting amino acids; Asp, Glu, Lys, Arg, Ser, Thr, Val and Trp. The altered MoFe protein from each of these mutants is designated as $\beta\text{-}95^{Asp}$, $\beta\text{-}95^{Glu}$, $\beta\text{-}95^{Lys}$, $\beta\text{-}95^{Arg}$, $\beta\text{-}95^{Ser}$, $\beta\text{-}95^{Thr}$, $\beta\text{-}95^{Val}$ and $\beta\text{-}95^{Trp}$, respectively. All mutant strains were derived from strain DJ527, which has an insertion mutation in the ***hoxKG*** genes that abolishes uptake-hydrogenase activity, but has an intact suite of ***nif*** genes. These mutants were constructed by John Cantwell and Valerie Cash at Virginia Tech.

3.2.2. Growth conditions, media and nitrogenase derepression

Small batches of ***Azotobacter vinelandii*** wild-type and eight mutant strains were grown at 30°C in Fernbach flasks on liquid Burk medium containing 0.01 mM Na_2MoO_4 to repress the alternative nitrogenase systems. Cultures were grown under air with shaking at 250 rpm. A fixed-nitrogen source of filter-sterilized urea was added to a final concentration of 20 mM. The growth of the culture was monitored using a Klett-Summerson meter (Klett Mfg. Co. Inc., New York) with a No. 54 filter. Cultures were grown in this fixed-nitrogen-containing Burk medium until they reached 200-240

Klett units. The cultures were then centrifuged at 10400xg for 20 minutes to remove the medium and the cell pellet was resuspended in nitrogen-free Burk medium. The cultures were allowed to derepress for four hours and then centrifuged at 10400xg for 20 minutes again to remove the medium. The cell pellet was stored at -70^{o}C until used.

Large-scale culture of wild-type ***A. vinelandii*** and the mutant strain containing β-95^{Asp} were achieved in a 28-liter fermentor (New Brunswick Scientific Company, New Brunswick, NJ) on 24 liters of Burk medium with 20 mM urea and 0.01 mM sodium molybdate. The air flow in the fermentor was controlled with a flow meter at 35-40 liters/min. and the culture was vigorously stirred at 250 rpm with a built-in stirrer. Each culture was allowed to grow up to 200-240 Klett units and then concentrated to 2 liters using a Watson-Marlow 60/S/R peristaltic pump and a Millipore (Pellicon) cassette filtration system with 0.22 A Pellicon filter in order to remove as much urea as possible. The 2-liter culture was then reinoculated into 24-liter nitrogen-free Burk medium and allowed to derepress for four hours. The culture medium was then removed by the Pellicon filtration system (as described above) and the cells were isolated by centrifugation. The cells obtained were then stored at -70^{o}C until used.

3.2.3. Crude-extract preparation

Cells were thawed, diluted and broken anaerobically as described in section 2.4.With material from the small-scale cultures of the eight mutants and wild-type, the extract was transferred anaerobically into centrifuge tubes and centrifuged for 90 min. at 98000xg at 4^{o}C. For material from the large-scale culture of wild-type and mutant strain with β-95^{Asp} substitution, which was to be used for MoFe protein purification, the extract was first transferred anaerobically to a stoppered flask full of argon and then the flask was immersed in a 70^{o}C water bath. The temperature of the cell extract inside the flask was monitored by a pre-inserted thermometer and was maintained at

55^{o}C for 5 min. Then, the heat-treated extract was cooled on ice and then transferred anaerobically to centrifuge tubes and centrifuged at 98000xg at 4^{o}C for 90 min. The supernatant was frozen dropwise into liquid nitrogen and stored in liquid nitrogen until used. Protein concentrations were measured as described in section 2.7.

3.2.4. Sodium dodecylsulfate polyacrylamide gel electrophoresis (SDS-PAGE)

SDS-PAGE was performed for on all nine crude extracts: β-95^{Asp}, β-95^{Glu}, β-95^{Lys}, β-95^{Arg}, β-95^{Ser}, β-95^{Thr}, β-95^{Val}, β-95^{Trp} and wild type, according to Laemmli (1970). 20 µg of each sample was loaded on a gel as described in section 2.6.

3.2.5. C_2H_2-Reduction and H^+-reduction assay at the crude-extract level

The MoFe-protein specific activity was measured in crude extracts for eight mutants and wild-type ***A. vinelandii***. Assays were performed in 9.25-ml reaction vials sealed with butyl rubber stoppers and aluminum seals. Each 1.0-ml reaction volume contained 25 mM Hepes-NaOH pH 7.4, 2.5 mM ATP, 5.0 mM $MgCl_2$, 30 mM creatine phosphate, 0.125 mg creatine phosphokinase and 20 mM $Na_2S_2O_4$ as described in section 2.8.2 and 2.8.3. An aliquot of 100 µl of crude extract was used plus 10 µl of pure wild-type Fe protein (121 µg) to ensure that the Fe protein-to-MoFe protein molar ratio was greater than 20:1. For C_2H_2-reduction assays, 10% of C_2H_2 was added into argon gas phase after degassing. For H^+-reduction assays, the reactions were performed under 100% argon. The reactions were performed at 30^{o}C for 5 min. and terminated by the addition of 0.25ml 0.5M Na_2EDTA, pH 7.5. The product of C_2H_2 reduction is C_2H_4 and its formation was quantified by gas chromatography as described in section 2.8.4. Calibrations were performed using standard gases of 1ppm C_2H_4 in helium and 1% H_2 in N_2 purchased from Scotty Specialty Gases (Plumsteadville, PA).

3.2.6 Electron paramagnetic resonance spectroscopy of crude extracts and purified MoFe proteins

Crude extracts of the eight mutant and wild-type strains of ***A. vinelandii*** and the purified β-95^{Asp} MoFe protein were prepared for EPR spectroscopy as described previously (Scott ***et al***., 1990). The spectra of the crude extracts and purified β-95^{Asp} MoFe protein were recorded on a Varian Associates E-line instrument operating at 9.17 GHz and 20 mW microwave power at 13K maintained by liquid helium boil-off.

3.2.7. Heat stability of the β-95^{Asp} nitrogenase at the crude-extract level

To test the heat stability of the β-95^{Asp} MoFe protein, both H^+-reduction and C_2H_2-reduction assays were performed under the same conditions as described in section 3.2.5. above for the crude-extract assays.However, the crude extracts were incubate at five different temperatures, namely, 60^{o}C, 55^{o}C, 50^{o}C, 45^{o}C and 40^{o}C, and then rapidly cooled on ice before performing the assay at 30^{o}C under 100% argon.

3.2.8 Purification of wild-type MoFe protein, wild-type Fe Protein and the altered β-95^{Asp} MoFe protein

The wild-type MoFe protein and Fe protein were purified from strain DJ527 using crude extracts prepared on a large scale as mentioned in section 3.2.3. Partial purification of wild-type MoFe protein and Fe protein was achieved by chromatography over a strong anion-exchange Q-sepharose (see section 2.5.1.). Further purification of wild-type MoFe protein was achieved by Sephacryl S-300 gel filtration chromatography (see section 2.5.2.) and Phenyl-Sepharose chromatography (see section 2.5.3.). The wild-type Fe protein isolated from the first Q-Sepharose column was further purified by

repeating a Q-Sepharose step. The altered β-95^{Asp} MoFe protein was found not to survive the phenyl-sepharose step. Thus, the purification of the β-95^{Asp} MoFe protein was achieved by Q-sepharose step followed by a modified Sephacryl S-300 step only (see section 2.5.2.). Exchange of buffers for all the purified proteins was achieved by using Sephacryl S-200 chromatography (see section 2.5.4.). At each step of the purification procedure, both the protein concentration (Smith ***et al***., 1985) and the H^+-reduction activity for both wild-type and β-95^{Asp} samples were evaluated (see section 2.8.2). The H^+-reduction specific activity of wild-type Fe protein was evaluated under the same conditions as for the MoFe protein except that MoFe protein-to-Fe protein molar ratio was optimized between 1:1 to 5:1.

3.2.9. Titration of the H^+-reduction, C_2H_2-reduction, and N_2-reduction activities for the β-95^{Asp} MoFe protein

Three series of assays were performed by changing the Fe protein-to-β-95^{Asp} MoFe protein molar ratio over the range from 1:1 to 40:1. All assay vials were set up exactly as described above (see section 3.2.5.) and allowed to run at 30^{o}C for 10 min. For assays under either a 100% argon or 90% argon plus 10% carbon monoxide (CO) gas phase, the H_2 product was quantified by gas chromatography as described in section 3.2.5. For assays under either a 90% argon/10% C_2H_2 or a 80% argon/10% C_2H_2/10% carbon monoxide (CO) gas phase, the H_2 and C_2H_4 products were quantified by gas chromatography as described in section 3.2.5. For assays under either 100% N_2 or 90% N_2/10% carbon monoxide, H_2 product was quantified by gas chromatography as described in section 3.2.5, and NH_3 (ammonia), the product of N_2 reduction, was quantified by the method mentioned in section 2.8.2. Wild-type MoFe protein control assays were performed in parallel. MgATP hydrolysis was measured for each assay (see section 2.8.4.) and the ratio of the number of moles of MgATP

hydrolyzed for each electron pair transferred to substrate (ATP/$2e^-$) was calculated also.

3.2.10 Reductant-independent MgATP hydrolysis by the β-95^{Asp} MoFe protein

It was found that, under 100% Ar, the ATP/$2e^-$ ratio decreased from 68±13 to 6.3±0.5 when the Fe protein-to-β-95^{Asp} MoFe protein ratio increased. This uncoupling of MgATP hydrolysis from electron transfer at low electron flux may reflect increasing reductant-independent ATP hydrolysis (see below). Thus, the low electron-flux ratio of Fe protein-to-β-95^{Asp} MoFe protein of 4-to-1 was selected for a time-course reaction that was performed with a limited amount of $Na_2S_2O_4$ under 100% Ar. In the 1-ml reaction volume, all reagents were at the same levels as described for the assays above, except that only 1 mM $Na_2S_2O_4$ was included. MgATP hydrolysis was measured (see section 2.8.4) for each sample and the ATP/$2e^-$ ratio was calculated. Control assays with wild-type MoFe protein were performed in parallel.

3.2.11 Carbon monoxide (CO) enhancement of activity at low electron flux for the β-95^{Asp} MoFe protein

Because an enhancement of catalytic activity by CO was observed at low electron flux in experiments described in section 3.2.9, an Fe protein-to-β-95^{Asp} MoFe protein ratio of 4:1 was selected to investigate further the CO-enhancement effect. A series of assays was set up as described above for the H^+-reduction activity measurements, except that the concentration of CO in the argon gas phase was varied from 10% to 0%. Reactions were performed at 30^oC in parallel with wild-type MoFe protein control experiments. H_2 produced in each assay was quantified as described in section 2.8.3. and ATP hydrolysis was measured as outlined in section 2.8.4, and the ATP/$2e^-$ ratio was calculated for each assay.

3.2.12. Activity assays for the β-95^{Asp} MoFe protein at lower flux with and without 10% CO added and in the presence of limited $Na_2S_2O_4$

The Fe protein-to-β-95^{Asp} MoFe protein ratio was fixed at 8:1 and the amount of β-95^{Asp} MoFe protein was increased from 0.1 mg/assay to 1.2 mg/assay. All reaction vials were set up as above except that the starting $Na_2S_2O_4$ concentration was fixed at 1 mM in the 1-ml reaction solution. The reactions were performed with and without 10% CO at 30^{o}C for 20 minutes. The H_2 product was quantified as above and its production is known to be linear with time for 30 min at least.

3.2.13 Metal analysis

The molybdenum and iron content of the purified β-95^{Asp} MoFe protein were determined using a Perkin-Elmer Plasma 400 Emission Spectrometer. All metal determinations were performed by J.T. Rinehart (Department of Human Nutrition, Foods and Exercise, Virginia Tech).

3.3. Results:

3.3.1 C_2H_2-reduction and H^+-reduction assays at the crude-extract level for eight mutants of *A. vinelandii* carrying substitutions at the β-95-Cys residue

The β-95-Cys residue of the MoFe protein is a strictly conserved residue among molybdenum-dependent nitrogenases from different organisms. All of the eight mutant strains having a site-specific point mutation at β-95-Cys were produced using site-directed mutagenesis and gene-replacement methods. Table 3-1 summarizes

the MoFe-protein specific activity for crude extracts prepared from nitrogenase-derepressed wild-type and the mutant strains along with their genotype and phenotype. The results of both C_2H_2-reduction and proton-reduction assays are shown in Table 3-1.

Most of the substitutions at residue β-95-Cys produce a Nif^- phenotype. Only the substitution of β-95-Cys with Asp gives a Nif^{slow} phenotype. The crude extracts from the Nif^- strains listed in Table 3-1 have no significant acetylene- and proton-reduction activity. However, the crude extract from the Nif^{slow} strain, which has the β-95-Cys to Asp substitution, does have both acetylene- and proton-reduction activity, although the activity is only about 15% compared to wild-type.

3.3.2 Crude extract EPR spectra.

The EPR spectra for the crude extracts from wild-type and the $\beta\text{-}95^{Asp}$ mutant are shown in Figure 3-1 and Figure 3-2, respectively From the analysis of the EPR spectra, only the $\beta\text{-}95^{Asp}$ and $\beta\text{-}95^{Trp}$ extract contain the signature signal of FeMoco as it occurs in wild-type with g values of about 4.3 and 3.7 and at only about 15% of its intensity. In contrast, the $\beta\text{-}95^{Arg}$, $\beta\text{-}95^{Val}$, $\beta\text{-}95^{Thr}$, $\beta\text{-}95^{Ser}$, $\beta\text{-}95^{Lys}$, $\beta\text{-}95^{Glu}$ and $\beta\text{-}95\text{-}^{Trp}$ extracts either do not have this signature signal or it is too weak for detection in extracts.

3.3.3. SDS-PAGE

SDS-PAGE of the crude extracts from eight mutant stains and wild-type strain are shown in Figure 3-3-1. The SDS-PAGE, gels showed that all strains expressed the nitrogenase MoFe protein but in different amounts. The $\beta\text{-}95^{Asp}$ substituted strain had

Table 3-1: The Crude Extract Specific Activity for mutants having a β-95-Cys residue substitution.

Strain	Substitution	Codon	Phenotype	Under[a] 10%C_2H_2		Under[b] argon
				C_2H_4	H_2	H_2
DJ527	none(Cys)	TGC	Nif^+	70	10	88
DJ1096	Asp	GAT	Nif^{slow}	9	3	12
DJ1082	Glu	GAA	Nif^-	0.1	0.8	0.4
DJ1084	Lys	AAA	Nif^-	0.2	0	0.6
DJ1080	Arg	AGA	Nif^-	0.1	0	0
DJ120	Ser	AGT	Nif^-	0.7	0.8	1.2
DJ1094	Thr	ACA	Nif^-	0.2	0	1.4
DJ1090	Trp	TGG	Nif^-	0.1	0	0.2
DJ1092	Val	GTT	Nif^-	1.0	0.1	1.0

a. MoFe-protein specific activity in crude extracts is listed as nmoles of C_2H_4 and H_2 produced per minute per mg total MoFe protein under a 10% C_2H_2/90% argon atmosphere in the presence of an optimal amount of purified Fe protein.

b. MoFe-protein specific activity in crude extracts is listed as nmoles of H_2 produced per minute per mg of total MoFe protein under 100% Ar atmosphere with an optimal amount of purified Fe protein present.

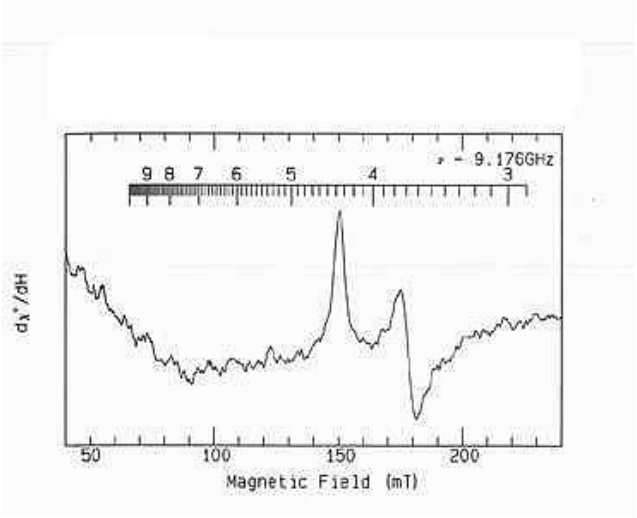

Figure 3-1. S=3/2 EPR Spectrum for Crude Extract of Wild-Type *A. vinelandii*. EPR spectrum was recorded at 9.17 GHZ and 20 mW at 13K maintained by liquid helium boil-off. Characterized responses at 150mT (g=4.3) and 175mT (g=3.7).

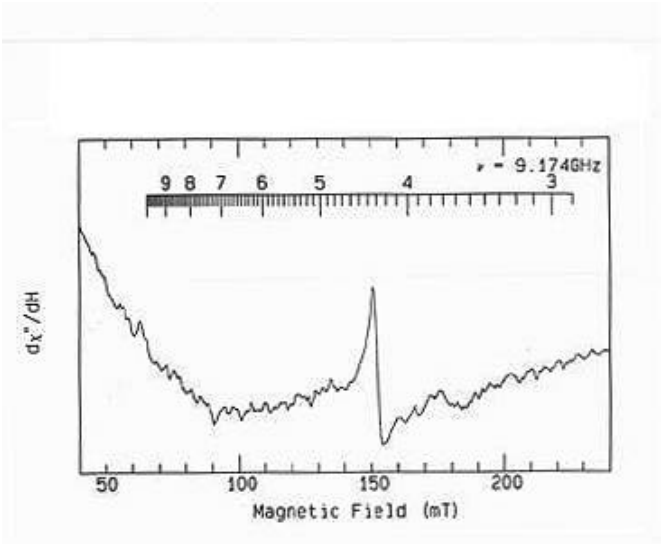

Figure 3-2. S=3/2 EPR Spectrum for Crude Extract of β-95^{Asp} *A. vinelandii*. EPR Spectrum was recorded at 9.17 GHZ and 20 mW at 13K maintained by liquid helium boil-off. The Major feature at 150mT (g=4.3) is due to containing Fe^{3+}. The MoFe protein is observable at 175 mT (g=3.7).

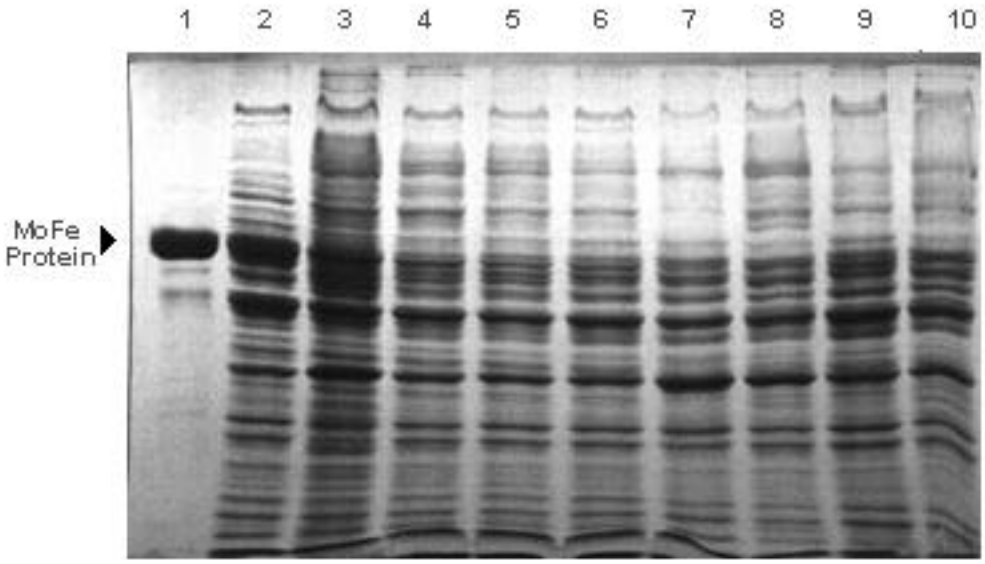

Figure 3-3-1. SDS-PAGE of crude extracts from mutant and wild-type strains. 20 µl of 1mg/ml crude extract from each strain was loaded. Lane 1, purified wild-type MoFe protein; Lane 2, wild-type crude extract; Lane 3, β-95^{Asp} crude extract ; Lane 4, β-95^{Glu} crude extract ; Lane 5, β-95^{Lys} crude extract ; Lane 6, β-95^{Arg} crude extract ; Lane 7, β-95^{Ser} crude extract ; Lane 8, β-95^{Thr} crude extract ; Lane 9. β-95^{Val} crude extract; and Lane 10, β-95^{Trp} crude extract

about 50% expression of MoFe protein compared to wild-type, but the others have less than 30% expression compared to wild-type.

3.3.4 Test for the heat stability of the nitrogenase activity in both wild-type and β-95^{Asp} substituted strains.

The heat stability test results are shown in Table 3-2. At the crude-extract level, the β-95^{Asp} substituted nitrogenase remained stable up to and including 55^{o}C for 5 minutes whereas, when temperature reached 60^{o}C, the β-95^{Asp} nitrogenase lost most of its proton-reduction activity. In contrast, the wild-type nitrogenase remains stable at 60^{o}C.

3.3.5 Purification of wild-type and β-95^{Asp} MoFe protein, and wild-type Fe protein.

The results from crude-extract activities and EPR spectra show an interesting phenotype for MoFe protein with a substitution of Asp at the β-95-Cys site. Thus, the β-95^{Asp} MoFe protein from stain DJ1096 was purified in order to further characterize its catalytic properties. Wild-type MoFe protein from DJ527 was purified in a parallel purification protocol except the phenyl-Sepharose step. Table 3-3 summarizes the purification procedure for the β-95^{Asp} and wild-type MoFe protein.

Twenty two-fold and fourteen-fold purification was achieved for wild-type and β-95^{Asp} MoFe protein, respectively. Twenty six percent and nineteen percent yields were achieved for the wild-type and β-95^{Asp} MoFe protein, respectively. SDS-PAGE (Figure 3-3-2) shows that both wild-type and β-95^{Asp} MoFe proteins contain two bands, which correspond to the α- and β-subunits of the MoFe protein. As judged by SDS-PAGE, purity of the wild-type MoFe protein is over 95% and the purity of the β-95^{Asp} is over

Table 3-2. Heat Stability of the β-95^{Asp} strain at Crude Extract Level.

Temp	β-95^{Asp} Crude Extract Specific Activty[a] (nmoles H_2/min.mg)	Wild-type Crude Extract Specific Activity[a] (nmoles H_2/min.mg)
40°C	6.6	54.5
45°C	7.1	55.5
50°C	6.7	56.0
55°C	6.5	57.5
60°C	2.0	52.5

a.Crude extracts were incubated for 5 min at the indicated temperatures before being rapidly cooled and then assayed at 30°C under 100% argon with an optimal amount of wild-type Fe protein added.

Table 3-3. MoFe Protein Purification from DJ1096 (β-95^{Asp}) and DJ527 (wild type)

Purification Step	Total Protein (gram)		Total Activity[a] mmol H_2/min/mg		Specific Activity[a] nmol H_2/min.mg		Fold of Purification		Yield (%)	
	WT	β-95^{Asp}	WT	β-95^{Asp}	WT	β-95^{Asp}	WT	β-95^{Asp}	WT	β-95^{Asp}
Crude Extract	11.3	7.4	1.1	0.14	94	19	1	1	100	100
Q-Sepharose	1.6	1.2	1.0	0.13	642	114	6.8	6	95	94
Sephacryl-300	0.8	0.1	0.9	0.03	1131	271	12.0	14	82	19
Phenyl-Sepharose	0.13	--------	0.28	-------	2074	--------	22	--------	26	------

a. Crude extracts were prepared using sonication followed by heat treatment at 55^{0}C for 5min and then centrifugation at 98000Xg for 90 minutes to remove the cell debris from the supernatant

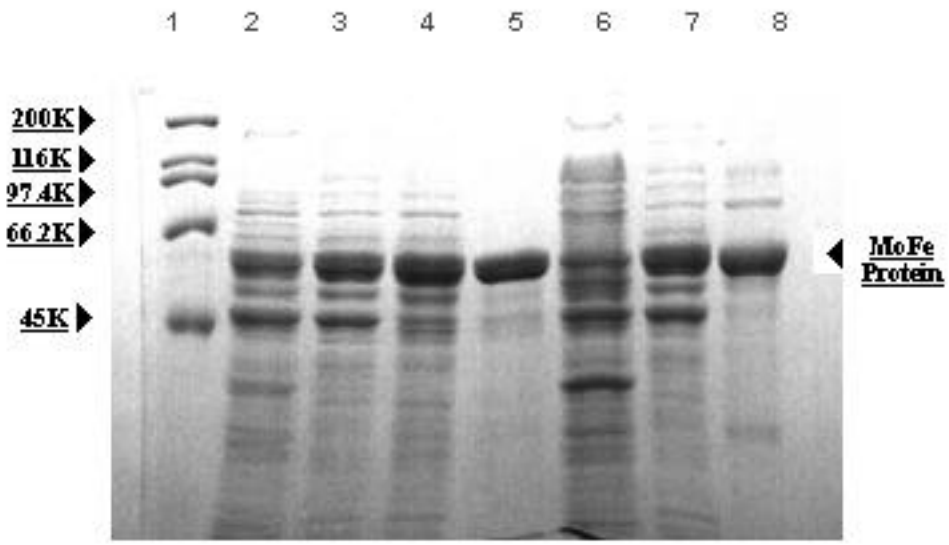

Figure 3-3-2. SDS-PAGE for each purification step of wild-type and β-95^{Asp} MoFe proteins. Lane 1: Molecular Weight Marker; Lane 2 - Lane 5 Wild-type MoFe purification: Lane 2: crude extract; Lane 3: Q-Sepharose ; Lane 4: Sephacryl S-300; Lane 5: phenyl-Sepharose; Lane 6- Lane 8: β-95^{Asp} purification; Lane 6: crude extract; Lane 7: Q-Sepharose; Lane 8: Sephacryl S-300.

90%. Figure 3-3-2 shows the SDS-PAGE for each purification step for both the wild-type and the β-95^{Asp} MoFe proteins.

The wild-type Fe protein was purified and assayed with an added optimal amount of wild-type MoFe protein. The highest Fe protein H^+-reduction specific activity was 2400 nmoles H_2/min/mg.

The wild-type Fe protein was purified as described in the experimental procedures section, and as was shown in SDS-PAGE (figure 3-3-3), 95% purity of the wild-type Fe protein was obtained.

3.3.6. H^+ reduction titration assay for β-95^{Asp} MoFe protein with wild-type Fe protein

In order to characterize the MoFe protein catalytic properties of the β-95^{Asp} MoFe protein. H^+ reduction titration assays with wild-type Fe protein were performed both under 100% Ar and 10% CO plus 90% Ar atmospheres. The parallel experiments for wild-type MoFe protein were performed as well. The results are shown in Figure 3-4-1 and Figure 3-4-2. It was found that at low electron flux, CO has a significant enhancement of H^+-reduction activity for β-95^{Asp}, but at high electron flux, CO did not have this effect. For wild-type MoFe protein, CO produces a 10-15% enhancement in H^+-reduction activity at both low and high electron flux. ATP hydrolyzed in the reaction has also been evaluated, and ATP/2e^- ratios were calculated for each assay. We find that, for the wild-type MoFe protein, the ATP/2e^- ratios remain constant at 6.0, with or without 10% CO in the reaction atmospheres. In contrast, the β-95^{Asp} MoFe protein reveals different features. Under 10% CO, the ATP/2e^- ratios remain constant at 6.5±0.5, but under 100% Ar (no CO), the ATP/2e^- ratio decreases from 67.5±13.5 to

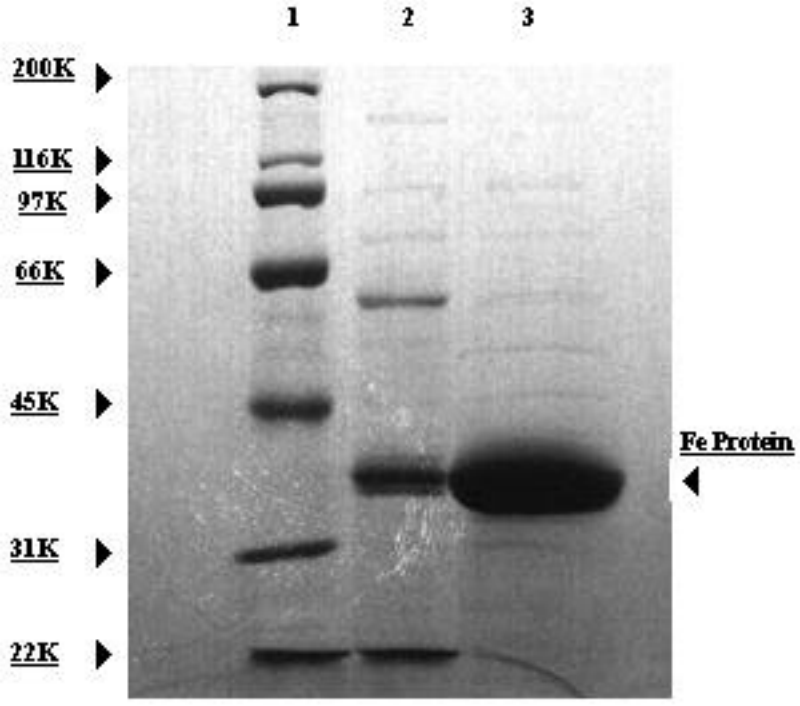

Figure. 3-3-3. Purification of Fe protein. Lane 1, MW marker; Lane 2, first Q-Sepharose; Lane 3, second Q-Sepharose.

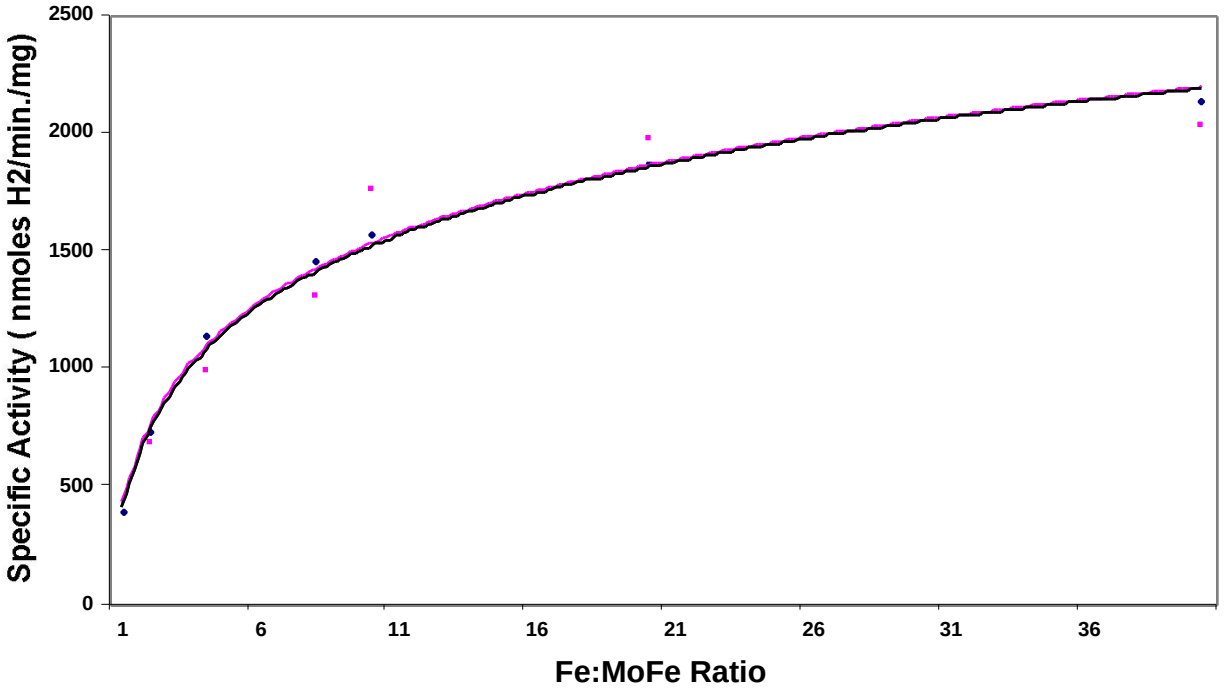

Figure.3-4-1. Proton-Reduction Titration of Wild-type MoFe Protein with Wild-type Fe Protein. The component protein ratio varies while wild-type MoFe protein concentration (0.1mg/ml) was kept constant. Assays were performed under Argon with( ) or without ( )10% CO, the specific activity is expressed as nmoles H_2 per min. per mg MoFe protein.

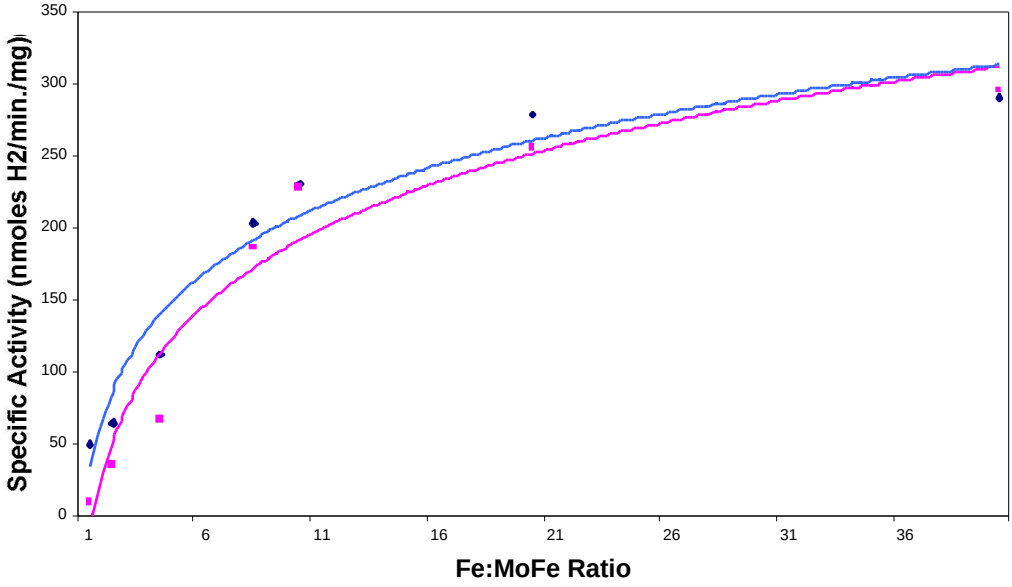

Figure.3-4-2. Proton-Reduction Titration of β-95-Asp MoFe Protein with Wild-type Fe Protein. The component protein ratio varies while wild-type MoFe protein concentration (0.1mg/ml) was kept constant. Assays were performed under Argon with (◆) or without 10% CO (■), the specific activity is expressed as nmoles H_2 per min. per mg MoFe protein.

Table 3-4. ATP/2e$^-$ ratio changes when electron flux increases for the β-95^{Asp} under 100% Ar.

Fe/β-95^{Asp} ratio	1:1	2:1	4:1	8:1	10:1	20:1	40:1	60:1
ATP/2e- ratio	67.5 ±13.5	19.5 ±3.5	14.5 ±1.0	7.2 ±0.3	7.8 ±0.5	7.1 ±0.7	6.7 ±0.5	6.3 ±0.5

6.3±0.5 when the electron flux increases (Table 3-4).

3.3.7. C_2H_2-reduction titration assay for the β-95^{Asp} MoFe protein with wild-type Fe protein

In order to compare any effects of the β-95^{Asp} substitution on C_2H_2 reduction, similar titration assays with wild-type Fe protein were performed both under 10% C_2H_2/90% Ar and under 10% C_2H_2/80% Ar/10% CO atmosphere. The parallel experiments for wild-type MoFe protein were performed as control. The results are shown in Figure 3-5-1 and Figure 3-5-2.

From Figure 3-5-1 and 3-5-2, for both β-95^{Asp} and β-95^{Cys} MoFe, C_2H_2 inhibits proton reduction and this inhibition can be relieved by CO. For β-95^{Asp}, under 10% C_2H_2/90% Ar, the maximum specific activity for C_2H_2 plus H_2 production is about 220 nmoles $2e^-$/min.mg. This value is lower than the maximum specific activity under 100% Ar, which is about 300 nmoles $2e^-$/min.mg. When CO is added to give a 10% CO 10%/C_2H_2/80% Ar atmosphere, no C_2H_4 is detected and the maximum specific activity increases about 22%. For wild-type MoFe protein, a maximum specific activity increase with CO added is about 15-20% and C_2H_4 is not detected with CO added as well. Under 10% C_2H_2/90% Argon atmosphere, the ratio of $2e^-$ transferred to C_2H_2 vs. to proton is different for wild-type and β-95^{Asp} MoFe protein, for wild-type MoFe protein, this ratio is about 6:1, while for β-95^{Asp} MoFe protein, it's about 4:1.

ATP hydrolyzed in each reaction was measured for each assay and ATP/$2e^-$ ratios were calculated. For the β-95^{Asp} MoFe protein, it was found that under 10% C_2H_2 without CO, the ATP/$2e^-$ ratio remains constant around 7.5±0.8 whereas with 10% CO,

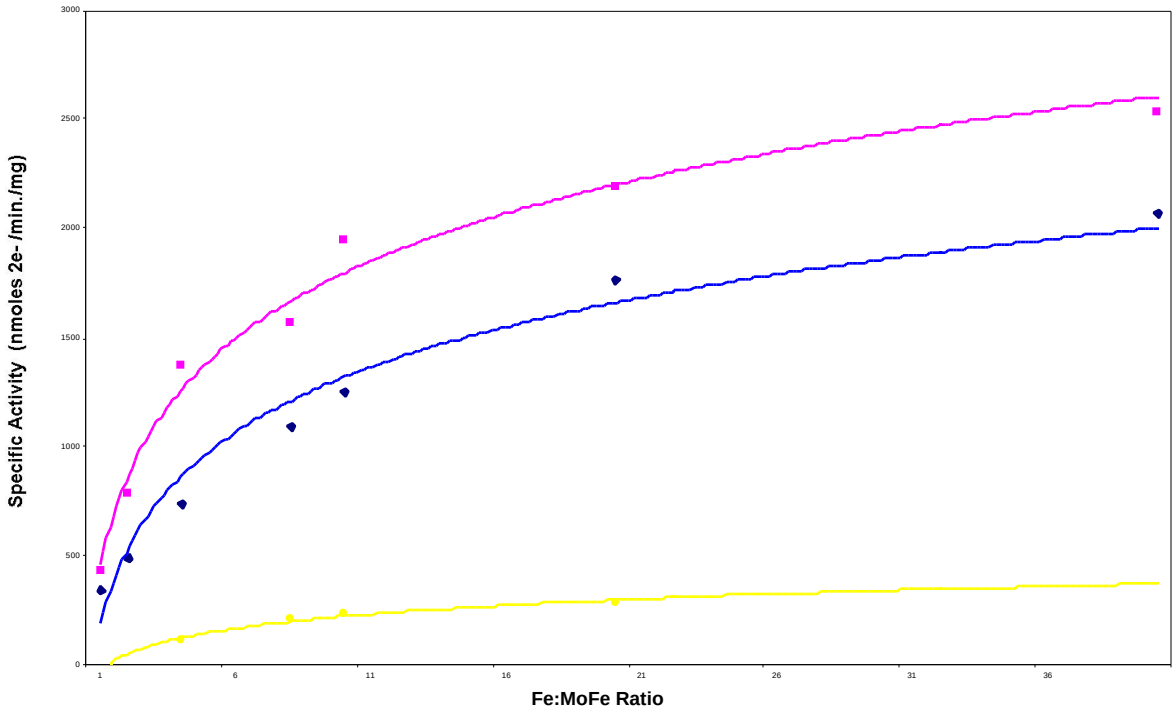

Figure 3-5-1. C_2H_2 Reduction Titration of Wild-type MoFe Protein with Wild-type Fe Protein. The component protein ratios were varied while the MoFe protein was fixed at 0.1 mg. Assays were performed under both 90% Argon/10% C_2H_2 (: H_2 Specific activity; : C_2H_4 specific activity) and 10% CO/10% C_2H_2 /80% Argon (: H_2 specific activity). The specific activity is expressed as nmoles of C_2H_4 or H_2 per minutes per mg MoFe protein.

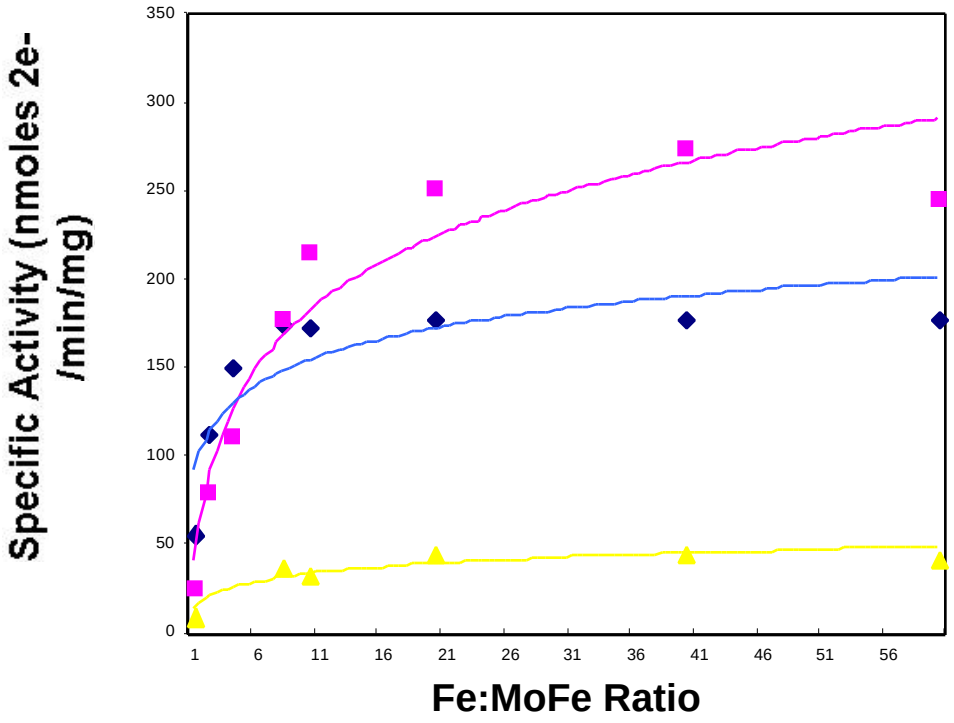

Figure 3-5-2. C_2H_2 Reduction Titration of β-95^{Asp} MoFe Protein with Wild-type Fe Protein. The component protein ratios were varied while the MoFe protein was fixed at 0.1 mg. Assays were performed under both 90% Argon/10% C_2H_2 (: H_2 specific activity; : C_2H_4 specific activity) and 10% CO/10% C_2H_2/80% Argon (: H_2 specific activity). The specific activity is expressed as nmoles of C_2H_4 or H_2 per minutes per mg MoFe Protein.

Table 3-5. ATP/2e$^-$ ratios decrease when electron flux increase for the β-95^{Asp} MoFe protein under 10%CO/10% C_2H_2/80% Argon

Fe: β-95^{Asp}	1:1	2:1	4:1	8:1	10:1	20:1	40:1	60:1
ATP/2e- Ratio	13.0± 0.2	8.7± 1.1	8.5± 0.3	7.4± 0.5	5.7± 0.2	6.7± 0.3	5.7± 0.2	6.6± 0.4

ATP/$2e^-$ ratio decreases from 13.0±0.2 to 5.7±0.2 as electron flux increase as shown in Table 3-5. For the wild-type, the ATP/2e- ratio remain 6.0±0.5.

3.3.8 N_2 fixation catalyzed by the β-95^{Asp} MoFe protein

It was found that the mutant carrying the β-95^{Asp} MoFe protein has a Nif^{slow} phenotype. This observation simply indicates that the β-95^{Asp} MoFe protein has some dinitrogen-fixation activity. In order to understand this activity better, N_2-reduction titration assays with wild-type Fe protein were performed under both 10% CO/90% N_2 and 100% N_2 atmospheres. The parallel experiments for wild-type MoFe protein were performed as a control. The results are shown in Figure 3-6-1 and 3-6-2.

The results show that N_2 can be fixed by β-95^{Asp} MoFe protein but at a lower efficiency compared to the wild-type. The titration curve is similar to that for wild-type MoFe protein. N_2 can partially inhibit H^+ reduction, and this inhibition can be relieved by the addition of 10% CO, which totally inhibits N_2-reduction. For wild-type MoFe protein, the ATP/$2e^-$ ratio remains constant at 6.5±0.5 under both 10% CO/90% N_2 and under 100% N_2 atmospheres. For the β-95^{Asp}, the ATP/$2e^-$ ratio remains constant at 11.0±0.7 under 100% N_2 and constant, but lower, at 7.5±0.9 under 10% CO/ 90% N_2 atmosphere. The electron distribution (expressed as the percentage of total electron that goes to H^+reduction) is also compared between wild-type and β-95^{Asp} MoFe protein under 100% N_2 (Table 3-6).

3.3.9 CO Enhancement for β-95^{Asp} at low flux

It was observed that at low flux, CO produced a significant enhancement of

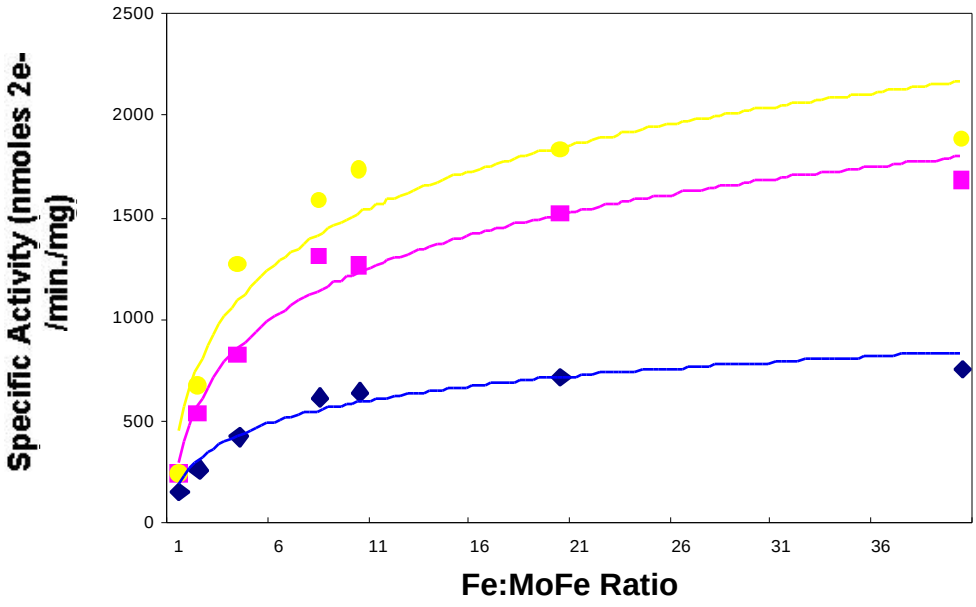

Figure 3-6-1. N_2 Reduction Titration of Wild-type MoFe Protein with Wild-type Fe Protein. The component protein ratios were varied while the MoFe protein was fixed at 0.1 mg. Assay were performed under both 100% N_2 (◆: H_2 specific activity; ■: 1.5 NH_3 specific activity) and 10% CO/90% N_2 (●: H_2 specific activity). The specific activity is expressed as nmoles of electron pairs to product per minute per mg MoFe Protein. This number is calculated as the nmoles H_2 product and 1.5 times the nmoles of NH_3 produced.

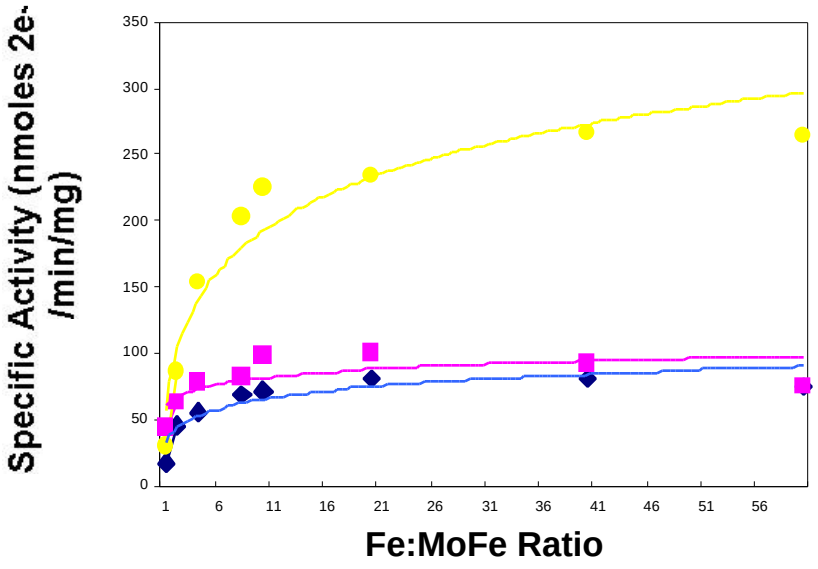

Figure 3-6-2. N_2 Reduction Titration of β-95^{Asp} MoFe Protein with Wild-type Fe Protein. The component protein ratios were varied while the MoFe protein was fixed at 0.1 mg. Assay were performed under both 100% N_2 (◆: H_2 specific activity; ■: 1.5 NH_3 specific activity) and 10% CO/90% N_2(●: H_2 specific activity). The specific activity is expressed as nmoles of electron pairs to product per minute per mg MoFe Protein. This number is calculated as the nmoles H_2 product and 1.5 times the nmoles of NH_3 produced.

Table 3-6. Electron distribution comparison under 100% N_2.

Fe: MoFe ratio	1:1	2:1	4:1	8:1	10:1	20:1	40:1	60:1
Wild-type(%)	38.8	33.8	34.0	32.1	34.0	32.4	31.5	30.6
β-95^{Asp} (%)	28.6	42.4	41.5	46.1	42.6	44.9	46.9	50.0

a. Electron distribution is calculated as the percentage of the electrons transferred to H^+ reduction, out of the total electrons transferred.

H^+-reduction specific activity for the β-95^{Asp} MoFe protein. To confirm this observation, a low flux ratio of 4:1 of Fe protein vs. β-95^{Asp} MoFe protein was selected to perform the H^+-reduction assay under a range of concentration from 0% CO to 10% CO. Wild-type controls were performed as well. Table 3-7-1 shows the results for β-95^{Asp} MoFe protein and Table 3-7-2 shows the results for wild-type MoFe protein.

It was found that the amount of ATP hydrolyzed in each assay remained same, only the H_2 produced varied for the β-95^{Asp} MoFe protein.

3.3.10 Limited $Na_2S_2O_4$ assay for the β-95^{Asp} MoFe protein at low flux (Fe: β-95^{Asp}= 8:1) with and without 10% CO.

In order to find out how CO affected the β-95^{Asp} MoFe protein H^+-reduction activity at low flux, and to determine whether it only altered the electron-transfer rate, or whereas electrons flowed to some other, as yet unknown, product, a 20-minute limited $Na_2S_2O_4$ assay experiment was designed. The Fe:β-95^{Asp} ratio was fixed at 8:1 and the amount of β-95^{Asp} MoFe protein increased from 0.1 mg to 1.2 mg in the assay. The results are shown in Figures 3-7-1 and 3-7-2. They show that in all experiments, all $Na_2S_2O_4$ present is used to produce H_2 and that CO increases the rate of H_2 evolution with the β-95^{Asp} MoFe protein.

3.3.11 Reductant-independent ATP hydrolysis by the β-95^{Asp} MoFe protein.

Because it was found that, under 100% argon, the ATP/$2e^-$ ratio decreases from 68±13 to 6.3±0.5 when the Fe: β-95^{Asp} ratio was increased, it was speculated that

Table 3-7-1: Enhancement by CO of H^+-reduction for the β-95^{Asp} MoFe protein at Fe: β-95^{Asp}= 4:1

CO concentration	10%	1%	0.1%	0.01%	0.0%
H_2 SPA*	181±1	155±8	103±13	59±1	54±2
ATP/$2e^-$	7.5±0	8.0±0	12.1±1.1	18.8±1.7	23.1±0.2

*SPA: specific activity, which is measured as nmoles H_2/min.mg

Table 3-7-2. Effect of CO on H^+-reduction by wild-type MoFe protein at Fe: MoFe=4:1

CO concentration	10%	1%	0.1%	0.01%	0%
H_2 SPA*	1121±76	1178±17	1090±21	1131±12	1085±27
ATP/2e-	4.8±0.5	4.6±0.1	5.3±0.2	5.0±0.1	5.3±0.1

*SPA: specific activity, which is evaluated as nmoles H_2/min.mg

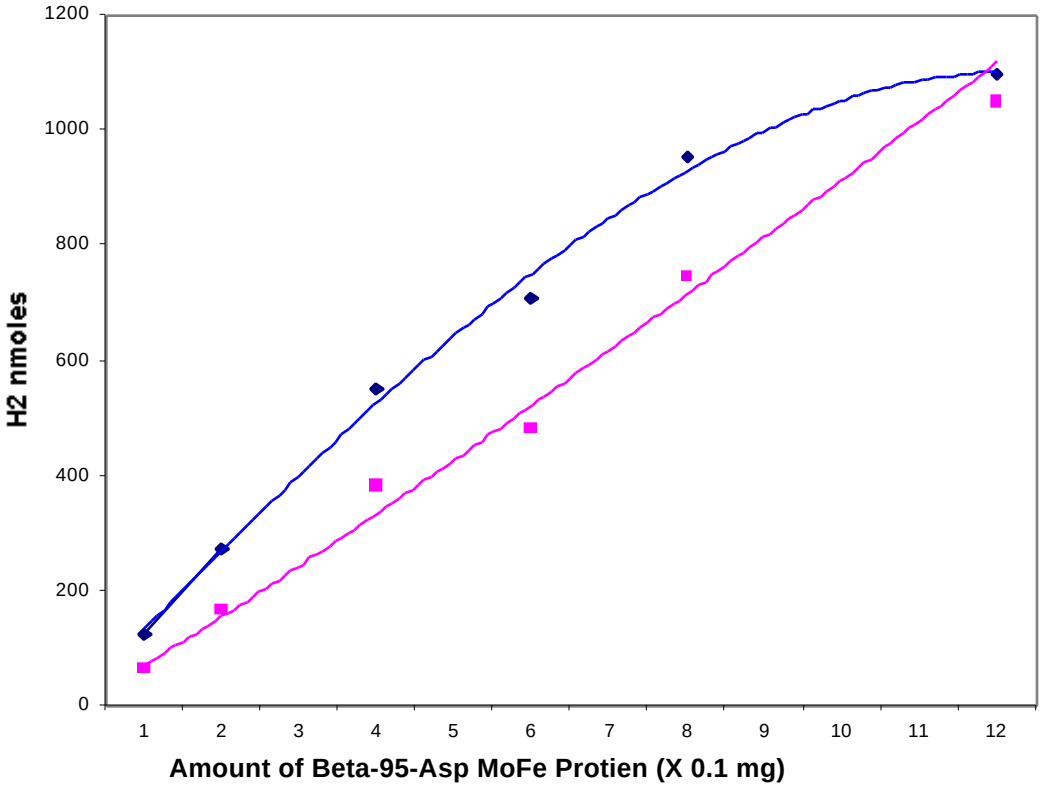

Figure 3-7-1. Limited Dithionite Assay of β-95^{Asp} MoFe Protein at Low Flux. The component protein ratio was fixed at Fe:MoFe=8:1 and the MoFe protein varied from 0.1mg to 1.2mg, the concentration of dithionite was fixed at 1.0-1.2 mM. Assays were performed under both 90% Argon/10% CO (◆) and 100% argon (■) for 20 minutes. The specific activity is expressed as nmoles of H_2 per minute per mg MoFe Protein.

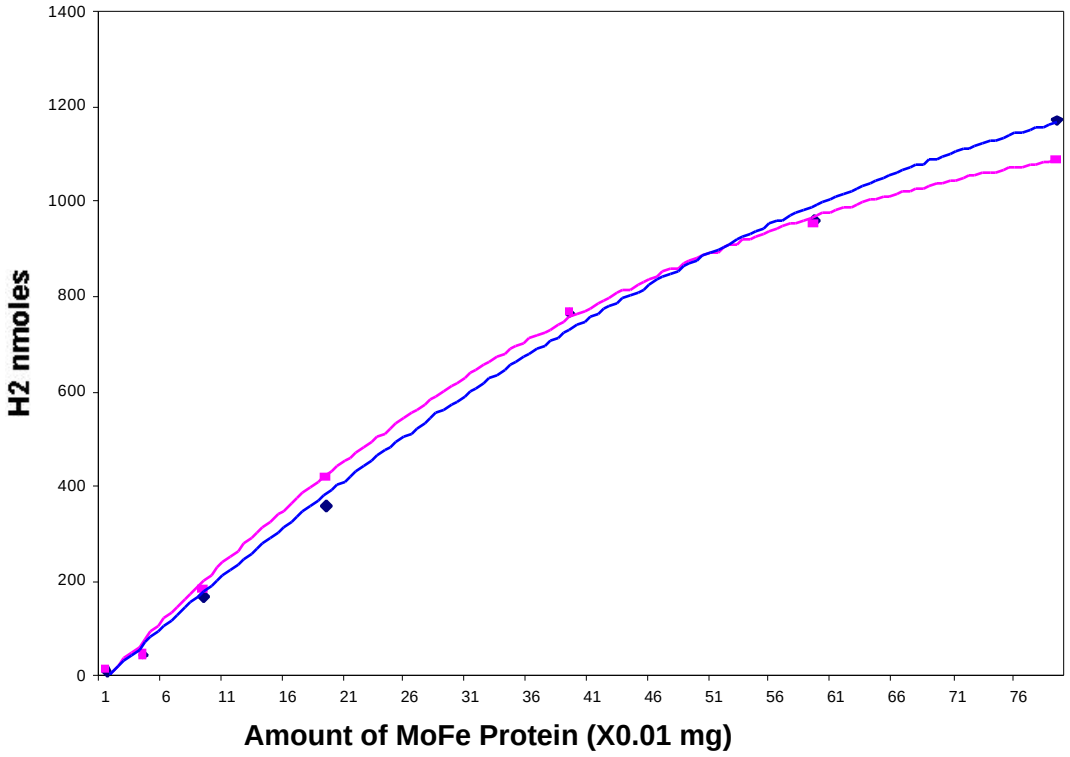

Figure 3-7-2. Limited Dithionite Assay of Wild-type MoFe Protein at Low Flux. The component protein ratio was fixed at Fe:MoFe=8:1 and the MoFe protein varied from 0.02mg to 0.8mg. The concentration of dithionite was fixed at 1.0-1.2 mM. Assay were performed under both 90% Argon/10% CO ( ) and 100% argon ( ) for 20 minutes. The specific activity is expressed as nmoles of H_2 per minute per mg MoFe protein.

reductant-independent ATP hydrolysis may be playing a role here. An experiment was designed to test reductant-independent ATP hydrolysis for the β-95^{Asp} MoFe protein using the wild-type MoFe protein as a control as described in section 3.2.10. The result is shown in Figure 3-8.

The reaction was performed with a limited amount of $Na_2S_2O_4$ (1mM, 1000 nmoles) under 10% Ar. The 1ml reaction volume includedeither 0.23mg wild-type or 0.1 mg β-95^{Asp} MoFe protein and the appropriate amount of the wild-type Fe protein (Fe: = 4:1), 25mM Hepes-NaOH pH 7.4, 2.5mM ATP, 5.0mM $MgCl_2$, 30mM creatine phosphate, 0.125 mg creatine phosphokinase. Reactions were stopped at 5 min., 10min., 15 min., 20min., 30min., respectively. ATP/2e- ratios were measured for each assay. The results show that, as time increases, the ATP/2e$^-$ ratio for β-95^{Asp} MoFe protein increases, but, for wild-type MoFe protein, the ATP/2e$^-$ ratio remains 9.0±1.0.

3.3.12 Electron Paramagnetic Resonance Spectrum of the partially purified β-95^{Asp} MoFe protein

The EPR spectrum for the β-95^{Asp} MoFe protein was shown in Figure 3-9. It reveals the typical signal for FeMoco at g=4.3 and g=3.6. It also has a signal at g=2.0, but this signal is not observed from the wild-type MoFe protein. We think this last signal maybe caused by the contamination.

3.3.13 Metal Analysis of the partially purified β-95^{Asp} MoFe protein.

Metal analyses for Mo and Fe were performed on duplicate samples of the β-95^{Asp} MoFe protein at two different concentrations. All four samples were found to contain 0.4 Mo atoms and 14.9 Fe atoms per molecule of MoFe protein compared to 2.0 Mo

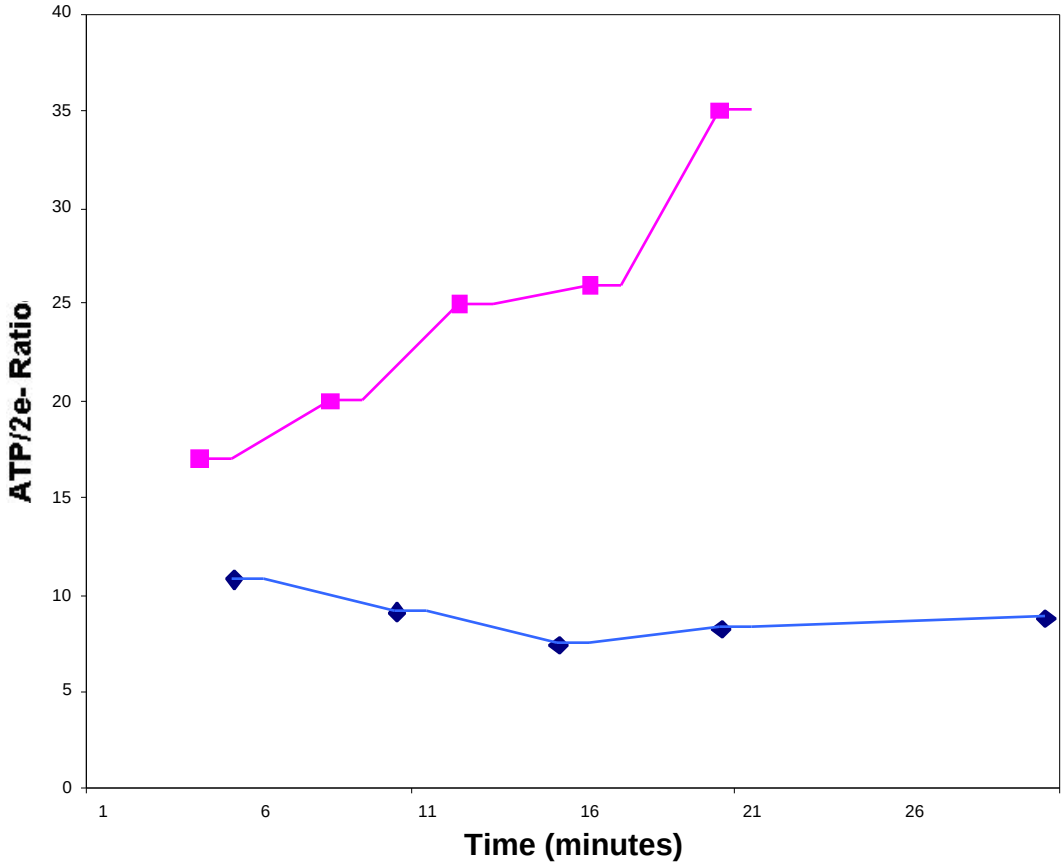

Figure 3-8. Reductant-independent ATP Hydrolysis Test of Wild-type (◆) and β-95^{Asp} (■) MoFe Proteins at Low Flux. The component protein ratio was fixed at Fe:MoFe=4:1 and the MoFe protein was fixed at 0.1mg. The concentration of dithionite was fixed at 1.0 mM and the assays were performed as a time-course under 100% argon.

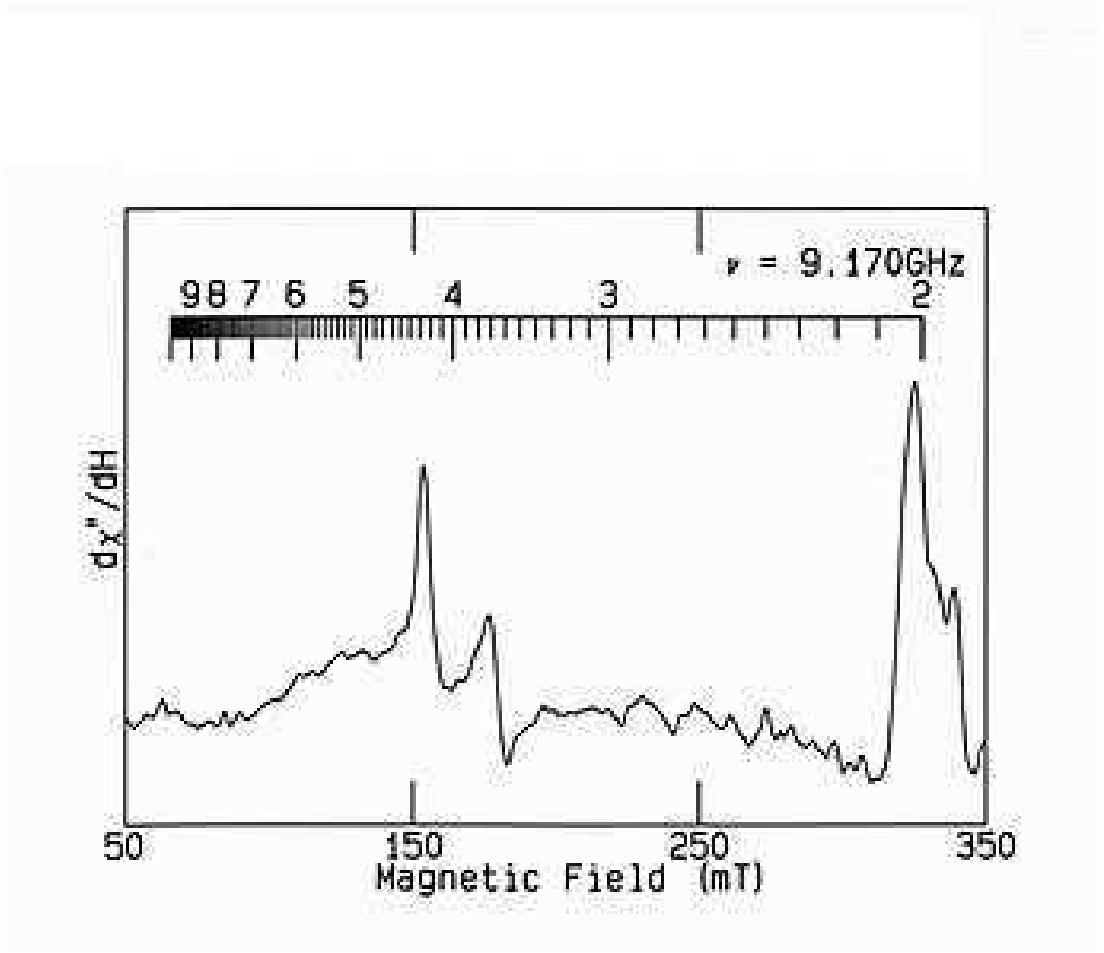

Figure 3-9. S=3/2 EPR Spectrum for the β-95^{Asp} MoFe Protein. The spectrum was recorded at 9.17 GHZ and 20 mW at 13K matained by liquid helium boil-off.
The typical signals for FeMoco at g=4.3 and g=3.6 were observed. A signal at g=2.0, is observed to be different from that is observed from the wild-type MoFe protein

and 30 Fe atoms expected for a purified, fully constituted MoFe protein. The Mo:Fe ratio for the β-95^{Asp} MoFe protein was thus found to be 1:37 compared to the expected 1:15.

3.4. Discussion

The currently accepted role of the P cluster is that of the primary acceptor of electrons from the Fe protein and their subsequent delivery intramolecularly to the FeMo-cofactor. This role is supported by the proposed structural models for the nitrogenase component proteins from ***A. vinelandii*** (Georgiadis ***et al***., 1992; Kim and Rees, 1992), the structure of the AlF_4^-/MgADP-stabilized complex of the two nitrogenase proteins (Schindelin et al., 1997) and the proposed docking model (Howard and Rees, 1996). The last two lines of support suggest that the P cluster is positioned directly in line between the prosthetic group of the electron donor (the Fe protein's [4Fe-4S] cluster) and the substrate-binding FeMo-co of the MoFe protein as would be expected if the P cluster was involved in electron acceptance from 4Fe-4S cluster and electron delivery to FeMoco.The structures of the nitrogenase MoFe protein in two of its available oxidation-reduction states (Peters ***et al.,*** 1997) show that, during the conformational interconversion of these two states, the distance between the central sulfur atom S1 and two of the Fe atoms in the sub-cluster associated with the β-subunit increase by 1 A or more. These observations also support the suggested role of the P cluster and by indicating that these redox-mediated structural changes may couple proton transfer to electron transfer.

The function of the P cluster has also been probed by directed mutagenesis studies, which introduce individual substitutions of P-cluster cysteinyl ligands. Previously, using the ***A. vinelandii*** MoFe protein, only α-88-Cys and β-153-Cys have been shown

to tolerate such replacements (Dean et al., 1990; May et al., 1991; J.S. Cantwell, Ph.D. thesis, Virginia Tech, 1998). Additionally, β-188-Ser is also substitutable by Gly (K. Fisher, personal communication). Our present study shows that β-95-Cys can also tolerate a substitution. The mechanistic significance of these observations is still under consideration but it is striking that the substitution of residues that coordinate the Fe atoms, which undergo movement as the MoFe protein cycles between the P^N and P^{ox} states, can be achieved without complete disruption of nitrogenase activity.

3.4.1. Substitutions at the β-95-Cys residue

In the present study, the strictly conserved β-95-Cys residue was targeted for several reasons. Firstly, β-95-Cys is located within the P cluster environment and serves as a coordinate ligand of the P cluster. Secondly, the counterpart of the β-95-Cys residue, the α-88-Cys residue, which also is involved in bridging the two partial Fe_4S_3 sub-clusters, can be replaced and still contain significant nitrogenase activity. Thus, it was reasonable to speculate that substitution at β-95-Cys may not always result in the complete loss of activity. Finally, the redox-dependent structural changes in the nitrogenase P-cluster suggest that β-188-Ser and α-88-Cys may serve to open and close an entrance for electrons arriving from the Fe protein, whereas the other cysteinyl ligands, especially the bridging β-95-Cys residue, may serve as hinges in the structural interconversion. Amino acid substitution at the β-95-Cys residue was undertaken in order to provide insight into the role played by the P-cluster in catalysis.

Crude-extract level EPR spectroscopy shows that mutant strains containing the β-95^{Trp}, β-95^{Lys}, β-95^{Glu}, β-95^{Ser} and β-95^{Asp} substitutions exhibit a typical FeMoco EPR signal, albeit very weakly, whereas those with the β-95^{Arg}, β-95^{Val} and β-95^{Thr}

substitutions either do not exhibit the typical FeMo cofactor EPR signal or the signal is too weak to be observed. However, the observation of FeMoco EPR signals from crude extracts of some, at least, of these mutant strains clearly suggests the possibility of nitrogenase activity and also demonstrates that the β-95-Cys residue is not required for insertion of the FeMoco into the apo-MoFe protein during maturation. However, the β-95-Cys residue must play an important role in electron/proton transfer to substrate because, among the 8 mutant strains studied, only the strain (DJ1096) with the Asp substitution at residue β-95 retains a Nif^{slow} phenotype and significant catalytic activity in crude extracts. It is possible that these substitutions interrupt the redox-driven conformational interconversion.

3.4.2. The β-95^{Asp} MoFe protein

The decision to purify the altered MoFe protein from mutant strain DJ1096 was prefaced by a determination of its heat stability because a heat step of 55°C for 5 minutes is part of the normal nitrogenase purification protocol. By monitoring the H_2-evolution activity, it was found that the β-95^{Asp} MoFe protein in crude extracts could tolerate 55°C for 5 minutes but, unlike wild type, it could not tolerate pre-incubation at 60°C for 5 minutes. This indication of inherent instability was confirmed during the Phenyl-sepharose chromatography step of purification. Although similar purification was achieved on Q-Sepharose (about 6-fold) and Sephacryl S-300 (about 13-fold) columns for both wild-type and β-95^{Asp} MoFe proteins, no active β-95^{Asp} MoFe protein-containing material could be recovered from Phenyl-sepharose chromatography. At a comparable state of purity, the wild-type and altered MoFe proteins had specific activities of 1131 and 271 nmol H_2 $(min.mg)^{-1}$, respectively, i.e., the inherent activity of the altered MoFe protein was about four-times less than that of wild type. The SDS-PAGE gel of the partially purified altered MoFe protein did not show many

contaminants and this observation suggests that some form of inactive apo-MoFe protein was co-purifying with the active β-95^{Asp} MoFe protein. Metal analysis confirmed that the majority of the material collected after the Sephacryl S-300 column was not holo-β-95^{Asp} MoFe protein. The Mo content was found to be equivalent to only 0.4 Mo atom per MoFe protein molecule, which indicates that only 20% of the collected material contained FeMoco. In contrast, the Fe analysis indicated 15 Fe atoms per MoFe molecule, which suggested 50% of the β-95^{Asp} MoFe proteins contain a full complement of Fe. Altogether, these data suggest that the preparation has 20% holo-protein, 30% FeMoco-deficient apo-protein and 50% of contaminating proteins. Because the specific activity of this preparation is only about 20% of that of wild-type MoFe protein, this conclusion indicates that the active, altered holo-protein present has a specific activity comparable to that of wild type. The EPR spectrum of the partially purified β-95^{Asp} MoFe protein, which shows a clean FeMoco signal around g=4 but extensive contamination with non-FeMoco signals around g=2, is also consistent with this conclusion. Further, the position and shape of the signals from the β-95^{Asp} MoFe protein at g values around 4 are identical with those of wild-type MoFe protein indicating that the β-95-Asp substitution has not, as expected, affected either the electronic state or the environment of FeMoco. Because no example exists of a protein containing FeMoco without P clusters, a reasonable hypothesis is that these prosthetic groups are inserted sequentially with the P cluster inserted first. Without the P cluster being present, FeMoco cannot be inserted. Thus, the stability of the P cluster and its polypeptide pocket will affect insertion of the FeMoco. This conclusion is affirmed by our observations resulting from the metal analyses.

3.4.3. Catalytic activities of the partially purified β-95^{Asp} MoFe protein

A survey of the catalytic activities of the partially purified β-95^{Asp} MoFe protein revealed some interesting differences to the comparable wild-type activities. The activities surveyed were: (1) H^+ reduction; (2) C_2H_2 reduction; (3) N_2 reduction; (4) CO inhibition of each of these reactions; and (5) MgATP hydrolysis for each reaction. The effects of each substrate and inhibitor were investigated by performing an electron flux titration. These experiments are performed by maintaining both substrate and inhibitor concentrations constant as well as keeping the amount of β-95^{Asp} MoFe protein constant and increasing the amount of Fe protein added. In this way, the molar ratio of Fe protein-to-MoFe protein increases throughout the titration from 1:1 to 40:1 and produces an increasing flux of electrons through the MoFe protein to substrate.

As occurs for wild type during catalyzed H^+ reduction, the increasing electron flux resulted in an increasing specific activity for the β-95^{Asp} MoFe protein until saturation was reached (at the much lower specific activity of 280 nmol(min.mg)$^{-1}$) at a Fe protein-to-MoFe protein of about 20:1. If the Fe protein is treated as a substrate of the MoFe protein, a K_m (as a ratio) for the interaction can be estimated from the titration curve (Figures 3-4-1 and 3-4-2). For the wild-type, this Km is about 4:1 whereas, for the β-95^{Asp} MoFe protein, it is about 6:1, which indicates that the protein-protein/electron transfer interaction has been somewhat perturbed by the β-95-Asp substitution.

When 10% CO was added and the titration curves re-evaluated in parallel, significant differences were found. For wild type, the typical increase in specific activity of about 10% was found throughout the titration range (Figure 3-4-1 and Table 3-7-2). However, with the β-95^{Asp} MoFe protein, a greater increase in H_2 evolution was observed with added CO but it was most significant at low flux, i.e., at Fe protein-to-MoFe protein molar ratios of 8:1 or less. The maximum difference in specific activity, a 2-3-fold increase under CO, occurred at a ratio of about 4:1.

Measurement of MgATP hydrolysis rates for these titration assays showed that, for each MoFe protein, they remained constant whether or not CO was present. Thus, the effect of CO with the β-95^{Asp} MoFe protein is on some aspect of substrate reduction and not on MgATP hydrolysis. This effect is clearly seen when these data are translated into the ratio, ATP/2e-, which reflects the number of moles of ATP hydrolyzed for each electron pair appearing as substrate. Based on two nucleotide-binding sites on each Fe protein, which usually delivers one electron, this ATP/2e$^-$ ratio would minimally be 4, but it is often measured experimentally as 5-6. For wild type with and without CO and for β-95^{Asp} MoFe protein with CO, this ratio varied between 5-7 (Tables 3-7-1 and 3-7-2) but, for β-95^{Asp} MoFe protein without CO, it increased to as high as about 70 (Table 3-4).

To determine if this CO-enhancement was common to all substrate reductions catalyzed by the β-95^{Asp} MoFe protein, similar titration experiments were performed under 10% C_2H_2/90% argon, 10% C_2H_2/10% CO/80% argon, 100% N_2 and 10% CO/90% N_2. In wild-type control experiments under 10% C_2H_2, typical results were obtained with about 10-15% of the electron flux appearing as H_2 and the remainder producing C_2H_4. With added CO, all electron flux produced H_2 (Figure 3-5-1). For all assays, the ATP/2e$^-$ values were about 6.

Using the β-95^{Asp} MoFe protein under 10% C_2H_2, a similar percentage of electron flux to that used by wild type appeared as H_2 but the total specific activity (C_2H_4 + H_2) at a 40:1 ratio was less (220 nmol product (min.mg)$^{-1}$) than under 100% argon when only H_2 was being produced (280 nmol (min.mg)$^{-1}$). When 10% CO was added, again all flux flowed to the production of H_2 but, additionally, the specific activity increased to about 270 nmols H_2 (min.mg)$^{-1}$. Similarly, under 100% N_2, the wild-type nitrogenase controls showed typical results with the H_2 produced accounting for an average of

35% of the electron flux (Table 3-6). The remaining flux produced NH_3. With added CO, all electron flux produced H_2. Again, the ATP/$2e^-$ values were about 6. The results under 100% N_2 with the β-95^{Asp} MoFe protein reflected its Nif^{slow} phenotype. In this case, an average of 46% of the electron flux produces H_2 (Table 3-6). With added CO, only H_2 is produced. As was found under 10% C_2H_2, the total specific activity (NH_3 + H_2) of the β-95^{Asp} MoFe protein under 100% N_2 is less than when 10% CO is present. With CO present, the specific activity increased to the expected 270 nmols $H_2(min.mg)^{-1}$.

This small inhibition of electron flux for the β-95^{Asp} MoFe protein under both 10% C_2H_2/90% argon and 100% N_2 is reminiscent of the inhibition observed under 100% argon because, just like that inhibition, it is completely reversed by CO. However, unlike the inhibition under 100% argon, the inhibition observed under either 10% C_2H_2/90% argon or 100% N_2 cannot be overcome simply by increasing flux. A difference in these inhibitory effects is also reflected in the ATP/$2e^-$ values for the experiments. Under C_2H_2 +/- CO, all ATP/$2e^-$ values were in the range 7.5 +/- 1.5, which reflects relatively good coupling between electron transfer and ATP hydrolysis. Thus, C_2H_2 must affect both electron flux and the rate of MgATP hydrolysis equally and its effect on both of these processes must be relieved by CO. In contrast, under 100% argon, the presence of CO is required for efficient coupling (Tables 3-4 and 3-7-1), otherwise MgATP hydrolysis continues at a normal rate and only electron flux is decreased. Thus, it appears that two separate inhibitory effects are operating. The first effect occurs under 100% argon and uncouples electron flux from ATP hydrolysis by decreasing electron flux only. It is apparently relieved by either CO or C_2H_2. The second, weaker, inhibitory effect acts on both electron flux and MgATP hydrolysis and is specific for the presence of C_2H_2. The situation under a N_2 atmosphere appears more complicated because the ATP/$2e^-$ ratio also decreased somewhat when CO was present from 11.0+/-0.7 under 100% N_2 to 7.5+/-0.9 with 10% CO present. These

observations suggest that the effect of N_2 reflects an intermediate situation in which a combination of the two inhibitory effects is operating.

The first of these inhibitory effects was initially investigated by studying the dependence of both the activity enhancement and MgATP coupling to electron flux on CO concentration. It was confirmed in assays performed at a Fe protein-to-β-95^{Asp} MoFe protein molar ratio of 4:1, where both effects were maximal. It was found that 1% CO was almost as effective as 10% CO but concentrations less than 1% were considerably less effective (Table 3-7-1). CO had no significant effect on either H_2-evolution activity or the coupling of MgATP hydrolysis to electron flux in wild type (Table 3-7-2).

The next question to answer was whether the decrease in electron flux observed in the absence of CO is real or is caused by some, unknown product of the reaction not being observed and measured. This question was investigated by conducting H_2-evolution activity assays (with or without CO) at a constant 8:1 Fe protein-to-MoFe protein molar ratio in the presence of limiting (1.2 mM) $Na_2S_2O_4$ for 20 minutes. The experimental variable was the absolute concentration of the nitrogenase proteins, which increased from 0.1 mg/ml to 1.2 mg/ml for the β-95^{Asp} MoFe protein and 0.1 mg/ml to 0.8 mg/ml for wild-type MoFe protein. For wild type, there was no significant difference in H_2-evolution activity between those assays containing CO and those without CO. In addition, both sets of assays showed that, at the highest nitrogenase concentration, all electrons from $Na_2S_2O_4$ appear as H_2 (Figure 3-7-2). The parallel β-95^{Asp} MoFe protein experiments confirmed the increase in the rate of H_2 evolution when CO was present but also showed that, at the highest nitrogenase concentrations, all electrons from $Na_2S_2O_4$ result in H_2 evolution (Table 3-7-1). So, given sufficient time and enzyme concentration, the β-95^{Asp}-substituted nitrogenase

will utilize all available electrons for H_2 production and, thus, no unexpected products are formed.

The uncoupling of electron flux from MgATP hydrolysis under 100% argon with nitrogenase utilizing the β-95^{Asp} MoFe protein was further investigated by performing time course assays with limited (1 mM) $Na_2S_2O_4$ at a constant 8:1 Fe protein-to-MoFe protein molar ratio with monitoring of the ATP/2e$^-$ ratio. Under these conditions, wild-type nitrogenase maintained a constant ATP/2e$^-$ ratio of 9+/-1 for 20 minutes. In contrast, the β-95^{Asp} MoFe protein exhibited a steadily increasing ATP/2e$^-$ ratio with time. It increased from 10 at 2 minutes to 35 after 20 minutes. This result is consistent with the observed uncoupling for the β-95^{Asp} MoFe protein and suggests that reductant-independent MgATP hydrolysis is occurring.

Reductant-independent MgATP hydrolysis has been shown to occur when dye-oxidized Fe protein complexes with MoFe protein (Thorneley ***et al***., 1991). This complex is capable of turning over MgATP in the absence of reductant. The individual proteins cannot hydrolyze MgATP on their own. It has been suggested that, once the nitrogenase complex has formed, MgATP hydrolysis is inevitable whether or not electron transfer occurs (Burgess and Lowe, 1996). In the last experiment, the initially high $Na_2S_2O_4$ concentration produces the lowest ATP/2e$^-$ ratio. Under these initial conditions, the reduced form of the Fe protein would be expected to be in excess but, as the $Na_2S_2O_4$ concentration decreases with time, the oxidized Fe protein would start to become dominant. Thus, at the later stages of the time course, the oxidized Fe protein would compete increasingly successfully for the β-95^{Asp} MoFe protein. The expected consequence of this situation would be steadily increasing reductant-independent MgATP hydrolysis, leading to ever-increasing uncoupling of MgATP hydrolysis from electron flux to product, which is consistent with the experimental result. The results from the C_2H_2-reduction and N_2-fixation titration assays with the β-

95^{Asp} MoFe protein show that the binding of substrate, not only CO, can decrease reductant-independent MgATP hydrolysis and, thus, maintain a constant ATP/2e$^-$ ratio.

Now that it has been shown that there is a definite decrease in the rate of electron flux when CO is absent, the question becomes one of now trying to identify the source of these two inhibitory effects. The major possibilities are in four general areas: (1) perturbations at the substrate-binding FeMoco; (2) disruption of the intra-MoFe protein electron-transfer pathway; (3) disruption of electron acceptance/donation by the P cluster; and (4) interference of the inter-molecular electron transfer from Fe protein to the MoFe protein. The third area is the most likely source of the changed catalytic properties because the β-95-Asp substitution is of a P-cluster ligand. Of the other three possibilities, inhibition by means of a perturbation at FeMoco and so an effect on substrate or inhibitor binding can be readily ruled out because the FeMoco center has not been affected by the β-95-Asp substitution as evidenced by its EPR spectrum. The other two areas of possibility cannot be ruled out on the available evidence. However, it is reasonable to speculate that the β-95-Asp substitution affects catalytic properties through an alteration in the vicinity of the P cluster.

One possibility is that the P cluster's capacity for accepting and delivering electrons has been affected. It could be unable now to reach a redox state required for catalysis. If so, it is not because the P cluster is unable to become oxidized. In that case, most oxidized P cluster states would be EPR-active and no new signals appear in the EPR spectrum. It is more likely that the P cluster in the β-95^{Asp} MoFe protein is unable to undergo as readily as wild type the structural interconversion described above. This is a likely possibility because β-95-Cys forms the hinge around which this interconversion must occur. It is unlikely that the binding of CO to the FeMoco site would affect action at the P cluster, so another possibility is that the β-95-Asp substitution has introduced a CO-binding site on the P cluster. Such binding sites

have been suggested previously without much evidence to support them. The binding of CO could displace a P-cluster ligand, one that is not bound normally with wild type, and thus facilitate the structural interconversion. Without the binding of CO, the P cluster could be unable to accept (or donate) electrons as rapidly as usual and this situation means that any Fe protein docking with this “stalled” MoFe protein cannot transfer its electron. It must then hydrolyze its bound MgATP and leave still its reduced state. To a lesser extent, C_2H_2 (and possibly N_2) might have the same effect. If so, then a consequence of its binding to the P cluster seems to be that, in overcoming this “stalling” problem and re-establishing good coupling of MgATP hydrolysis to electron flux, a second inhibitory effect is introduced. This second form of inhibition results in a general overall slow down and C_2H_2 binding to the P cluster may be affecting the Fe protein-MoFe protein interaction possibly decreasing the affinity of the MoFe protein for the Fe protein. However, we have gathered no evidence to support this line of speculation.

Chapter 4. References.

Anderson, G.L., Howard, J.B., 1984, ***Biochemistry* 23**, 2118-2133.

Appl M., 1976, ***Nitrogen* 100**, 47-49.

Arber, J.M., Dobson, B.R., Eady, R.R., Stevens, P., Hasnain, S.S., Garner, C.D., Smith, B.E., 1987, ***Nature* 325**, 372-374.

Arber, J.M., Dobson, B.R., Eady, R.R., Hasnain, S.S., Garner, C.D.,Matsushita, H., Nomura, M., Smith, B.E., 1989, ***Biochem. J.* 258**, 733-737

Arnold, W., Rump, A., Klipp, W., Priefer, U.B., Puhler, A., 1988, ***J. Mol. Biol*. 203**, 715-738.

Beynon, J., Ally, A., Cannon, M., Cannon, F., Jacobson, M.R., Cash, V. L., Dean, D., 1987, ***J. Bacteriol.* 169**, 4024-4029

Beynon, J., Cannon, M., Buchanan -Wollaston, V., Ally, A., Setterquist, R., Dean, D., Cannon, F., 1988, ***Nucleic Acids Res.* 16**, 9860

Bolin, J.T., Ronco, A.E., Mortenson, L.E., Morgan, T.V.,Williamson,M., Xuong, N-h., 1990, In ***Nitrogen fixation:Achievements and objectives*** (Gresshoff, P.M., Roth, L.E., Stacy, G., Newton, W.E., eds) Chapman and Hall, New York & London. pp. 117-124

Brigle, K.E., Newton, W.E., Dean, D.R., 1985, ***Gene* 37**, 37-44

Brigle, K.E., Setterquist, R.A., Dean, D.R., Cantwell, J.S., Weiss, M.C., Newton, W.E., 1987, ***Proc. Natl. Acad. Sci. USA* 84**, 7066-7069

Brigle, K.E., Weiss, M.C., Newton, W.E., Dean, D.R., 1987, ***J. Bacteriol***. **169**, 1547-1553

Buikema, W.J., Klingensmith, J.A., Gibbon, S.L., Ausubel, F.M., 1987, ***J. Bacteriol.*** **169**, 1120-1126

Buikema, W.J., Szeto, W.W., Lemley, P.V., Orme-Johnson, W.H., Ausubel, F., M., 1985, ***Nucleic Acid Res.*** **13**, 4539-4555

Bulen, W.A., 1976,In ***Proc. 1st Symp. Nitrogen Fixation Vol 1***, (Newton, W.E., Nyman, C.J. eds.) Washington State University Press. pp. 177-186

Bulen, W.A., LeComte, J.R., 1966, ***Proc. Natl.Acad. Sci. USA*** **56**, 979-986

Bulen, W.A., Burns, R., LeComte, J.R., 1965, ***Proc. Natl. Acad. Sci. USA*** **53**, 532-539

Burgess, B.K., 1983, in ***Advances in Nitrogen fixation Research*** (Veeger, C., Newton, W.E., eds) Martinus Nijhoff. The Hague. pp 103-114

Burgess, B.K., 1990, ***Chem. Rev.*** **90**, 1377-1406.

Burgess, B.K., 1993, in ***Molybdenum Enzyme, Cofactor and Models*** (Stiefel, E., Coucouvanis, D., Newton, W.E.,eds) American Chemical Society, Washington D.C. pp. 144-169

Burgess, B.K., Lowe, D.J., 1996, ***Chem. Rev***. **96**, 2983-3011

Burgess, B.K., Stiefel, E.I., Newton, W.E., 1980, ***J. Biol. Chem***. **355**, 353-356

Burns, A., Watt, G.D., Wang, Z.C., 1985, ***Biochemistry* 24**, 3932-3936

Burns R.C., Hardy R.W.F. (1975), ***Nitrogen Fixation in Bacteria and Higher Plants*, *Springer-Verlag, Berlin.***

Burris, R.H. 1979 ***A Treatise on Dinitrogen Fixation***, (Hardy, R.W.F., Bottomly, F., Burris, R.H., eds) Wiley, New York.

Cannon, M., Cannon, F., Buchanan-Wollaston, V., Ally, D., Ally, A., Beynon, J., 1988, ***Nucleic Acid Res.* 16**, 11379

Chan, M.K., Kim, J., Rees, D.C., 1993, ***Science* 260**, 792-794

Chen, J., Christiansen, J., George, S.J., van Elp, J.,Tittsworth, R.C., Hales, B.J., Al-Ahamad, S., Coucouvanis, D., Bolin, J.T., Cramer, S.P., 1993, ***J. Am. Chem. Soc.* 535**, 231-242

Chen, J., Christiansen, J., Tittsworth, R.C., Hales, B.J., George, S.J., Coucouvanis, D., Cramer, S.P.,1993, ***J. Am. Chem. Soc.* 115**, 5509-5515.

Chen L., Cavin, N., Tsruta, H., Eliezer, D., Burgess, B.K., Doniach, S., Hodgson, K.O., 1994, ***J. Biol. Chem.* 269**, 3290-3294

Chlisnell, J.R., Premakumar, R., Bishop, P.E., 1988, ***J. Bacteriol***. **170**, 27-33

Corbin, J.L., 1978, ***Anal. Biochem***. **84**, 340-342

Davis, L.C., 1980, ***Archiv. Biochem. Biophys.* 204**, 270-276

Dean, D.R., Setterquist, R.A., Brigle, K.E., Scott, D.J., Laird, N.F., Newton, W.E., 1990, ***Mol. Microbiol***. **4(9)**, 1505-1515

Dean, D.R., Jacobson, M.R., 1992, ***In Biological Nitrogen Fixation***. (Stacey, G., Burris, R. H., Eavans, H. J., eds) Chapman and Hall, New York, pp 763-834

Dean, D.R., Brigle, K.E., May, H.D., Newton, W.E., 1988, ***In Nitrogen Fixation-Hundred Years After***. (Bothe, H., de Bruijn, F.J., Newton, W.E., eds) Gustav Fischer, Stuttgurt, pp 107-113

Deits, T.L., Howard, J.B., 1990, ***J. Biol. Chem***. **265**, 3859-3867

Deits, T.L., Howard, J.B., 1989, J. Biol. Chem***.* 264,** 6619

Delwiche C.C., 1977, ***Ambio*** **6**, 106

Denefle, P., Kush, A., Norel, F., Paquelin, A., and Elmerich, C., 1987, ***Mol. Gen. Genet.*** **207,** 280-287

Dilworth, M.J., 1966, ***Biochim. Biophys.Acta***. **127**, 285

Dilworth, M.J., Thorneley, R.N.F., 1981, ***Biochem. J***. **193**, 971-983

Dilworth, M.J., Eady, R.R., Eldridge, M.E., 1988, ***Biochem. J***. **249**, 745-751

Dilworth, M.J., Eady, R.R., Robson, R.L., Miller, R.W., 1987, ***Nature (London)*** **327**, 167-168.

Dilworth, M.J., Eldridge, M.E., Eady, R.R., 1992, ***Anal. Biochem***. **206**, 6-10

Drummond, M., Whitty, P., Wooton, J., 1986, ***EMBO J.*** **5**, 441-447

Drummond, M.H., 1985, ***Biochem. J.*** **232**, 891-896

Drummond, M.H., Wootton, J.C., 1987, ***Mol, Microbiol. J.*** **1**, 37-44

Eady, R.R. (1992) In ***The Procaryotes***, Second edition, Vol.**1**. (Balows, A. Truper, H.G., Dworkin, M., Harder, W., Schleifer, K.H. eds) Springer-Verlag. pp. 534-553

Elmerich, C., Houmard, J., Sibold, L., Manheimer, I., Charpin, N., 1978, ***Biochimie*** **165,** 181-189

Ennor, A.H., 1957, ***Method in Enzymol***. **3**, 850-856

Ernst C.A., 1928, ***Fixation of Atmospheric Nitrogen***, van Nostrand Co., New York.

George, G.N., Coyle, C.L., Hales, B.J., Cramer, S.P., 1988, ***J. Am. Chem. Soc.,*** **110**, 4057-4059

Georgiadis, M.M., Komiya, H., Chakrabarti, P., Woo, D., Kornuc, J.J., Rees, D.C., 1992, ***Science*** **257**, 1653-1659.

Hageman, R.V., Burris, R.H. 1978, ***Proc. Natl. Acad. Sci. USA*** **75**, 2699-2706

Hageman R.V. Burris, R.H., 1978, ***Biochemistry.*** **17**, 4117

Hagen, W.R., Eady, R.R., Dunham, W.R., Haaker, H., 1985, ***J. Biol. Chem.* 261**, 15301-15306

Hales, B.J., Case, E.E., Morningstar, J.E., Dzeda, M.F.,Mauterer, L.A., 1986, ***Biochemistry* 25**,7251-7255

Hardy, R.W.F., 1979, ***A Treatise on Dinitrogen Fixation, Section 2***, (Hardy, R.W.F. and Burns, R.C. eds) Wiley and Sons, New York. pp515-568

Hardy, R.W.F., Jackson, E.K., 1967, ***Fed. Proc., Fed. Am. Soc. Exp. Biol*. 26**, 725

Hardy, R.W.F., Burns, R.C., Holsten, R.D., 1973, ***Soil Biol. Biochem***. **5**, 47-81

Hardy, R.W.F., Knight, E. Jr., 1967, ***Biochim. Biophys. Acta* 139,** 69-90

Hausinger, R.P., Howard, 1983, ***J. Biol. Chem.* 258**, 13486-13492

Hawkes, T.R., Smith, B.E., 1983, ***Biochem. J.* 209**, 43-50

Hawkes, T.R., McLean, P.A., Smith, B.E., 1984, ***Biochem. J.***, **217,** 317-321.

Holland, D., Zilberstein, A., Zamir, Sussman, J., 1987, ***Biochem. J.* 247**, 277-285

Hoover, T.R., Roberson, A.D., Cerny, R.L., Hayes, E.N., Imperial, J., Shah, V.K., Ludden, P.W., 1987, ***Nature* 329**, 855-857

Hoover, T.R., Imperial, J., Ludden, P.W., Shah, V.K., 1989, ***Biochemistry* 28**, 2768-2771

Hoover, T.R., Imperial, J., Liang, J., Ludden, P.W., Shah, V.K., 1988, ***Biochemistry*** **27**, 3647-3652

Homer, M.J., Paustian, T.D., Shah, V.K., Roberts, G.P. 1993, ***J. Bacteriol.*** **175**, 4907-4910

Houmard, J., Bogusz, D., Bigault, R., Elmerich, C., 1980, ***Biochimie*** **62**, 267-275

Howard, K.S., McLean, P.A., Hansen, F.B., Lemley, P.V., Koblan, K.S., Orme-Johnson, W.H. 1986, ***J. Biol. Chem***. **261**, 772-778.

Howard, J.B., Rees, D.C., 1994, ***Annu. Rev. Biochem.*** **63**, 235-264

Howard, J.B., Davis, R., Moldenhauer, B., Cash, V.L., Dean, D., 1989, ***J. Biol. Chem.*** **264**, 11270-11274

Howard, J.B., Rees, D.C., 1994, ***Annu. Rev. Biochem.*** **63**, 235-264

Howard J.B., Rees, D.C., 1996, ***Chem. Rev.*** **96**, 2965-2982

Hwang, J.C., Chen, C.H., Burris, R.H., 1973, ***Biochim. Biophys. Acta***., **292**, 256-270

Hwang, J.C., Burris, R.H., 1972, ***Biochim. Biophys. Acta.*** **283**, 339-350

Imperial, J., Hoover, T.R., Madden, M.S., Ludden, M.S., Shah, V.K., 1989, ***Biochemistry*** **28**, 7796-7799

Ioannidis, I., Buck, M., 1987, ***Biochem. J.*** **247**, 287-291

Jackson, E.K., Parshall, G.W., Hardy, R.W.F., 1968, ***J.Biol. Chem.*** **243**, 4952-4958

Jacobson, M.R., Cash, V.L., Weiss, M.C., Laird, N.F., Newton, W.E., Dean, D.R. 1989, ***Mol.Gen. Genet***. **219**, 49-57

Kaluza , K., Hennecke, H., 1984, ***Mol. Gen. Genet***. **196**, 35-42

Kelly, M., 1968, ***Biochem. J.*** **107**, 1-6

Kelly, M., Postgate, J.R., Richards, R.L., 1967 ***Biochem. J.*** **102**, 1c-3c

Kent, H.M., Ioannidis, I., Gormal, C., Smith, B.E., Buck, M., 1989, ***Biochem. J.*** **264**, 257-264

Kim, J., Rees, D.C., 1992a, ***Science*** **257**, 1677-1659

Kim, J., Rees, D.C., 1992b, ***Nature*** **360**, 553-560

Kim, J., Woo, D., Rees, D.C., 1993, ***Biochemistry*** **32**,7104-7115

Knowles, P.F., Marsh, D., Rattle, H.W.E., 1976, ***Magnetic Resonance of Biomolecules***. Wiley, New York.

Kurtz, D.M, Jr., McMillan, R.S., Burgess, B.K., Mortenson, L.E., Holm, R.M.. 1979, ***Proc. Natl. Acad. Sci. USA*** **80**, 4723-4727

Lammers P.J., Haselkorn, R.,1983, ***Proc. Natl. Acad. Sci. USA*** **80**, 4723-4727

Lanzilotta, W.N., Fisher, K, Seefeldt, L.C., 1996, ***Biochemistry***, **35** , 7188-7196

Leigh, G.J., 1981, ***The Significance of Current Research on Chemical Nitrogen Fixation. Chemistry and Industry***. pp. 664-667

Li, J.G., Burgess, B.K.M., Corbin, J.L., 1982, ***Biochemistry*** **21**, 4393-4402

Lowe, D.J., 1992, ***In Electron and proton transfer in chemistry and biology***. (Muller, A., Ratajczak, H., Jungle, W., Diemann, E., eds) Elsevier, Amsterdam. pp. 149-165

Lowe, D.J., Thorneley, R.N.F., 1984a, ***Biochem. J***. **224**, 877-886

Lowe, D.J., Thorneley, R.N.F., 1984b,***Biochem. J.*** **224**, 895-901

Lowe, D.J., Fisher, K., Thorneley, R.N.F., 1993, ***Biochem. J.*** **292,** 93-98

Lowery, R., Chang, C., Davis, L., McKenna, M.C., Stephens, P.J., Ludden, P., 1989, ***Biochemistry*** **28**, 1206-1212

MacNeil, T., MacNeil, D., Roberts, G.P., Supiano, M., A., Brill, W.J., 1978, ***J. Bacteriol.*** **136**, 252-266

Martin, A.E., Burgess, B.K., Iismma, S.E., Smartt, C.T., Jacobson, M.R., Dean, D.R., 1989, ***J. Bacteriol.*** **171**, 3162-3167

Masharak, P., Smith, M.C., Armstrong, W.H., Burgess, B.K., Holm, R.H., 1982, ***Proc. Natl. Acad. Sci. USA*** **79**, 7056-7060

May, H.D., Dean, D.R., Newton, W.E., 1991, ***Biochem. J.***, **227**, 457-464

Mazur, B.J., Chui, C.F., 1982, ***Proc. Natl. Acad. Sci. USA*** **79**, 6782-6786

McKenna, C.E., Jones, J.B., Eran, H., Huang, C.W., 1979, ***Nature*** (London) **280**, 611-612.

McLean, P.A., Dixon, R.A., 1981, ***Nature*** (London) **292**, 655-656

Merrick, M., Filser, M., Dixon, R., Elmerich, C., Sibold, L., Houmard, J., 1980, ***J. Gen. Microbiol.*** **117**, 509-520

Meyer, J., Gaillard, J., Moulis, J.-M., 1988, ***Biochemistry*** **27**, 6150

Miller, A.F., Orme-Johnson, W.H. 1992, ***J. Biol. Chem***. **267**, 9398-9408

Morgan, T.V., Prince, R.C., Mortenson, L.E., 1986, ***FEBS Lett.*** **206**, 4-8

Morningstar, J.E., Johnson, M.K., Case, E.E., Hales, B.J., 1987, ***Biochemistry*** **26**, 1795-1800

Mortenson, L.E., 1964, ***Proc. Natl. Acad. Sci. USA*** **52**, 272-279

Mortenson,L.E., Thorneley, R.N.F., 1979, ***Annu. Rev. Biochem.*** **48**, 387-418

Moustafa, E., Mortenson, L.E., 1967, ***Nature*** **216**, 1241-1242

Mozen, M.M., Burris, R.H., 1954, ***Biochim. Biophys. Acta***. **14,** 577-578

Murrel, S.A., Lowery, R.G., Ludden, P.W., 1988, ***Biochem. J***. **251**, 609-612

Newton, W.E., 1992, In ***Biological Nitrogen Fixation*** (Stacy, G., Burris, R.H., Evans, H.J., eds) , Chapman and Hall, New York, NY, pp 877-929

Newton, W.E., Gheller, S.F., Schultz, F.A., Burgess, B.K., Conradson, S.D., McDonald, J.W., Hedman, B., Hodgson, K.O., 1985, I***n Nitrogen Fixation Research Progress*** (Evans, H.J., Bottomley, P.J., Newton, W.E., eds) Martinus Nijhoff , Dordrecht, the Netherlands, pp 5729-5735

Palmer, G., 1985, ***Biochem. Soc. Trans***. **13**, 548- 560

Palmer G., 1972, ***Biochem. Biophys. Res. Commun.*** **48**, 1525-1532

Paul, W., Merrick, M., 1987, ***Eur. J. Biochem.*** **170**, 259-265

Paul, W., Merrick, M., 1989, ***Eur. J. Biochem.*** **178**, 675-682

Paustian, T.D., Shah, V.K., Roberts, G.P., 1990, ***Biochemistry*** **29**, 3515-3522

Peters, J.W., Fisher, K., Newton, W.E., Dean, D.R., 1995, ***J. Biol. Chem.*** **270**, 27007-27013

Peters, J.W., Stowell, M.H.B., Soltis, S.M, Finnegan, M.G., Johnson, M.K., Rees, D.C., 1997, ***Biochemistry*** **36**, 1181-1187

Pope, M.R., Murrel, S.A., Ludden, P.W., 1985, ***Proc. Natl. Acad. Sci. USA*** **82**, 3173-3177

Puhler, A., Klipp, W., 1980, In ***Biology of Inorganic Nitrogen and Sulfur*** (Bothe, H., Trebst, eds). Springer-Verlag, Berlin.1980, pp. 276-286

Rawlings, D.E., 1989, ***Gene* 69**, 337-343

Rawlings, J., Shah, V.K., Chrisnell, J.R., Brill, W.J., Zimmermann, R., Munck, E., Orme-Johnson, W.H., 1978, ***J. Biol. Chem.* 253**, 1001-1004.

Rees, D.C., Howard, J.B., 1983, ***J. Biol. Chem.* 258**,12733-12734

Riedel, G.E., Ausubel, F.M., Cannon, F.M., 1979, ***Proc. Natl. Acad. Sci. USA* 76,** 2866-2870

Rivera-Ortiz, J.M., Burris, R.H., 1975, ***J. Bacteriol***. **123,** 537-545

Roberts, G.P., Brill, W.J., 1980, ***J. Bacteriol.* 144**, 210-216

Roberts, G.P., MacNeil, T., MacNeil, D., Brill, W.J., 1978, ***J. Bacteriol.* 136**, 267-279

Robson, R.L., 1984, ***FEBS Lett.* 173**, 394

Robson, R.L., Eady, R.R., Richardson, T.H., Miller, R.W., Hawkins, M, Postgate, J.R., 1986, ***Nature* 322**, 388-390

Rubinson, J.F., Corbin, J.L., Burgess, B.K., 1983, ***Biochemistry* 22,** 6260-6268

Ryle, M.J., Seefeldt, L.C., 1996, ***Biochemistry* 35**, 4766-4775

Schill, R., 1977, In ***Modern Practice of Gas Chromatography*** (Grob, R.L., ed), Wiley, New York, London, Sydney, Toronto, pp. 289-364

Schindlin, H., Kisher, C., Schlessman, J.L., Howard, J.B., Rees, D.C., 1997, ***Nature*** **387**, 370-376

Schollhorn, R., Burris, R.H., 1967, ***Proc. Natl. Acad. Sci. USA*** **57**, 1317-1323

Schollhorn, R., Burris, R.H., 1967, ***Proc. Natl. Acad. Sci. USA*** **58**, 213-216

Schollhorn, R., Burris, R.H., 1966, ***Fed. Proc***. **25**, 710

Scott, D.J., Dean, D.R., Newton, W.E., 1992, ***J. Biol. Chem***. **267**, 20002-20010

Scott, D.J., May, H.D., Newton, W.E., Brigle, K.E., Dean, D.R., 1990, ***Nature*** **343**, 188-190

Scott, D.J., Rolfe, B.G., Shine, J., 1981, ***J. Mol. Apl.Genet.*** **1,** 71-78

Setterquist, R., Brigle, K.E., Beynon, J., Cannon, M., Ally, A., Cannon, F., Dean, D.R., 1988, ***Nucleic Acid Res.*** **16**, 5215

Shah, V.K., Davis, L.C., Brill, W.J., 1975, ***Biochim. Biophys. Acta***. **384**, 353-359

Shah, V.K., Chlisnell, J.R., Brill, W.J., 1978, ***Biochem. Biophys. Res. Commun***. **81**, 232-236.

Shah, V.K., Davis, L.C., Gordon, J.K., Orme-Johnson, W.H., Brill, W., 1973, ***Biochim. Biophys. Acta.*** **292,** 246-255.

Shah, V.K., Stacey, G., Brill, W.J., 1983, ***J. Biol. Chem***. **258,** 12064-12068

Shah,V.K., Brill, W.J., 1977 ***J. Proc. Natl. Acad. Sci. U.S.A*** **74**, 3249-3253

Shen, J., 1994, Ph.D. dissertation: ***Roles of MoFe Protein α-274-Histidine, α-276-tyrosine and α-277-arginine residues in Azotobacter vinelandii nitrogenase catalysis***, Virginia Tech, Blacksburg, Virginia, pp 20-21.

Silvelster, W.B., Musgrave, D.R., 1991, In ***Biology and Biochemistry of Nitrogen Fixation*** (Dilworth, M.J., and Glenn, A.R., eds), Elsevier, Amsterdam, pp. 162-186

Simpson, F.B., Burris, R.H., 1984, ***Science*** **224**, 1095-1097

Smith, B.E., Bishop, P.E., Dixon, R.A., Eady, R.R., Filler, W.A., Lowe, D.J., Richard, A.J.M., Thomson, A.J., Thorneley, R.N.F., Postgate, J.R., 1985, In ***Nitrogen Fixation Research Progress*** (Evans, H.J., Bottomley, P.J., Newton, W.E., eds) Martinus Nijhoff : Dordrecht, the Netherlands, pp 597-603

Smith, B.E., Bishop, P.E., Dixon, R.A., Eady, R.R., Filler W.A., Lowe, D.J., Richards, A.J.M., thompson, A.J., Thorneley, R.N.F., Postgate, J.R., 1985, In ***Nitrogen Fixation Progress.*** (Evans, H.J., Bottomley, P.J., Newton, W.E., eds), pp. 597-603

Smith, B.E.,Lowe, D.J., Bray, R.C., 1973,***Biochem. J.*** **135**, 331-341

Smith, B.E., Eady, R.R., Lowe, D.J., Gormal,C., 1988, ***Biochem. J.*** **250**, 299-302

Steinbauer, J., Wenzel, W., Hess, D., 1988, ***Nucleic Acid Res.*** **16**, 719

Stephens, P.J., McKenna, C.E., McKenna, M.C., Nguyen, H.T., Lowe, D.J., 1982 in ***Electron Transport and Oxygen Utilization*** (Ho, C., ed), Elsevier Biomidical, New York, pp405-409

Stiefel, E.I., 1973, ***Proc. Natl. Acad. Sci. USA*** **70**, 988-992

Strandberg, G.W., Wilson, P.A., 1968, ***Can. J. Microb***. **14**, 25-31

Sundaresan, V., Ausubel, F.M., 1981, ***J. Biol. Chem.*** **256**, 2808-2812

Surerus, K.K., Hendrich, M.P., Christie, P.D., Rottgardt, D., Orme-Johnson, W.H., Munck, E., 1992, ***J. Am. Chem. Soc.*** **114**, 8579-8590

Thomann, H., Bernardo, M., Newton, W.E., Dean, D.R., 1991, ***Proc. Natl. Acad. Sci. USA*** **88**, 6620-6623

Thony, B., Kaluza, K., Henneke, H., 1985, ***Mol. Gen. Genet***.**198**, 441-448

Thorneley, R.N.F., Lowe, D.J., 1984a, ***Biochem. J.*** **224**, 887-894

Thorneley, R.N.F., Lowe, D.J., 1984b, ***Biochem. J***. **224**, 903-909

Thorneley, R.N.F., Eady, R.R., Lowe, D.J., 1978, ***Nature*** **272**, 557-558

Thorneley, R.N.F., Lowe, D.J., 1983, ***Biochem. J.*** **215**, 393-403

Ulgalde, R.A., Imperial, J., Shah, V.K., Brill, W.J. 1984, ***J. Bacteriol.*** **159**, 888-893

Vancini C.A. 1971, ***Synthesis of Ammonia***, CRC Press Cleveland,Ohio.

Walker, G.A., Mortenson, L.E., 1973, ***Biochem. Biophys. Res. Commun.*** **53**, 904-909

Walker, G.A., Mortenson, L.E., 1974, ***Biochemistry*** **13**, 2382-2388

Walker, J.E., Saraste, M., Runswick, M.J., Gay, N.J., 1982, ***EMBO J.*** **1**, 945

Wang, S.-Z., Chen, J.-S., Johnson, J.L., 1988, ***Biochemistry*** **27**, 2800-2810

Weinman, J.J., Fellows, F.F., Gresshoff, P.M., Shine, J., Scott, K.F., 1984, ***Nucl. Acid. Res***. **12**, 8329-8344

Willing, A.H., Georgiadis, M.M., Rees, D.C., Howard, J.B., 1989, ***J. Biol. Chem***. **264**, 8499-8503

Willing, A.H., Howard , J.B., 1990, ***J. Biol. Chem***. **265**, 6596-9599

White, T.C., Harris, G.S., Orme-Johnson, W.H. 1992, ***J. Biol. Chem***. **267**, 24007-24016

Wolle, D., Kim, C.-H., Dean, D.R., Howard, J.B.,1992, ***J. Biol. Chem***. **267**, 3667-3673

Yates, M.G., 1991, in ***Biological Nitrogen Fixation*** (Stacey, G., Burris, R.H. and Evans, H.J., eds), Chapman and Hall, New York, pp. 685-735

Zimmerman, R., Munck,E., Brill, W.J., Shah, V.K., Henzl, M.T., Rawlings, J., Orme-Johnson , W.H. 1978, ***Biochem. Biophys. Acta.*** **537**, 185-207

Zheng, L., White, R.H., Cash, V.L., Jack, R.F., Dean, D.R. 19***93, Proc. Natl. Acad. Sci. USA*** **90**, 2754-2758

Zovoisky, E.J., 1945, ***J. Phys. USSR*** **9**, 211-216

Zumft, W.G., Mortenson, L.E., Palmer G., 1974, ***Eur. J. Biochem.*** **46**, 525-535

Vita

Haibing Xie was born on January 11, 1968 in Zhoushan, P.R.China. He graduated from Fudan University in Shanghai with a Bachelor of Science in Genetics in 1990, and he received a Master of Science in Molecular Biology from Fudan University in Shanghai in August, 1995. He came to the Dept. of Biochemistry, Virginia Polytechnic Institute and State University, where he completed his Master's degree requirement in August 1998.